UNIVERSITY OF CALIFORNIA, SAN DIEGO

Signaling from the asters and spindle midzone is required to promote cytokinesis in the early *C. elegans* embryo

A dissertation submitted in partial satisfaction of the requirements for the degree Doctor of Philosophy

in

Biomedical Sciences

by

Lindsay Kyle Lewellyn

Committee in charge:

Professor Karen Oegema, Chair
Professor Arshad Desai
Professor Don Cleveland
Professor Larry Goldstein
Professor Laurie Smith

2010

ProQuest LLC
789 East Eisenhower Parkway
P.O. Box 1346
Ann Arbor, MI 48106-1346

The Dissertation of Lindsay Kyle Lewellyn is approved, and it is acceptable in quality and form for publication on microfilm and electronically:

_____

_____

_____

_____

_____

Chair

University of California, San Diego

2010

Dedication

I would like to dedicate this thesis to my parents, Michael and Kathy Lewellyn, who have always been my greatest supporters.

Table of Contents

List of Figures

List of Tables

Acknowledgements

I would first like to acknowledge my husband, Brian, who has given me so much unconditional support throughout my time as a graduate student. He always helped to remind me of the big picture whenever things got hard. I would also like to thank Karen, who has been a great mentor: she really pushed me to do my best work and to never be satisfied with anything less. I would also like to thank Arshad, my co-mentor, and the rest of the OD lab past and present, who made these years unforgettable. I have learned so much from everyone in the lab, especially Amy Maddox, who taught me everything about worms and cytokinesis. Julie Canman and Julien Dumont have been great bay mates, sharing their scientific expertise, and always making lab fun. I also want to acknowledge the other students in the lab that helped me survive – Sharsti Sandall, Joost Monen, Nate Portier, Tony Essex, and Molly Bush.

Chapter 2, in full, was published under the following citation: *Mol. Biol. Cell*, 2009 Nov 4(Epub), Lewellyn L, Dumont J, Desai A, and Oegema K. The dissertation author was the primary researcher and author of this paper.

Chaper 3, in full, was published under the following citation: *Science*, 2008 Dec 5;322(5907):1543-6, Canman JC, Lewellyn L, Laband K, Smerdon SJ, Desai A, Bowerman B, and Oegema K. The dissertation author was

second author of this paper and performed the experiments and data analysis for Fig. 1C,D, 3, 4, S2, S3, and S4.

Chapter 4 is currently being prepared for submission for publication. Lewellyn L, Maddox AS, Desai A, and K Oegema. The dissertation author was the primary investigator and author of this material.

Vita

2003 Bachelor of Sciences, University of North Carolina, Chapel Hill

2010 Doctor of Philosophy, University of California, San Diego

PUBLICATIONS

Maddox A.S., **Lewellyn L.**, Desai A., and K. Oegema. (2007) Anillin and the septins promote asymmetric ingression of the cytokinetic furrow. *Dev Cell*. 12(5): 827-35.

Canman J.C., **Lewellyn L**., Laband, K., Smerdon, Desai A., Bowerman, B. and K. Oegema. (2008) Inhibition of Rac by the GAP activity of centralspindlin is essential for cytokinesis. *Science* 322(5907): 1543-6.

Essex, A., Dammerman, A., **Lewellyn, L**., Oegema, K., and A. Desai (2009) Systematic analysis in *Caenorhabditis elegans* reveals that the spindle checkpoint is composed of two largely independent branches. *Mol Biol Cell* 20(4):1252-67.

Lewellyn L., Dumont, J., Desai A., and K. Oegema. (2009) Analyzing the effects of delaying aster separation on furrow formation during cytokinesis in the *C. elegans* embryo. *Mol. Biol. Cell* Nov. 4 (Epub ahead of print)

Lewellyn L., Maddox, A.S., Desai A., and K. Oegema. (*in preparation*) Centralspindlin and the chromosomal passenger proteins independently promote furrow ingression in the *C. elegans* embryo

ABSTRACT OF THE DISSERTATION

Signaling from the asters and spindle midzone is required to promote cytokinesis in the early *C. elegans* embryo

by

Lindsay Kyle Lewellyn

Doctor of Philosophy in Biomedical Sciences

University of California, San Diego, 2010

Professor Karen Oegema, Chair

Cytokinesis is the final step of the cell division that physically separates a single cell into two daughter cells following chromosome segregation. In order to insure that each daughter cell receives the proper genetic complement, cytokinesis must be both spatially and temporally coupled to chromosome segregation. Cytokinesis is accomplished by formation and

constriction of a contractile ring made up of actin, myosin, anillin, and the septins. One of the critical questions in the field is how does the cell maintain precise spatial and temporal control over the assembly and constriction of the contractile ring? Although the precise molecular signals are still being debated, it is known that signals from the anaphase spindle are critical for furrow formation and ingression.

Using the early *C. elegans* embryo I have found that integration of signals from astral microtubules and the spindle midzone is critical for the formation of a single furrow during cytokinesis. During early anaphase, astral microtubules provide an inhibitory signal to prevent accumulation of contractile ring proteins in the anterior and posterior of the cell, leading to their enrichment in the equatorial region. Proper separation of the asters is important for this early signal, since delaying or preventing aster separation disrupts the equatorial enrichment of anillin and myosin and delays furrow formation. Following this initial signal from the astral microtubules, a positive signal from the midzone – mediated by Centralspindlin and the Chromosomal Passenger Complex (CPC) - drives furrow ingression and completion. Although the initial patterning of contractility and the timing of furrow formation are unaffected, depletion of Centralspindlin or the CPC leads to a decrease in the rate of ingression and failure of cytokinesis. My work has also shown that Centralspindlin and the CPC are involved in distinct pathways to promote furrow ingression. The key role of the Centralspindlin complex is to inactivate

the small GTPase, Rac, whereas the role of the CPC is likely through promoting contractile ring disassembly through regulation of anillin and/or septin.

Chapter 1: Introduction

1.1 Cytokinesis and the Spindle

Mitosis is the process by which the genetic material contained within the cell nucleus is equally divided into two daughter nuclei. Walther Flemming was one of the first scientists to describe and illustrate this process in the late 1800s. Flemming described mitosis in two steps – a progressive step in which the threadlike structures (chromosomes) were condensed and aligned, and the regressive phase, in which the threads were separated and two daughter nuclei were formed. Since this early description of the process, the field of mitosis has grown and become more specialized, allowing groups to focus on specific stages or structures involved in cell division (Rev. Paweletz 2001). This work focuses almost exclusively on the later stage of mitosis, which Flemming called the regressive phase (anaphase and telophase), and cytokinesis. Cytokinesis is the process that follows chromosomes separation, and it physically separates the cell to form two daughter cells, each containing a single nucleus. Cytokinesis is accomplished by formation and constriction of a contractile ring made up of anillin, myosin, the septins, and Anillin (Rev. Eggert, Mitchison et al. 2006). To insure that each daughter cell receives exactly one set of the genome, the assembly of the contractile ring must be both spatially and temporally coupled to chromosome segregation.

One of the critical questions in the field is how does the cell maintain precise control over formation and constriction of the contractile ring? Although the field is still trying to determine the exact nature of this signal, one thing that is known is that the anaphase spindle, which is made up of microtubule polymers, is continuously required. If the microtubules are depolymerized during early- to mid-anaphase, cytokinesis completely fails; however, if the microtubules are disrupted during late-anaphase or after ingression has initiated, there will be a late failure of cytokinesis (Larkin and Danilchik 1999). Because of this effect, most work on cytokinesis has focused on how microtubules of the anaphase spindle (or associated molecules) communicate to the equatorial cortex to promote formation and constriction of the contractile ring.

Most of the early cytokinesis studies were done using large echinoderm embryos, in which the spindle, or mitotic apparatus, was clearly visible. Raymond Rappaport is considered by most to be the father of cytokinesis, pioneering work in the field using a combination of drug treatments and physical manipulations to investigate the role of the anaphase spindle in cytokinesis (Rev. Rappaport 1996). In one classic experiment, a glass rod was pressed into the center of a dividing embryo, causing it to assume a doughnut shape. After the first mitosis, one side of the cell cleaved, forming a horseshoe shaped embryo. During the second mitosis, two separate spindles were formed in the embryo, and multiple furrows were observed. Initially,

furrows formed across the two spindles, between the separating chromosomes, as would normally occur during cytokinesis. Later, an additional furrow was formed between the asters of the adjacent spindles, which did not contain chromosomes between them (Rappaport 1961). This work provided the field with two key observations: (1) neither chromosomes nor the spindle were necessary for furrow formation, and (2) two adjacent asters were sufficient to induce furrow formation.

1.1.1 Microtubule Populations of the Anaphase Spindle

When discussing the anaphase spindle, a number of different microtubule populations are usually referred to, which should be defined before further discussion. First, are the astral microtubules, which emanate radially from the two microtubule organizing centers, or centrosomes. The astral microtubules are usually considered to be dynamic, and they contact the cortex with the highest density in the polar region and the lowest density at the equator (Wolpert 1960; Schroeder 1981; Dechant and Glotzer 2003; Strickland, Wen et al. 2005). The dynamic nature of these microtubules is likely critical for cytokinesis, since treatment of cells with taxol, a microtubule-stabilizing drug, causes cytokinesis failure (Shannon, Canman et al. 2005). One popular theory, termed “polar relaxation,” posits that dynamic astral microtubules provide a negative signal that inhibits cortical contractility in the polar regions, thereby specifying contractility in the equator (Wolpert 1960).

By measuring the tension in dividing sea urchin eggs, Schroeder (1981) proposed a variation on this theory – the “global contraction, astral relaxation” model. In this model, there is an initial, global increase in cortical tension that occurs during anaphase, and the role of the asters is to inhibit this cortical tension in the polar regions. White and Borisy (1983) went on to generate a computer model that expanded on this idea, showing that the differences in cortical tension generated by the asters could theoretically explain division of spherical cells.

Although the precise mechanism of this inhibitory signal is not known, a number of experiments support the role of the asters in suppressing contractility. Forcing cells to enter anaphase in the absence of microtubules (after treatment with nocodazole), led to contractility over the entire cortex (Canman, Hoffman et al. 2000), suggesting that the presence of microtubule polymer helps to suppress contractility. Partial depolymerization of microtubules (Hird and White 1993) in the early *C. elegans* embryo led to formation of a small spindle in the posterior, perpendicular to the normal plane of division. In these embryos, cortical contractions were observed in the anterior, away from the position of the spindle, and phalloidin staining showed an enrichment of f-actin in those regions of contractility. More recently, Werner et al. (2007) showed that in other conditions that generate small posterior spindles, cortical myosin was observed to flow away from the spindle

toward the anterior of the cell. Therefore, this data suggests that the asters normally inhibit contractility.

Although the “astral relaxation” model proposed by White and Borisy (1983) nicely predicted division in spherical cells, it was less accurate in predicting the outcome of a number of different experimental manipulations (summarized Rappaport 1996). More recent work has shown that dynamic astral microtubules are not essential for furrow formation. Treatment of cells with low doses of nocodazole, which depolymerizes dynamic astral microtubules, broadened the width of the furrow, but it did not cause failure of division (Foe and von Dassow 2008). Therefore, although they might not be required for cytokinesis, dynamic astral microtubules may play a role in refining the plane of division.

Another model proposes that instead of providing an inhibitory signal, the asters could be stimulating furrow formation, referred to as “equatorial stimulation.” Rappaport showed that placing blocks between the asters and the polar surfaces did not affect furrow formation, but placing blocks between the asters and the equatorial surface disrupted furrow formation (Rappaport and Conrad 1963; Rappaport and Rappaport 1983; Rev. Rappaport 1986), suggesting that the asters are providing a positive signal to the equator that is required for cytokinesis. In a set of papers published in 1989, Devore et al. and Harris and Gewalt proposed that the distal tips of the astral microtubules provide a positive signal to promote furrowing. This positive signal is only

strong enough to induce cytokinesis in the equatorial region, where the cortex experiences the additive effect from both asters (Devore, Conrad et al. 1989; Harris and Gewalt 1989). Not only does their model describe normal division, but it also successfully predicts the outcome of a number of experimental perturbations previously described.

More recent work has defined a subset of stable astral microtubules that could be mediating this positive signal. This population of microtubules is more closely associated with the chromosomes, where they may pick up factors that promote their stabilization. These microtubules contact the equatorial region of the cortex, and they are associated with regions of active myosin accumulation (Canman, Cameron et al. 2003; Foe and von Dassow 2008). In monopolar cells that are induced into anaphase, furrow ingression will occur at regions of the cortex that are contacted by these stable astral microtubules (Canman, Cameron et al. 2003). Although cells treated with taxol during early anaphase will ultimately fail cytokinesis, contractility was observed in regions of the cortex that were contacted by a stable microtubule (Shannon, Canman et al. 2005). Therefore, this work suggests that stable astral microtubules could provide a positive signal to induce furrow ingression in the equatorial region.

1.1.2 Aster Separation and Cytokinesis

In 1903, Teichmann used a number of different methods to induce cytokinesis failure in sea urchin embryos, leading to the formation of cells with multiple asters. Similar to Rappaport's experiment with the torus shaped embryos, he saw that furrowing could occur between aster pairs that were not connected by a spindle and chromosomes. Moreover, furrowing did not occur between every aster pair, and the depth of the furrows correlated with the separation of the asters from each other. He attributed this observation to the idea that the asters take up aggregated cytoplasm, and as they separate, they effectively help to clear the equatorial region of this aggregation and thereby promote constriction of the cell (Teichmann 1903). Because of this activity, separation of the asters is critical to generate a region of the cell that is capable of cleaving. Rappaport also reported that there was a specific extent of aster separation that was important for furrow formation. If the asters were too far apart, furrowing would not occur; however, if the distance from the spindle to the cortex was decreased, then this block to furrowing could be overcome (Rappaport 1969). This effect was explained in the context of the equatorial stimulation model, which requires that the equatorial surface experience an additive signal from both asters. As the distance between the asters increases, the area of the equatorial cortex that experiences this additive signal decreases and eventually the cytoplasm (and not the cortex) is receiving the additive effect from the two asters. Therefore, whether the signal

is positive or negative, it appears that proper aster separation is critical to deliver that signal to the cortex to induce furrow formation.

1.1.3 Spindle Midzone

The third subpopulation of microtubules that is part of the anaphase spindle and promotes cytokinesis is the spindle midzone, a set of antiparallel bundles of microtubules that forms between the separating chromosomes. It is known that the (+) ends of the microtubules are orientated toward the midline of the spindle, forming a narrow zone of overlap; however, the location of the (-) ends has been unclear (Mcdonald, Pickettheaps et al. 1977; Mastronarde, Mcdonald et al. 1993). Incorporation of fluorescent tubulin near the midline of the midzone suggests that there is some addition of tubulin at the (+) ends, but fluorescence recovery after photobleaching (FRAP) experiments showed that there is also sliding of the antiparallel microtubules apart during anaphase (Saxton and McIntosh 1987), likely through the action of motor proteins that localize to these bundles. Therefore, the spindle midzone is a structure that elongates during anaphase through the combination of microtubule polymerization at the (+) ends and sliding of the filaments against each other.

The spindle midzone is thought to provide a positive signal to induce furrow formation. Perforation of a cell between the spindle midzone and the cortex prevents furrowing on the far side of the cortex (Rappaport and

Rappaport 1983; Cao and Wang 1996). One possibility is that the bundles themselves are critical for the signal. In grasshopper spermatocytes, the chromosomes and spindle poles can be removed, and furrowing will still occur in regions of the cortex associated with microtubule bundles (Alsop 2003). Further, in cells treated with a topoisomerase II inhibitor, in which chromosome separation was prevented, furrowing was associated with regions of bundle formation (Wheatley, O'Connell et al. 1998). Although the location of cytokinetic furrows has been closely linked to microtubule bundles (Wheatley and Wang 1996), there is also strong support for the role of a number of complexes that localize to these bundles in providing the key driving force for furrow formation (Rev. Glotzer 2005). For example, if two cells are fused to produce a mitotic heterokaryon, there is a correlation between formation of a "Rappaport furrow" between the adjacent asters not connected by a spindle, and localization of INCENP, a member of the Chromosomal Passenger Complex that normally localizes to the midzone (Eckley, Ainsztein et al. 1997). Therefore, the key role of the bundles could be to provide a platform to localize critical signaling molecules during anaphase.

Formation of the midzone bundles is dependent on a microtubule bundling protein - PRC1 (also known as SPD-1 in *C. elegans*, Feo in *Drosophila*, Ase1 in budding yeast). PRC1 binds to microtubules, and electron microscopy shows that it is able to form bridges between aligned microtubules. If it is overexpressed in cells, PRC1 will induce ectopic bundle formation.

PRC1 has 2 Cdk1 phosphorylation sites, which inhibit microtubule bundling prior to anaphase onset (Mollinari 2002), insuring that the bundling capacity of the protein is under strict temporal regulation. In human cells or *Drosophila,* disruption of the spindle midzone by depletion of PRC1 or feo respectively leads to failure of cytokinesis (Mollinari, Kleman et al. 2002; Verni 2004; Mollinari, Kleman et al. 2005), suggesting that the spindle midzone is part of an integral signal that drives cell division.

In *C. elegans*, depletion of the PRC1 homolog, SPD-1, disrupts formation of the spindle midzone and leads to a spindle snapping phenotype at anaphase onset, since the astral pulling forces are no longer resisted by the spindle midzone. Although the midzone bundles are severely disrupted, embryos depleted of SPD-1 complete the first embryonic divisions (although there is often failure in later divisions; Verbrugghe 2004). Therefore, in this large embryo, the antiparallel bundles themselves are not required for cytokinesis, making it an ideal system to study the contributions of the astral and midzone microtubules.

1.2 Centralspindlin Complex

The Centralspindlin Complex is a heterotetrameric complex made up of two molecules of the kinesin motor protein, ZEN-4/Mklp1/Pavarotti, and two molecules of the Rho family GTPase activating protein (GAP), CYK-

4/MgcRacGAP/RacGAP50c. Depletion or disruption of the either member of the Centralspindlin complex leads to disruption of the spindle midzone and cytokinesis failure (Rev. Glotzer 2005).

1.2.1 Centralspindlin Complex formation and localization

In *C. elegans*, the two components of the Centralspindlin Complex are able to self-assemble, with the N-terminus of CYK-4 interacting with the central domain of ZEN-4. The intact complex is able to induce bundling of microtubules *in vitro*, whereas the individual components are not (Mishima, Kaitna et al. 2002). The N-terminus of ZEN-4/Mklp1 contains the motor domain, which is able to support microtubule gliding *in vitro* (Mishima, Pavicic et al. 2004); however, the motor activity is not required for its proper localization or for its role in cytokinesis. Expression of an ATP binding mutant of Mklp1 or its homologs (CHO1 or Pavarotti) did not prevent microtubule binding, but it did broaden the region of the midzone where the complex was localized (Matuliene and Kuriyama 2002; Minestrini, Harley et al. 2003). This suggests that the kinesin might be walking toward the (+) ends of microtubules during anaphase, resulting in the enrichment of the Centralspindlin complex in a narrow region of the midzone. Another possibility is that the motor could additionally be transporting the complex along stable astral microtubules to the equatorial cortex (Odell and Foe 2008), where it could be promoting cortical contractility.

Similar to PRC1, phosphorylation of the motor domain by the kinase, Cdk1, inhibits the ATPase activity and decreases both microtubule binding and activity in the gliding assay. This inhibitory phosphorylation may be removed by the phosphatase, Cdc14, which also localizes to the spindle midzone during anaphase (Mishima, Pavicic et al. 2004). Thus, the microtubule binding and bundling activities of ZEN-4/Mklp1 are also precisely regulated during the cell cycle.

1.2.2 Centralspindlin Complex and Rho GTPases

Most work on the Centralspindlin complex has focused on the ability of the GAP component to regulate members of the Rho family of small GTPases, which include Rho, Rac, and Cdc42. The Rho family members are small G proteins that cycle between an active, GTP-bound form, and an inactive, GDP-bound form. In their active forms, Rho family members interact with their downstream effectors to promote rearrangement of the actin cytoskeleton. Previously, it has been shown that Rac and Cdc42 are important regulators of lamellapodia and filopodia formation respectively, whereas Rho is required for cytokinesis in all systems. In its active, GTP-bound from, RhoA interacts with a number of different effectors including myosin kinases, which promote the activation of myosin motors, and formins, which promote formation of filamentous actin (Bement, Miller et al. 2006).

A number of models for the role of the Centralspindlin complex during cytokinesis have been proposed, including: (1) inactivation of Rho during the late stages of cytokinesis via activity of the RhoGAP, (2) promoting the cycling of RhoA during cytokinesis, also via the RhoGAP, (3) recruitment of the RhoGEF, ECT-2, which activates Rho, to the midzone, or (4) regulation of another small GTPase, Rac.

Initially, the role of the Centralspindlin Complex was thought to be via the GAP activity of the CYK-4 subunit, which catalyzes the enzymatic activity of Rho family GTPases: mutation of the GAP domain leads to failure of cytokinesis (Hirose 2001; Somers and Saint 2003). *In vitro*, CYK-4 was shown to be active towards all 3 members of the Rho family of GTPases – Rho, Rac, and Cdc42 – although it was most active towards Rac and Cdc42 (Jantsch-Plunger, Gonczy et al. 2000). Because Rho is the only member that is required for cytokinesis, it was proposed that CYK-4 was likely promoting inactivation of Rho during late cytokinesis to turn off the contractile machinery and allow for the completion of cell division. If CYK-4 were acting primarily to inactivate Rho, a second possibility is that the GAP activity was increasing the rate of Rho cycling during ingression. Modeling by Bement (2006) showed that the transitioning of Rho through the GTPase cycle promotes formation of a narrow zone of activity, which would be critical to limit the zone of contractility.

A third model that has been proposed is that the critical role for the Centralspindlin complex is to promote localization of the RhoGEF, ECT-2 to the spindle midzone. In human cells and *Drosophila*, MgcRacGAP/RacGAP50c has been shown to interact with ECT-2/Pebble, and depletion of Centralspindlin disrupts localization of ECT-2 on the midzone (Somers and Saint 2003; Yuce 2005; Nishimura 2006). Localization of the RhoGEF to the spindle midzone would provide a mechanism to locally activate Rho in the equatorial region following anaphase onset, making it an attractive model for midzone-based signaling. However, displacing ECT-2 from the spindle midzone did not disrupt cytokinesis in human cells (Chalamalasetty, Hummer et al. 2006), which suggests that localization of the GEF to the spindle midzone may not be essential.

The final model for the role of the Centralspindlin complex during cytokinesis is via regulation of another GTPase, Rac. Although phosphorylation of CYK-4 did modestly increase its GAP activity toward Rho, CYK-4 always showed higher GAP activity toward Rac and Cdc42 *in vitro* (Jantsch-Plunger, Gonczy et al. 2000; Minoshima, Kawashima et al. 2003). Therefore, it seemed possible that Rac or Cdc42 might be the actual target(s) of CYK-4 *in vivo*. Along these lines, it was shown that in *Drosophila* eye imaginal discs, depletion of RacGAP50c was enhanced by mutations in Rho and suppressed by mutation of Rac (D'Avino, Savoian et al. 2004), suggesting that the target of the GAP activity was Rac and not Rho. Fluorescence

Resonance Energy Transfer (FRET)-based probes demonstrated that there is a decrease in Rac activity in the equatorial region during cytokinesis (Yoshizaki, Ohba et al. 2003), and expression of a constitutively active Rac construct leads to cytokinesis failure (Muris, Verschoor et al. 2002; Yoshizaki, Ohba et al. 2003). Therefore, this suggests that during cytokinesis, there is a down-regulation of Rac activity in the equator, which is critical for ingression, and the midzone-localized Centralspindlin Complex could be fulfilling this role.

1.4 Chromosomal Passenger Complex (CPC)

Another important midzone-localized complex is the Chromosomal Passenger Complex (CPC), a four-member complex made up of the kinase, AuroraB, as well as INCENP, Survivin, and Borealin. The CPC gets its name from its dynamic localization during mitosis - first localizing to the chromosomes, then concentrating on the inner centromeres, and later transitioning onto the spindle midzone during anaphase. Fluorescence recovery after photobleaching (FRAP) experiments have shown that the complex is highly dynamic at the centromere, but it becomes stably associated with the spindle midzone during anaphase and throughout telophase (Murata-Hori and Wang 2002). Disruption or depletion of the CPC leads to errors in chromosome segregation, disorganization of the spindle midzone, and cytokinesis failure (Rev. Ruchaud, Carmena et al. 2007).

1.4.1 Localization of the CPC

A number of different studies have tried to dissect the regions of the complex that contribute to its localization throughout mitosis. INCENP is the largest member of the complex, and it acts as a scaffold to interact with the other three members. INCENP itself is a substrate of AuroraB, and phosphorylation of the C-terminal IN-box region promotes further activation of the kinase (Bishop 2002). The C-terminal coiled-coil region of INCENP binds to microtubules, and if this region is overexpressed, it will coat the entire spindle; however, this microtubule binding region is not required for localization of the complex to the spindle midzone (Mackay, Ainsztein et al. 1998). It is actually the N-terminus of INCENP that is necessary to localize the CPC to the centromere and transfer to the spindle midzone during anaphase (Ainsztein, Kandels-Lewis et al. 1998; Mackay, Ainsztein et al. 1998). In addition to the chromosomes and spindle midzone, the CPC also localizes to the equatorial cortex in mammalian cells prior to furrow ingression (Eckley, Ainsztein et al. 1997; Wheatley, Carvalho et al. 2001; Murata-Hori and Wang 2002). If cells are treated with nocodazole, the CPC remains localized on the chromosomes as well as on the entire cortex. Further, if cells are treated with taxol to stabilize microtubules, the CPC is seen at the (+) ends of microtubules that are near the cortex, but not on the cortex itself (Wheatley, Carvalho et al.

2001). This suggests that astral microtubules can deliver the CPC to the equatorial cortex.

The site of action of the CPC during cytokinesis has remained a bit of a mystery, although it is known that localization of the complex to the centromere is not required for its role in cytokinesis or for its subsequent localization on the spindle midzone (Lens, Rodriguez et al. 2006; Vader, Kauw et al. 2006). If the CPC is tethered to the centromere by fusing CenpB to INCENP, cytokinesis fails (Eckley, Ainsztein et al. 1997). This suggests that although localization to the centromere is dispensable, liberating the complex from the centromere is required for cytokinesis.

1.4.2 Targets of the CPC during Cytokinesis

One of the critical roles of the CPC is to promote cytokinesis, although the mechanism by which this is achieved is still not understood. It is known that the kinase activity of Aurora B is required for its function during cytokinesis (Murata-Hori and Wang 2002; Honda, Korner et al. 2003), and a number of targets have been identified, including histone H3, myosin regulatory light chain (MRLC), CENP-A, INCENP, MgcRacGAP, vimentin, desmin, survivin, and MCAK (Rev. Vagnarelli and Earnshaw 2004). However, none have been demonstrated to be the key regulator of cytokinesis. One possibility is that the critical role of the CPC is to promote localization and/or activity of the Centralspindlin Complex. Both members of the Centralspindlin

Complex are phosphorylated by AuroraB (Minoshima, Kawashima et al. 2003; Guse, Mishima et al. 2005; Neef, Klein et al. 2006), but the functional importance of these sites is still unclear. These regulatory sites may control the specificity of the GAP domain of CYK-4 (Minoshima, Kawashima et al. 2003) or promote nuclear import of Centralspindlin during late ingression (Neef, Klein et al. 2006). In addition, although disruption of the CPC does perturb the localization of the Centralspindlin Complex (Kaitna, Mendoza et al. 2000; Giet and Glover 2001; Verbrugghe 2004; Zhu, Bossy-Wetzel et al. 2005), this could be a secondary consequence of disruption of the spindle midzone structure, and it might not be due to a strict requirement for the CPC in promoting Centralspindlin's localization.

1.5 Midzone and Asters

Until recently, the role of the asters and the midzone have been described separately, but both structures exist within the cell during early anaphase, and both could be providing signals that converge upon the equatorial cortex to promote furrow formation. To dissect the role of the two different sets of microtubules, Bringmann and Hyman (2005) performed a spindle cutting experiment in the *C. elegans* embryo. During anaphase, a UV microbeam was used to sever the spindle between the separated chromosomes and one of the asters: this led to a situation in which the position midway between the asters was spatially distinct from the position of

the midzone. In these embryos, two furrows were observed – an initial furrow at the midpoint between the asters, and a second furrow that corresponded to the position of the midzone. This led the authors to propose a model in which the asters and the midzone provide two sequential, redundant signals to promote furrow formation and ingression. However, because the signals normally overlap, it is a way for large embryonic cells to insure that a single, robust furrow is formed.

In this and later work, Bringmann et al. went on to characterize the molecules required for the two different signals. They showed that the aster-based furrow was dependent on Gα subunits (GOA-1/GPA-16), its upstream activators, GPR-1/2, and the DEP-domain protein, LET-99, which is required to restrict the localization of GPR-1/2 to the posterior of the embryo (Bringmann, Cowan et al. 2007). Interestingly, signaling by the Gα pathway is also required to promote separation of the asters during anaphase (Gonczy 2005), which is reminiscent of the early work of Rappaport and others (Rev. Rappaport 1996) showing that proper aster separation (not too much or too little) is critical for cytokinesis. The midzone-based furrow was dependent on the microtubule bundling protein, SPD-1, the Centralspindlin Complex, and the CPC (Bringmann and Hyman 2005). Therefore, this work has suggested that signaling from the asters and the spindle midzone redundantly promote cytokinesis and ensure that the process happens robustly.

Chapter 2: Analyzing the effects of delaying aster separation on furrow formation during cytokinesis in the *C. elegans* embryo

2.1 Summary

Signaling by the centrosomal asters and spindle midzone coordinately directs formation of the cytokinetic furrow. Here, we explore the contribution of the asters by analyzing the consequences of altering inter-aster distance during the first cytokinesis of the *C. elegans* embryo. Delaying aster separation, using TPXL-1 depletion to shorten the metaphase spindle, leads to a corresponding delay in furrow formation, but results in a single furrow that ingresses at a normal rate. Preventing aster separation, by simultaneously inhibiting TPXL-1 and Gα signaling-based cortical forces pulling on the asters, delays furrow formation and leads to the formation of multiple furrows that ingress towards the midzone. Disrupting midzone-based signaling, by depleting conserved midzone complexes, results in a converse phenotype: neither the timing nor number of furrows is affected, but the rate of furrow ingression is decreased 3-fold. Simultaneously delaying aster separation and disrupting midzone-based signaling leads to complete failure of furrow formation. Based on these results, we propose that signaling by the separated

asters executes two critical functions: 1) it couples furrow formation to anaphase onset by concentrating contractile ring proteins on the equatorial cortex in a midzone-independent fashion; 2) it subsequently refines spindle midzone-based signaling to restrict furrowing to a single site.

2.2 Introduction

The cytokinetic furrow assembles in response to signals from the anaphase spindle, thereby coupling cytokinesis spatially and temporally to chromosome segregation (Eggert, Mitchison et al. 2006). Furrow formation is directed by signals from the centrosomal asters and spindle midzone (Oegema and Mitchison 1997; Maddox and Oegema 2003; Glotzer 2005; Eggert, Mitchison et al. 2006); however, the nature of these signals and how they coordinately specify the formation of a single furrow at a unique site remains an important current challenge. An influential experiment addressing the relative roles of aster and midzone-based signaling was recently performed in the *C. elegans* embryo (Bringmann and Hyman 2005). In this experiment, the connection between the aster and chromosomes on one side of the spindle was severed with a UV microbeam immediately following anaphase onset. Cortical forces pulling on astral microtubules moved the liberated aster away from the midzone with the attached aster, spatially separating the plane bisecting the asters from the center of the spindle midzone. In this situation, two furrows formed: an initial furrow in the plane

bisecting the asters followed a few minutes later by a second furrow over the midzone. These results led to the conclusion that the asters and midzone provide sequential, redundant signals that promote furrow formation.

Recent work has suggested that dynamic astral microtubules promote furrow formation by inhibiting the accumulation of contractile ring proteins on the polar cortex, leading to their relative enrichment at the cell equator (Werner et al., 2007; Chen et al., 2008; Zhou and Wang, 2008), a role analogous to the classic polar relaxation mechanism originally proposed by Wolpert, which was later refined by Borisy and White (Wolpert 1960; White and Borisy 1983). Support for this idea comes from the *C. elegans* embryo, where mis-regulation of the microtubule-severing protein, katanin, destabilizes microtubules and leads to formation of a small spindle in the embryo posterior and accumulation of excess myosin on the opposite anterior cortex (Werner, Munro et al. 2007). Similarly, in grasshopper spermatocytes asymmetrically positioned asters, or placement of a mechanically “deconstructed” spindle on one side of the cell, results in the accumulation of cortical actin on the opposite side of the cell (Chen et al., 2008). An inhibitory role for the asters has also been proposed based on work in vertebrate cells and in sea urchin embryos. In vertebrate cells, phases of myosin loss were shown to balance phases of myosin recruitment on the polar cortex, whereas at the cell equator, fewer disassembly phases led to myosin accumulation (Zhou and Wang 2008). Similarly, sea urchin embryos undergoing anaphase onset in the presence of

nocodazole, at levels sufficient to depolymerize astral microtubules, accumulate high levels of activated myosin II over the entire cell cortex, rather than specifically at the cell equator. Treatment of sea urchin embryos with lower levels of nocodazole, which allowed cytokinesis to occur, led to increased levels of activated myosin II over a substantially broader region of the equatorial cortex than in controls (Foe and von Dassow 2008). This result suggests that in addition to inhibiting the contractility of the polar cortex, dynamic astral microtubules also act on the equatorial cortex to limit the width of the contractile region.

Insight into the role of the asters in furrow formation can be obtained by analyzing the effect of varying inter-aster distance, thereby redistributing the spatial cues that the asters provide. In a classic set of experiments, Rappaport demonstrated that increasing inter-aster distance in manipulated sea urchin embryos inhibits furrowing: this inhibition can be overcome by moving the spindle closer to the cell surface (Rappaport 1969). Early cytologists also reported that decreased inter-aster distance correlates with reduced furrowing activity (Rev. Rappaport 1996). The effect of experimentally reducing the rate of aster separation after anaphase onset has been investigated in the *C. elegans* embryo by inhibiting Gα signaling, which normally generates cortical forces that pull on the asters after anaphase onset to promote spindle elongation (Gonczy 2005). Disrupting Gα signaling does not result in a cytokinesis defect on its own. However, when combined with

inhibition of the spindle midzone-localized signaling complexes - Centralspindlin or the Chromosomal Passenger Complex (CPC) - disrupting Gα signaling leads to a synthetic defect in furrow formation (Dechant and Glotzer 2003; Verbrugghe and White 2007). Whether this synthetic defect is a consequence of reducing inter-aster distance (Dechant and Glotzer 2003) or reflects a direct role for the Gα pathway in mediating aster-based signaling has remained controversial (Bringmann, Cowan et al. 2007; Verbrugghe and White 2007). Thus, the effect of reducing inter-aster distance on furrow formation has remained an important open question.

Here we develop a controlled system to analyze the effects of reducing inter-aster distance on the cortical accumulation of contractile ring proteins and furrow formation during the first cytokinesis of the *C. elegans* embryo. We accomplish this by using TPXL-1 depletion to shorten the metaphase spindle, thereby introducing a delay between anaphase onset and the time when aster separation is comparable to that at anaphase onset in controls (Ozlü, Srayko et al. 2005). Because kinetochore microtubules exert forces that counter astral pulling forces, simultaneous inhibition of kinetochore assembly restores aster separation in TPXL-1 depleted embryos, providing an important control that ensures that effects on cytokinesis are due to reduced inter-aster distance and not to a direct role for TPXL-1. Our results suggest that signaling by the separated asters controls furrow formation in a midzone-independent fashion by focusing global cortical contractility triggered by anaphase onset to the cell

equator. Subsequently, aster-based signaling also confines the midzone-based signal to restrict furrow formation to a unique site.

2.3 Materials and Methods

2.3.1 Strains and live imaging

The genotypes of all strains used are listed in Supplemental Table I. The strains OD58 (Audhya, Hyndman et al. 2005), OD38, and OD73 (Maddox, Lewellyn et al. 2007) were described previously. The strain JJ1473 expressing NMY-2:GFP (Nance, Munro et al. 2003) was a gift of Edwin Munro. Strains were maintained at 20^{o} and live imaging was performed on newly fertilized embryos mounted as previously described (Oegema, Desai et al. 2001). For most experiments, embryos were filmed using a spinning disk confocal mounted on a Nikon TE2000-E inverted microscope equipped with a krypton-argon 2.5W water-cooled laser (Spectra-Physics, Mountain View, CA) and a charge-coupled device camera (Orca-ER; Hamamatsu, Hamamatsu, Japan). Acquisition parameters, shutters, and focus were controlled by MetaMorph software (Molecular Devices, Downington, PA). In all cases a 60x, 1.4 NA PlanApochromat lens with 2x2 binning was used. For cortical imaging, 4 z-sections were collected at 1μm intervals at each timepoint. Furrow diameters were measured in end-on projections generated from 11x2.5μm z-stacks collected at 20s intervals. The region of the furrow was isolated,

projected, and rotated 90^{o} using MetaMorph software to generate an end-on view. Embryos co-expressing GFP:AuroraB^{AIR-2} and RFP^{mCherry}:Histone H2B (OD224) were imaged on a Andor Revolution spinning disc confocal system controlled by the Andor iQ software (Andor Technology, Belfast, Ireland) equipped with an electron multiplication back-thinned charge-coupled device camera (iXon) and solid state 100 mW lasers. Embryos were imaged with a 60x, 1.4 NA PlanApochromat lens with a 1.5x optivar and no binning.

2.3.2 Quantification of cortical contractile protein accumulation

Analysis of the post-anaphase accumulation of cortical GFP:Anillin and NMY-2:GFP as a function of embryo length was performed on maximum-intensity projections of four-plane z-series containing the embryo cortex. A line bisecting the embryo was drawn from the anterior to posterior tips of the embryo, and MetaMorph software was used to generate an average intensity linescan (50 pixels wide, ~1/2 of the width of the embryo) for each timepoint. Embryos were divided into 20 equal length segments from anterior (0% embryo length) to posterior (100% embryo length), and the mean GFP:Anillin/NMY-2:GFP in each segment, after subtraction of a background measurement for that segment made just prior to anaphase onset (120-160s after NEBD; before detectable accumulation), was calculated for each timepoint. The values for each data set were normalized by dividing all

intensity values by the average maximum value for controls (55-65% embryo width at 280s after NEBD) imaged in parallel.

2.3.3 Analysis of GFP:AuroraB^{AIR-2}

The graph in Figure 2.4B was generated by drawing a 40 pixel wide box along the spindle axis in images of control and *tpxl-1(RNAi)* embryos acquired 120 seconds after anaphase onset and generating a linescan of average fluorescence intensity vs. position along the spindle axis. After subtracting the cytoplasmic background (average of the final 5 values of the linescan, nearest the embryo posterior) from all values, the traces from 5-6 individual embryos were aligned by setting the fluorescence intensity maximum for each scan to position=0. After aligning, the average fluorescence intensity at each position along the spindle axis was calculated for the set of scans and plotted.

2.3.4 RNA-mediated interference

dsRNAs were prepared as described (Oegema, Desai et al. 2001), using the primers listed in Supplemental Table II to amplify regions from N2 genomic or specific cDNAs. L4 hermaphrodites were injected with dsRNA and incubated at 20˚C for 45-48 hours. For double depletions, RNAs were mixed to obtain equal concentrations for each RNA. For single depletions done in parallel with double depletions, the dsRNA corresponding to the target was mixed with an equal concentration of a control RNA made by amplifying a

region of the yeast gene *CTF13* that does not have significant homology with any *C. elegans* gene.

2.3.5 Immunofluorescence

Immunofluorescence was performed as described previously (Oegema, Desai et al. 2001; Desai, Rybina et al. 2003) using a 20 minute methanol fixation. Antibodies against the C-terminal 108 amino acids of ZEN-4 were generated by using the primers (cgcgaattccaacagggttacgttaatccaaaat and cgcttccgtcgacttactttcgtgtgctcggagat) to amplify the corresponding region from a gene specific cDNA. The fragment was digested with EcoRI/SalI and cloned into pGEX6P-1 (GE Healthcare Life Sciences) digested with the same enzymes. A purified GST fusion was injected into a rabbit. Affinity purification was performed using standard procedures after coupling a fragment generated by removal of the GST by cleavage with PreScission protease (GE Healthcare Life Sciences) to a 1 ml NHS HiTrap column (GE Healthcare Life Sciences). Affinity purified polyclonal antibodies against the C-terminal peptide of AIR-2 (C)RAEKQQKIEKEASLRNH were generated as described previously (Desai, Rybina et al. 2003). Immunofluorescence was performed with FITC labeled α-tubulin antibodies (DM1-α; Abcam, Cambridge, MA) and antibodies to ZEN-4 and AIR-2 directly labeled with Cy3 or Cy5 as described previously (Francis-Lang, Minden et al. 1999). Images were acquired using a 100X, 1.35 NA Olympus U-PlanApo oil objective lens mounted on a

DeltaVision system (Applied Precision) that included an Olympus IX70 microscope equipped with a CoolSnap CCD camera (Roper Scientific). All fixed images are projections of 3D widefield data sets that were computationally deconvolved using Softworx software (Applied Precision).

2.3.6 Western Blotting

Western blotting of control and *tpxl-1(RNAi)* worms was performed as described (Hannak, Kirkham et al. 2001). Western blots were initially probed using 1 µg/ml rabbit anti–TPXL-1 (Ozlü, Srayko et al. 2005), which was detected using a HRP-conjugated secondary antibody (1:10,000; Bio-Rad Laboratories). The same blot was subsequently probed for α-tubulin using the monoclonal DM1α (1:100; Sigma-Aldrich) followed by an alkaline-phosphatase–conjugated anti-mouse secondary antibody (1:3,750; Jackson ImmunoResearch Laboratories).

2.4 Results

2.4.1 A controlled system to analyze the effects of delaying aster separation on cytokinesis

We began by developing a controlled system to manipulate anaphase aster separation based on depletion of the spindle protein TPXL-1, the *C. elegans* ortholog of TPX2 (Özlü *et al.*, 2005). TPXL-1 depletion shortens the

kinetochore microtubules that connect the chromosomes to the spindle poles, thereby reducing metaphase spindle length. Importantly, TPXL-1 depletion is a well-characterized perturbation previously shown to have no effect on cell polarity, the kinetics or amount of γ-tubulin recruited to centrosomes, or the rates of centrosomal microtubule nucleation or microtubule growth (Ozlü, Srayko et al. 2005; Srayko, Kaya et al. 2005). In addition, the asters in control and TPXL-1 depleted embryos move at a similar velocity and reach a similar final position after spindle severing using a UV laser (Özlü *et al.*, 2005), which in light of recent modeling (Kozlowski, Srayko et al. 2007) suggests that TPXL-1 depletion does not substantially alter either the number of astral microtubules or the Gα signaling mediated forces that position the asters.

TPXL-1 depletion shortens the kinetochore microtubules that connect the chromosomes to the spindle poles, reducing the length of the metaphase spindle from ~15 to 5 μm (Fig. 2.1A,B; Ozlü, Srayko et al. 2005). The short spindles remain centered within the embryo so that the spindle center is the same distance from the equatorial cortex as in control embryos (Fig. S2.1). Anaphase onset also occurs with the same timing in control and TPXL-1 depleted embryos, ~180s after nuclear envelope breakdown (180 $\pm$ 14.7s SD in *tpxl-1(RNAi)*, n= 13; 173 $\pm$ 11.2s SD in control, n=9). After anaphase onset, the rate of spindle elongation in TPXL-1 depleted embryos is similar to that in controls (Fig. 2.1B). However, due to the shorter initial spindle length, it takes 170s for the spindle to reach a length comparable to that at anaphase onset in

controls (Fig. 2.1A,B). After anaphase onset, inter-aster distance in TPXL-1 depleted embryos increases at a linear rate for ~170s, after which it plateaus at a value comparable to that at anaphase onset in control embryos (Fig. 2.1B). Thus, TPXL-1 depletion introduces a ~3 minute delay between anaphase onset and the point when the asters achieve a normal extent of separation, allowing us to assess the effect of this delay on furrow formation.

Because the TPXL-1 depletion-mediated decrease in spindle length requires kinetochore-microtubule attachments (Ozlü, Srayko et al. 2005), aster separation can be rescued by preventing kinetochore assembly via co-depletion of the inner kinetochore component HCP-4 (the *C. elegans* CENP-C homolog). The ability to rescue aster separation in TPXL-1 depleted embryos provides an important control to ensure that effects on cytokinesis are due to the delay in aster separation and not a direct role for TPXL-1. HCP-4 depletion leads to premature aster separation due to the absence of kinetochore microtubules, which normally resist the outward-directed cortical pulling forces acting on the asters (Oegema, Desai et al. 2001). Embryos depleted of HCP-4 or co-depleted of TPXL-1 and HCP-4 exhibit a similar pattern of premature aster separation (Fig. 2.1A,B; Movie S1). Quantitative immuno-blotting confirmed that TPXL-1 levels were reduced to a similar extent when depleted on its own or in conjunction with HCP-4 (Fig. 2.1C). Thus, comparing the consequences of co-depleting TPXL-1 & HCP-4 to those of

depleting TPXL-1 alone provides a controlled system to characterize the consequences of delaying aster separation on cytokinesis.

2.4.2 Delaying aster separation leads to a corresponding delay in furrow formation but does not alter the ingression rate

To examine the effect of delaying aster separation on cytokinesis, we analyzed embryos expressing a GFP-labeled plasma membrane probe (Audhya, Hyndman et al. 2005). To score furrow formation unambiguously, we measured the time between NEBD and "furrow involution"- the first appearance of a furrow composed of two adhered back-to-back plasma membranes in a side view of the embryo (*purple arrowheads* in Fig. 2.2A). Relative to controls, furrow involution was delayed by ~190s in TPXL-1 depleted embryos (Fig. 2.2A,B; Movie S2). To measure the kinetics of furrow ingression, z-stacks were collected and the region containing the furrow was rotated by 90^{o} and projected to generate an end-on view of the division plane (Fig. 2.2C). The diameter of the circular hole between the daughter cells was measured at each timepoint. This analysis revealed that after furrow formation in TPXL-1 depleted embryos, the rate of furrow ingression and the ultimate success of cytokinesis were indistinguishable from controls (Fig. 2.2D; compare the *orange* and *grey* curves).

To ensure that the delay in furrow formation was not due to a direct role for TPXL-1 in cytokinesis, we next examined embryos co-depleted of TPXL-1

& HCP-4. Depletion of HCP-4 on its own led to a modest delay of ~55s in furrow involution and a slight decrease in the ingression rate (Fig. 2.2A-D). This phenotype is common to perturbations that disrupt kinetochore function (*data not shown*) and likely results from the consequences of disrupting chromosome segregation on assembly of the spindle midzone. Co-depletion of HCP-4 & TPXL-1 rescued the 190s delay in furrow involution resulting from TPXL-1 depletion back to the modest delay seen in embryos depleted of HCP-4 alone (Fig. 2.2A,B). Thus, the delay in furrow formation in TPXL-1 depleted embryos is a consequence of delaying aster separation and does not reflect an independent role for TPXL-1 in promoting cytokinesis. The fact that delaying aster separation leads to a matched delay in furrow formation indicates that separated asters are required to temporally couple furrow formation to anaphase onset.

2.4.3 Aster separation is required for the equatorial enrichment of contractile ring proteins following anaphase onset

To understand how delaying aster separation delays furrow formation, we next examined the consequences of delaying aster separation on the cortical accumulation of GFP fusions with two contractile ring components, Anillin (GFP:Anillin^{ANI-1}; Fig. 2.3; Movie S3) and the heavy chain of myosin II (NMY-2:GFP; Fig. S2.2). The post-anaphase pattern of equatorial accumulation was essentially identical for the two markers (Fig. 2.3A-C; Fig.

S2.2A,B); however, the equatorial accumulation of Anillin was easier to quantify. This is because, in addition to its localization to the contractile ring, myosin II also localizes to an anterior cap that forms prior to anaphase onset and contributes to the maintenance of cell polarity (Fig. S2.2A; Guo and Kemphues 1996; Severson and Bowerman 2003; Munro 2004), whereas Anillin does not.

In control embryos, GFP:Anillin and NMY-2:GFP accumulated on the equatorial cortex during the 100s following anaphase onset (180-280 seconds after NEBD), forming a band that peaked at ~60% of embryo length. Furrow involution occurred ~10s after the equatorial band reached its maximum intensity (Fig. 2.3C; 280s). In TPXL-1 depleted embryos, GFP:Anillin and NMY-2:GFP also accumulated on the cortex during the 100s following anaphase onset. However, instead of being concentrated at the cell equator, patches of GFP:Anillin and NMY-2:GFP were distributed over the entire cortex (Fig. 2.3A,D; Fig. S2.2A,C; Movie S3). Quantitative analysis revealed a slight enrichment of cortical GFP:Anillin on the anterior and posterior corticies relative to the cell equator (Fig. 2.3C, arrowheads in graphs for 240 and 280s timepoints) – a pattern inverse to that seen in controls at this time. Thus, our results indicate that separated asters are critical for the equatorial enrichment of contractile ring proteins following anaphase onset.

After a ~3 minute delay, the inter-aster distance in TPXL-1 depleted embryos is similar to that at anaphase onset in control embryos. At this point,

an equatorial band of GFP:Anillin and NMY-2:GFP has formed on the cortex, reaching ~50% of the levels in controls (Fig. 2.3C; 440s). The 3 minute delay in the equatorial accumulation of GFP:Anillin and NMY-2:GFP (Fig. 2.3A,C; Fig. S2.2A,B) paralleled the ~3 minute delay in furrow involution (Fig. 2.2A,B). Co-depletion of HCP-4 along with TPXL-1 rescued the delay in the equatorial accumulation of GFP:Anillin and NMY-2:GFP to yield a pattern similar to that in controls (Fig. 2.3A,C; Fig. S2.2A,B; Movie S3). We note that while GFP:Anillin and NMY-2:GFP accumulated with normal timing, the equatorial accumulation persisted for ~40s longer in embryos depleted of HCP-4 alone or HCP-4 & TPXL-1 (Fig. 2.3A,C), due to the delay in furrow involution resulting from HCP-4 depletion (Fig. 2.2A,B). Together these results show that the delays in the equatorial accumulation of contractile ring proteins and furrow formation in TPXL-1 depleted embryos are due to the delay in aster separation and not to a specific role for TPXL-1 in cytokinesis.

2.4.4 TPXL-1 depletion does not significantly alter the localization of midzone-localized signaling complexes

TPXL-1 depletion leads to matched delays in aster separation, the equatorial recruitment of contractile ring proteins, and furrow formation. These delays are rescued when aster separation is restored by co-depletion of the kinetochore protein HCP-4, suggesting that they are a direct consequence of the effect of TPXL-1 on the kinetics of aster separation, rather than an

unintended consequence of TPXL-1 depletion on another process, such as assembly of the spindle midzone. To confirm this conclusion, we analyzed the effect of TPXL-1 depletion on the localization of Centralspindlin and the Chromosomal Passenger Complex (CPC), two midzone-localized complexes required for cytokinesis (Powers, Bossinger et al. 1998; Raich, Moran et al. 1998; Schumacher, Golden et al. 1998; Jantsch-Plunger, Gonczy et al. 2000; Kaitna, Mendoza et al. 2000; Severson, Hamill et al. 2000). Immunofluorescence revealed that TPXL-1 depleted embryos exhibited mild defects in chromosome segregation due to the dramatically shortened spindle (Fig. 2.4A). However, the localization of AuroraB^{AIR-2} kinase, the essential enzymatic component of the CPC, and the Centralspindlin component, ZEN-4, appeared similar between control and *tpxl-1(RNAi)* embryos (Fig. 2.4A). Live imaging of embryos co-expressing GFP:AuroraB^{AIR-2} and mCherry:Histone H2B confirmed the presence of a robust midzone (Fig. 2.4B; Movie S4). Comparison of the GFP:AuroraB^{AIR-2} fluorescence intensity along the spindle axis 120 seconds after anaphase onset (corresponds to the time of furrow formation in controls) revealed that peak levels were similar in *tpxl-1(RNAi)* embryos compared to controls; however, the distribution was slightly narrower (Fig. 2.4B). We conclude that midzone structure is largely normal in TPXL-1 depleted embryos.

2.4.5 Furrows form with normal timing but ingress at a reduced rate following inhibition of centralspindlin or the chromosomal passenger complex

To understand the relative contributions of signaling by the asters and midzone during cytokinesis, we tested whether inhibition of midzone-localized proteins would result in a delay in furrow formation comparable to that resulting from delaying aster separation. Using the methods we developed to characterize TPXL-1 depleted embryos, we analyzed the phenotype of embryos depleted of three different midzone proteins– the Centralspindlin component ZEN-4, the CPC component AuroraB^{AIR-2}, and SPD-1, a microtubule-binding protein required for the stable bundling of midzone microtubules (Vebrugghe and White, 2004). Depletion of any of these midzone components disrupts the formation of midzone microtubule bundles and leads to premature spindle pole separation (Fig. 2.5A). Depletion of AuroraB^{AIR-2} additionally results in defects in meiotic and mitotic chromosome segregation, which likely underlies the different aster separation kinetics for this depletion compared to depletion of SPD-1 or ZEN-4 (Fig. 2.5A). Although, midzone microtubules failed to form stable bundles (Fig. S2.3), the equatorial recruitment of contractile ring proteins and furrow formation occurred with normal timing in SPD-1 depleted embryos (Figs. 2.5B; 2.6A,B), and the rate of furrow ingression and success of the first cytokinesis were not different from controls (Fig. 2.5C,D). The ability of SPD-1 depleted embryos to undergo a

normal division may be due to the fact that the CPC and Centralspindlin continue to localize to microtubules in the midzone region, despite the failure to form stable microtubule bundles (Fig. S2.3).

In contrast to depletion of SPD-1, depletion of ZEN-4 or AuroraB^{AIR-2} led to penetrant failure of the first cytokinesis (Fig. 2.5C). Interestingly, in ZEN-4 or AuroraB^{AIR-2} depleted embryos, the equatorial recruitment of contractile ring proteins and furrow formation occurred with normal timing (Fig. 2.5B; 2.6A,B), but the subsequent rate of furrow ingression was dramatically (~3-4 fold) reduced compared to controls (Fig. 2.5C,D). Thus, inhibiting midzone signaling leads to a phenotype that is the opposite of that resulting from delaying aster separation. Delaying aster separation delays furrow formation but does not affect the rate of furrow ingression, whereas inhibiting midzone signaling does not affect the timing of furrow formation, but reduces the rate of furrow ingression. The mirror image relationship between these phenotypes suggests that the asters govern the initial patterning of cortical contractility and the timing of furrow formation, after which a handoff is made to the spindle midzone, which controls furrow ingression.

2.4.6 Midzone-localized signaling complexes become essential for furrow formation when aster separation is delayed

The opposing phenotypes resulting from delaying aster separation and inhibiting midzone signaling suggest that simultaneous inhibition of aster

separation and midzone signaling would abolish furrow formation. To test this idea, we co-depleted TPXL-1 and either ZEN-4 or Aurora B^{AIR-2}. The kinetics of aster separation in the co-depleted embryos were similar to those in embryos depleted of TPXL-1 alone (Fig. 2.7A,B); however furrow involution was completely abolished (Fig. 2.7C, Movie S5). This suggests that when aster separation is delayed, furrow formation becomes dependent on Centralspindlin and the CPC.

2.4.7 Multiple furrows form and simultaneously ingress towards the spindle center when aster separation is prevented

Although they are initially closer together, the asters in TPXL-1 depleted embryos separate after anaphase onset at the same rate as in controls, due to the action of cortical pulling forces mediated by the Gα signaling pathway (Gonczy 2005). Thus, the asters ultimately achieve a normal extent of separation and furrowing proceeds. In an attempt to determine if the midzone can direct furrowing in the presence of unseparated asters, we examined the consequences of simultaneously depleting TPXL-1 and disrupting Gα signaling. As predicted, co-depletion of TPXL-1 & GPR-1/2, essential components of the Gα signaling pathway, reduced both the inter-aster distance at anaphase onset and the rate of post-anaphase aster separation (Fig. 2.8A,B).

Although the asters never reached the same degree of separation as in controls, co-depleted embryos formed furrows after a delay of ~ 4 minutes (Fig. 2.8E; compared to ~3 minutes in embryos depleted of TPXL-1 alone). Strikingly, in ~80% of the TPXL-1 & GPR-1/2 depleted embryos, extra ingressions formed over the central third of the embryo (Fig. 2.8C,D). In ~50% of co-depleted embryos, the multiple ingression sites matured into extra double-membrane furrows that simultaneously progressed towards the spindle center; in the other 30%, the ectopic ingression sites did not resolve into extra furrows (Fig. 2.8C,D; Movie S6). Once formed, furrows always ingressed along a trajectory towards the spindle center, rather than straight into the embryo from their point of origin. Consistent with the formation of multiple furrows, the equatorial accumulation of GFP:Anillin occurred later and over a substantially broader region when aster separation was prevented by co-depletion of TPXL-1 & GPR-1/2 than when aster separation was delayed by TPXL-1 depletion (Fig. S2.4). In 75% of embryos, the first furrows to contact the midzone from opposite sides of the embryo formed a stable connection and cytokinesis succeeded; however, in the remaining ~25% of cases, cytokinesis failed.

Cumulatively, these results suggest that when aster separation is prevented, the midzone is ultimately able to drive furrow formation. However, in the absence of support from the separated asters, the midzone-based

signal is not sufficient to limit furrow formation to a single plane, and multiple furrows form and ingress towards the spindle center simultaneously.

2.5 Discussion

In a classic set of experiments in flattened dispermic echinoderm eggs, Rappaport (1969) showed that increasing inter-aster distance by ~25% blocked furrowing over the normal range of spindle to surface distances. The ability of these over-separated asters to promote furrow formation could be rescued by moving the asters 2-fold closer to the cortex. Here we perform the converse experiment, using a genetic perturbation to examine the effect of reducing inter-aster distance on furrow formation. TPXL-1 depletion shortens the metaphase spindle so that at anaphase onset, inter-aster distance is 1/3 of its normal value; after anaphase onset, inter-aster distance increases linearly (for 170s) until it reaches a value comparable to that at anaphase onset in controls. By introducing this delay in aster separation, we observed a 190s delay in furrow formation. This result suggests that an inter-aster distance comparable to that at anaphase onset in control embryos is required to form a furrow during the normal post-anaphase window. Therefore, a unifying conclusion that emerges from Rappport's experiments and our work is that furrow formation is remarkably sensitive to changes in inter-aster distance. We note that when aster separation is prevented (by co-depletion of TPXL-1

and disruption of Gα signaling-based cortical pulling forces), not only is cytokinesis is significantly delayed, but multiple furrows form and ingress toward the spindle midzone. Thus, although aster separation is required to couple furrow formation to anaphase onset and to properly specify furrow position and number, furrows can ultimately form in the presence of unseparated asters.

2.5.1 Delaying aster separation delays the equatorial accumulation of contractile ring proteins and furrow formation

We chose to manipulate aster separation using TPXL-1 depletion because it is an extensively characterized perturbation that has only one known phenotype - reducing the length of the kinetochore microtubules that connect the chromosomes to the spindle poles (Özlü *et al.* 2005, Srayko *et al.*, 2005, Portier *et al.*, 2007). TPXL-1 is an activator of the mitotic kinase Aurora A (Özlü *et al.* 2005). Aurora A has multiple functions in the early *C. elegans* embryo including control of spindle length, regulation of cell polarity, centrosome maturation, and promoting timely nuclear envelope breakdown (Schumacher *et al.*, 1998, Hannak *et al.*, 2001, Portier *et al.*, 2007). However, of these, only spindle length control is mediated by TPXL-1. Depletion of TPXL-1 does not affect cell polarity, centrosome maturation, or nuclear envelope breakdown, indicating that these processes are mediated by other Aurora A activator(s) (Özlü *et al.* 2005, Srayko *et al.*, 2005, Portier *et al.*,

2007). Nevertheless, it was important to control for the possibility that TPXL-1 has a direct, unidentified role in cytokinesis. To do this, we used HCP-4 depletion, which rescues the spindle shortening phenotype of TPXL-1 depletion by disrupting the kinetochore microtubules that connect the chromosomes to the spindle poles (Oegema *et al.*, 2001; Özlü *et al.,* 2005). TPXL-1 depletion led to matched delays in aster separation, the equatorial accumulation of contractile ring proteins, and furrow formation. Co-depletion of HCP-4 and TPXL-1 restored the timing of contractile ring protein accumulation to that observed in controls, and the timing of furrow formation to that observed in HCP-4 depletion alone, indicating that the observed effects are the result of a delay in aster separation rather than a specific consequence of inhibiting TPXL-1.

2.5.2 Signaling by the separated asters concentrates contractile ring proteins on the equatorial cortex and generates a midzone-independent signal for furrow formation

Our data show that aster separation is essential for the temporal coupling between furrow formation and anaphase onset. When aster separation is delayed, we observed an inverted pattern of contractile ring protein accumulation following anaphase onset - ectopic accumulation of contractile ring proteins on the polar cortex and a relative lack of accumulation on the equatorial cortex (Fig. 2.3). In light of prior work indicating that

microtubule asters inhibit the accumulation of contractile ring proteins (Wolpert 1960; White and Borisy 1983; Werner, Munro et al. 2007; Foe and von Dassow 2008; Zhou and Wang 2008), we propose a model to explain this result in which the separated asters promote furrow formation by preventing the accumulation of contractile ring proteins on the polar cortex, thereby restricting their accumulation to the cell equator (Fig. 2.9).

The separated asters likely provide modulate a transient, global up-regulation of contractility triggered by anaphase onset (Canman et al., 2000; Foe et al., 2000; Shuster and Burgess, 2002; Straight et al., 2003; Foe and von Dassow, 2008) that is independent of the midzone complexes (Fig. 2.9A; top row). In TPXL-1 depleted embryos, the transient cell cycle progression driven wave of contractility is over by the time the asters separate, depriving them of their ability to generate a midzone-independent signal for furrow formation. This would also explain why furrow formation requires midzone-localized signaling complexes when aster separation is delayed but not when the asters separate with normal timing (Fig. 2.7). An inhibitory mechanism for the asters is attractive, because in addition to explaining how separated asters pattern the cortical accumulation of contractile proteins triggered by anaphase onset to promote furrow formation, it also suggests that unseparated asters would prevent the midzone-based signal from acting on the equatorial cortex. The ectopic inhibition of cortical contractility by the unseparated asters would

explain why the midzone complex-dependent furrows in TPXL-1 depleted embryos do not form until after the asters separate.

The spindle severing experiments of Bringmann and Hyman (2005) indicated that the asters provide an initial signal for furrow formation that is independent of a second signal from the spindle midzone. The opposite phenotypes we observed following TPXL-1 depletion versus inhibition of midzone signaling provide strong support for the idea that the asters control the initial stages of furrow formation in a midzone-independent fashion. Delaying aster separation leads to an inability to properly pattern cortical contractility following anaphase onset and delays furrow formation. By contrast, inhibition of midzone signaling by depletion of essential components of either the Centralspindlin or the Chromosomal Passenger Complex does not affect the equatorial accumulation of contractile ring proteins or the timing of furrow formation.

2.5.3 Aster-based inhibition refines midzone-based signaling to confine furrow formation to a unique site

Preventing aster separation, by simultaneously inhibiting TPXL-1 and Gα signaling-based cortical forces pulling on the asters, leads to an increased delay in cytokinesis onset, followed by the simultaneous formation of multiple furrows that ingress towards the midzone. We explain this result by proposing that in addition to controlling furrow formation in a midzone-independent

fashion, astral inhibition also interacts with the midzone-based signal to limit furrow formation to a single site (Fig. 2.9A; bottom row). The fact that unseparated asters do not prevent furrowing indefinitely suggests that the asters eventually lose the ability to inhibit cortical contractility (see Fig. 2.9B). Loss of this inhibition occurs ~4 min after anaphase onset; a timepoint after completion of cytokinesis in control cells. We favor a model in which the separated asters limit furrow formation to a unique site by spatially restricting the region of the cortex where contractile ring proteins are able to accumulate in response to the midzone-based signal (Fig. 2.9A,B). In the absence of inhibition by the asters, midzone signaling generates a broad contractile region, and multiple furrows form and ingress towards the midzone simultaneously. The idea that inhibition by the asters provides spatial information that refines midzone-based signaling is consistent with a recent study in sea urchin embryos in which increased levels of activated myosin II were observed over a substantially broader region of the equatorial cortex when astral microtubules were partially depolymerized by low dose nocodazole treatment (Foe and von Dassow 2008).

In the model we propose, aster-based inhibition is a constant that acts throughout cytokinesis. Initially, aster-based inhibition patterns anaphase onset triggered contractility to prime the equatorial cortex for ingression and to promote the formation of an initial furrow. Later, aster-based inhibition confines the midzone-based signal to the equatorial plane to limit furrow

ingression to a single site. Our model differs from the model of Bringmann and Hyman (2005), who proposed that the asters and midzone provide sequential redundant positive signals, in two key respects. In our model the asters are inhibitory; they modulate contractile signals but do not generate them on their own. In addition, the aster and midzone signals in our model function together rather than being functionally redundant, since the midzone-based signal requires input from aster-based inhibition to confine its action to a unique site.

2.6 Acknowledgements

We thank Rebecca Green, Julie Canman, Amy Maddox, Ana Carvalho, and Chris Campbell for critical reading of the manuscript, and Yuji Kohara (National Institute of Genetics, Mishima, Japan) for gene specific cDNAs. K.O. and A.D. receive salary and additional support from the Ludwig Institute for Cancer Research. K.O. was a Pew Scholar in the Biomedical Sciences. L.L. was supported by the NIH/NIGMS funded UCSD Genetics Training Program (T32 GM008666) and a training grant from the National Cancer Institute.

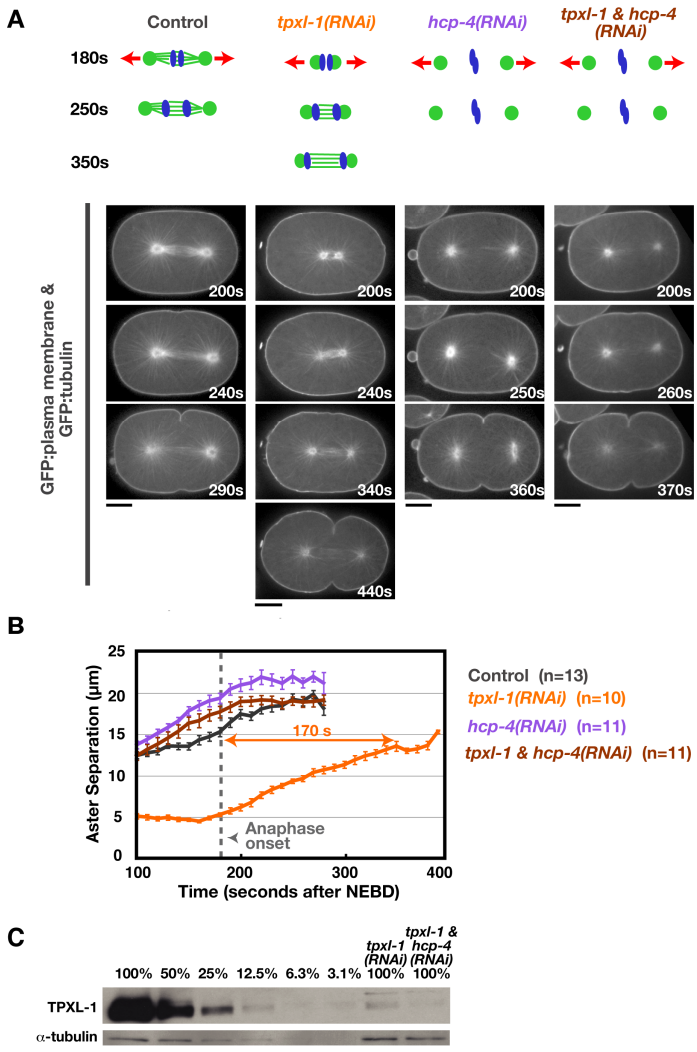

Figure 2.1 TPXL-1 depletion introduces a delay between anaphase onset and the point when the asters achieve a normal extent of separation.
(A) Schematics summarize the effects of each perturbation. Kinetochore microtubules, which resist cortical forces that pull on astral microtubules (red arrows), are absent in hcp-4(RNAi) embryos. Confocal images of embryos co-expressing GFP:β-tubulin and a GFP plasma membrane probe. Times are in seconds after NEBD. Scale bars are 10 µm. (B) Mean aster-to-aster distance, measured from the sequences in A, is plotted versus time in seconds after NEBD. Error bars are the SEM. Dotted line marks the mean time of anaphase onset in control and TPXL-1 depleted embryos. (C) Western blot of control, *tpxl-1(RNAi)*, and *tpxl-1 & hcp-4(RNAi)* worms. Serial dilutions of the control lysate were used to quantify the amount of TPXL-1 in the RNAi samples (percentage of amount in 100% control indicated above each lane). RNAi of tpxl-1 alone and tpxl-1 & hcp-4 reduced TPXL-1 levels to 7.4 and 5.6% of that in controls, respectively.

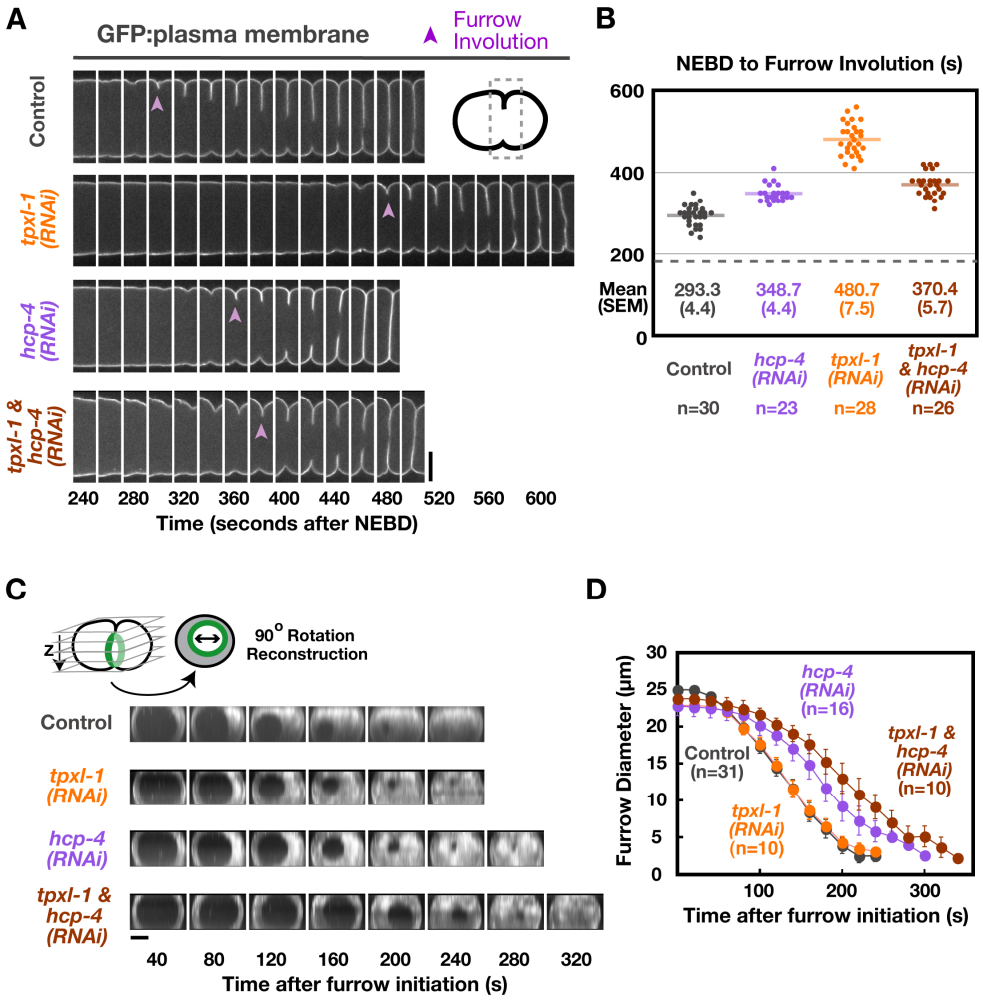

Figure 2.2 Delaying aster separation leads to a corresponding delay in furrow formation but does not alter the ingression rate.

(A) Montages of the equatorial region from central plane images of embryos expressing a GFP plasma membrane probe. Furrow involution is indicated (purple arrowheads). (B) The interval between NEBD and furrow involution, measured in embryos co-expressing GFP:β-tubulin and a GFP plasma membrane probe, is plotted for individual embryos. Solid line indicates the mean. Dashed line indicates the mean time of anaphase onset in controls. (C) Spinning disk confocal optics were used to image control, *tpxl-1(RNAi), hcp-4(RNAi)*, and *tpxl-1&hcp-4(RNAi)* embryos expressing the GFP plasma membrane probe. For each timepoint, 11 images were collected at 2.5 µm intervals in z and an "end-on" view of the division plane was obtained by isolating the region of the furrow from the image stack, rotating it by 90o, and generating a maximum intensity projection. Representative projections from timelapse series are shown for each condition. (D) Mean furrow diameter was measured from end on reconstructions generated as in C and plotted versus time. Times in C and D are in seconds after furrow initiation, the time when the first detectable ingression was visible. Error bars are SEM. Scale bars are 10 µm.

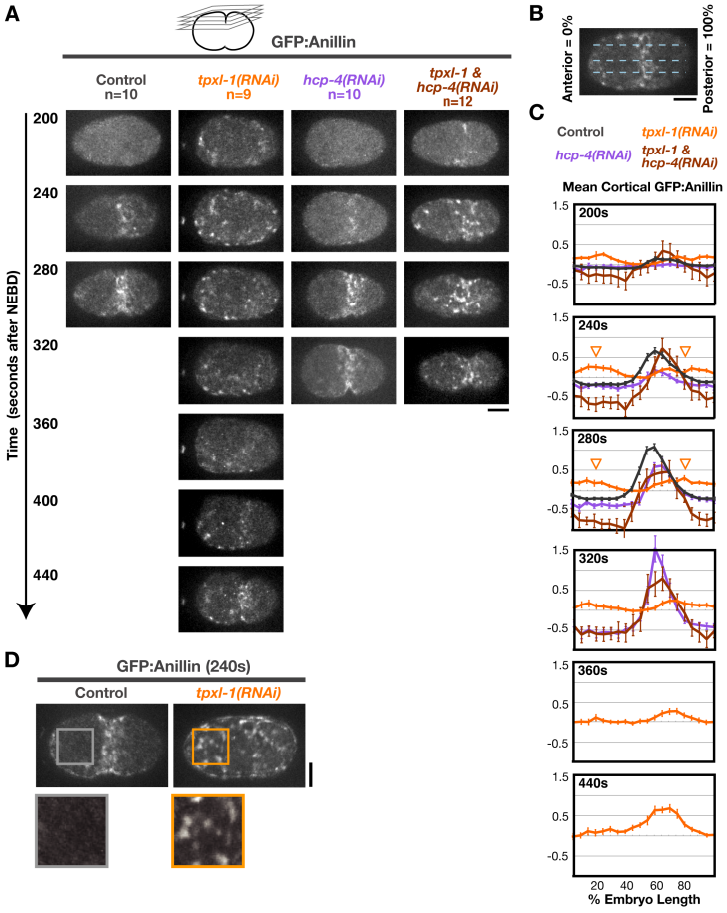

Figure 2.3 Delaying aster separation prevents the equatorial enrichment of contractile ring proteins during the early post anaphase interval.
(A) Images of the cortex in embryos expressing GFP:Anillin. Images are maximum intensity projections of 4 z-sections collected at 1µm intervals (see schematic). (B) Schematic illustrating the method used to analyze cortical GFP:Anillin distribution. A 50 pixel wide line (~1/2 the embryo width) was drawn, and embryos were divided into 20 equal length segments from anterior (0%) to posterior (100%). (C) The mean post-anaphase accumulation of cortical GFP:Anillin is plotted as a function of embryo length. The mean GFP:Anillin in each segment, after subtraction of a background measurement made prior to anaphase onset, is plotted for each timepoint. Values were normalized by dividing by the average maximum value for controls. In TPXL-1 depleted embryos, a slight enrichment of cortical GFP:Anillin is observed on the polar corticies (arrowheads in graphs for 240 and 280s timepoints) relative to the equator. Error bars are SEM. (D) Examples of cortical GFP:Anillin accumulation in control and *tpxl-1(RNAi)* embryos 240 seconds after NEBD. Boxed regions are magnified 2x. Times are in seconds after NEBD. Scale bars are 10 µm.

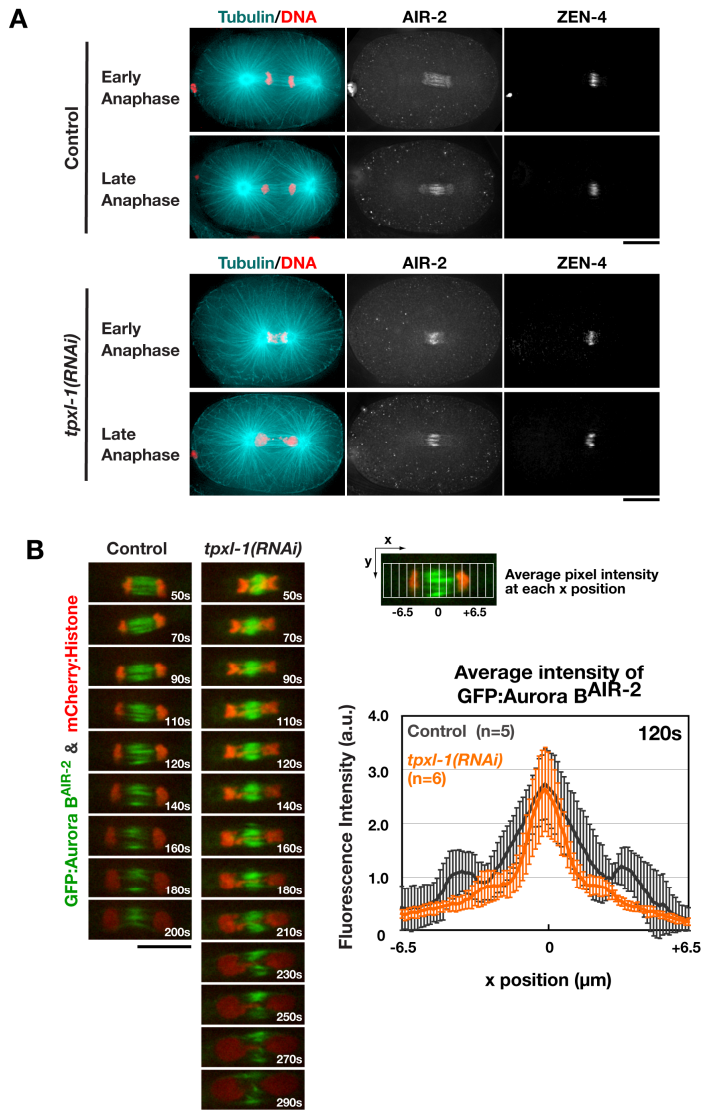

Figure 2.4 TPXL-1 depletion does not significantly alter the localization of midzone-localized signaling complexes.

(A) Fixed control and *tpxl-1(RNAi)* embryos were stained to visualize DNA, α-tubulin, ZEN-4, and AIR-2. 3D widefield data stacks were collected and computationally deconvolved. Maximum intensity projections of the central region of representative early (*top*) and late (*bottom*) anaphase embryos are shown. (B) Single plane confocal images of the spindle in embryos expressing GFP:AuroraB^{AIR-2} and mCherry:Histone H2B. Times are relative to anaphase onset. Graphs show the average GFP:AuroraB^{AIR-2} fluorescence intensity as a function of position along the spindle axis (see diagram) in control and *tpxl-1(RNAi)* embryos 120 seconds after anaphase onset, which corresponds to the time of furrow involution in controls. Values are plotted over the length of the midzone, with the zero position corresponding to the fluorescence intensity maximum. Error bars are the standard deviation. Scale bars are 10 µm.

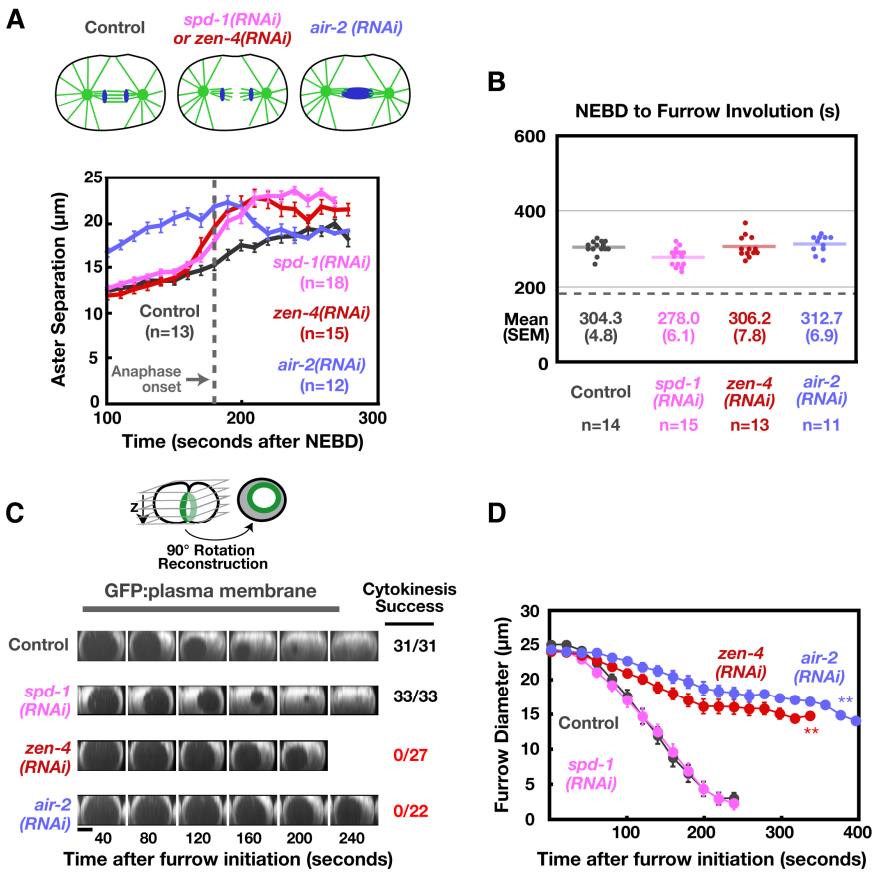

Figure 2.5 Furrows form with normal timing but ingress at a reduced rate following inhibition of centralspindlin or the Chromosomal Passenger Complex.

(A) Schematics summarize the effects of each perturbation on chromosome segregation and anaphase spindle structure. The mean aster-to-aster distance, measured from confocal images of embryos co-expressing GFP:β-tubulin and a GFP plasma membrane probe, is plotted versus time in seconds after NEBD for each condition. The control curve from Fig. 2.1B is reproduced for comparison. Dotted line indicates anaphase onset in controls. Error bars are SEM. (B) The interval between NEBD and furrow involution, measured in embryos co-expressing GFP:β-tubulin and a GFP plasma membrane probe, is plotted for individual embryos. The data for the control embryos is reproduced from Fig. 2.2B for comparison. Solid line indicates the mean. Dashed line indicates the mean time of anaphase onset in controls. (C) Spinning disk confocal optics were used to acquire z-series of control, *spd-1(RNAi)*, *zen-4(RNAi)*, and *air-2(RNAi)* embryos expressing the GFP plasma membrane probe, and reconstructions yielding an "end-on" view of the division plane were generated. Representative projections from timelapse series are shown for each condition. The fraction of embryos that completed the first cytokinesis is indicated to the right. Scale bar is 10 µm. (D) Mean furrow diameter was measured from end on reconstructions generated as in C and is plotted versus time. The control curve is reproduced from Fig. 2.2D for comparison. Times in C and D are in seconds after furrow initiation, the time when the first detectable ingression was visible. Error bars are the 90% confidence interval for the mean. Double asterisks indicate furrow regression.

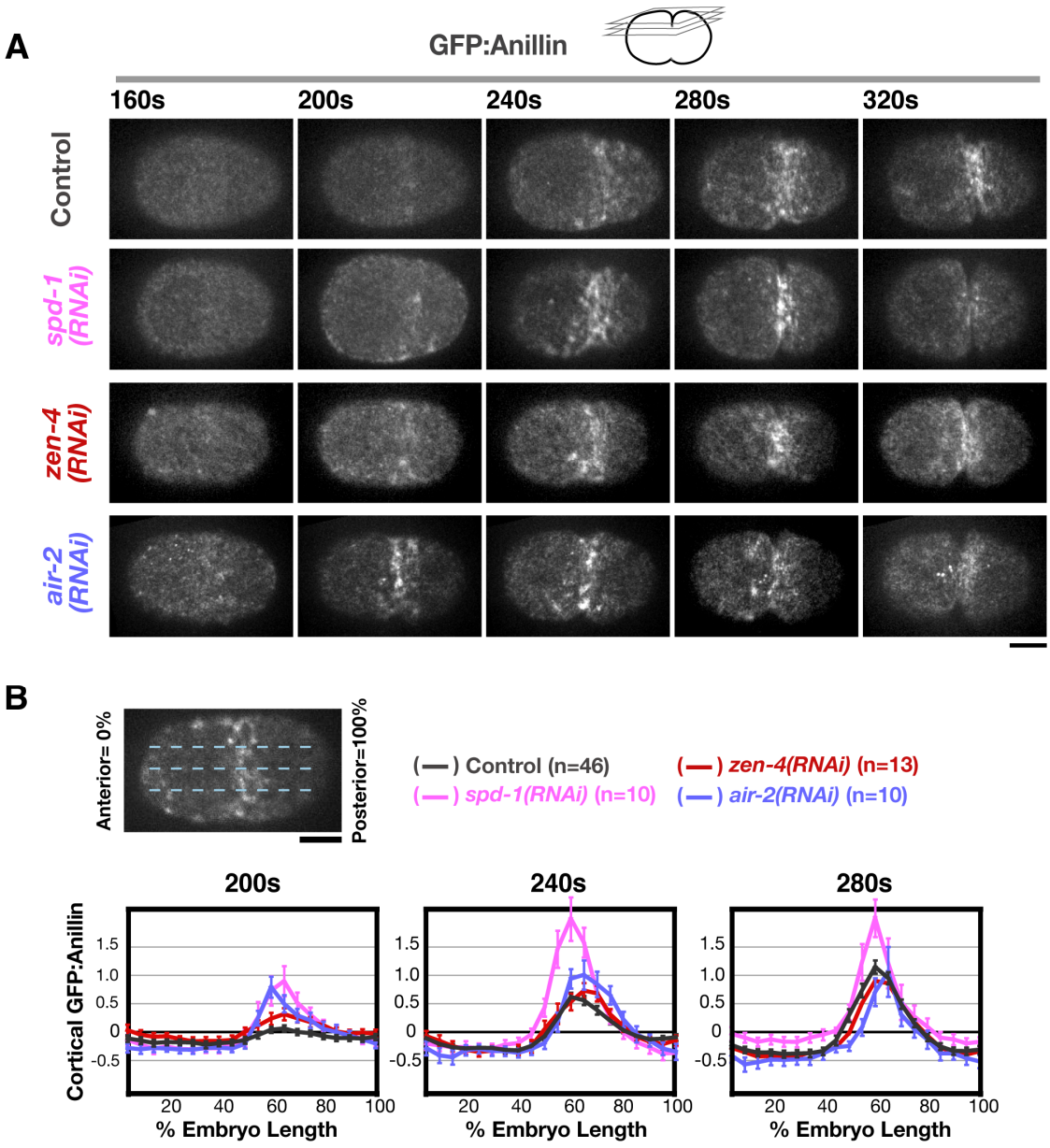

Figure 2.6 GFP:Anillin accumulates on the equatorial cortex with normal timing following depletion of SPD-1, ZEN-4 or AuroraB^{AIR-2}.
(A) Spinning disk confocal optics were used to image the cortex in control (n=46), *spd-1(RNAi)* (n=10), *zen-4(RNAi)* (n=13), and *air-2(RNAi)* (n=10) embryos expressing GFP:Anillin. Images are maximum intensity projections of 4 cortical sections collected at 1µm z intervals. (B) The mean post-anaphase accumulation of cortical GFP:Anillin was quantified as a function of embryo length (as described for Fig. 2.3) for control, *spd-1(RNAi)*, *zen-4(RNAi)*, and *air-2(RNAi)* embryos at the indicated time points after NEBD. Error bars are SEM. Scale bar is 10 µm.

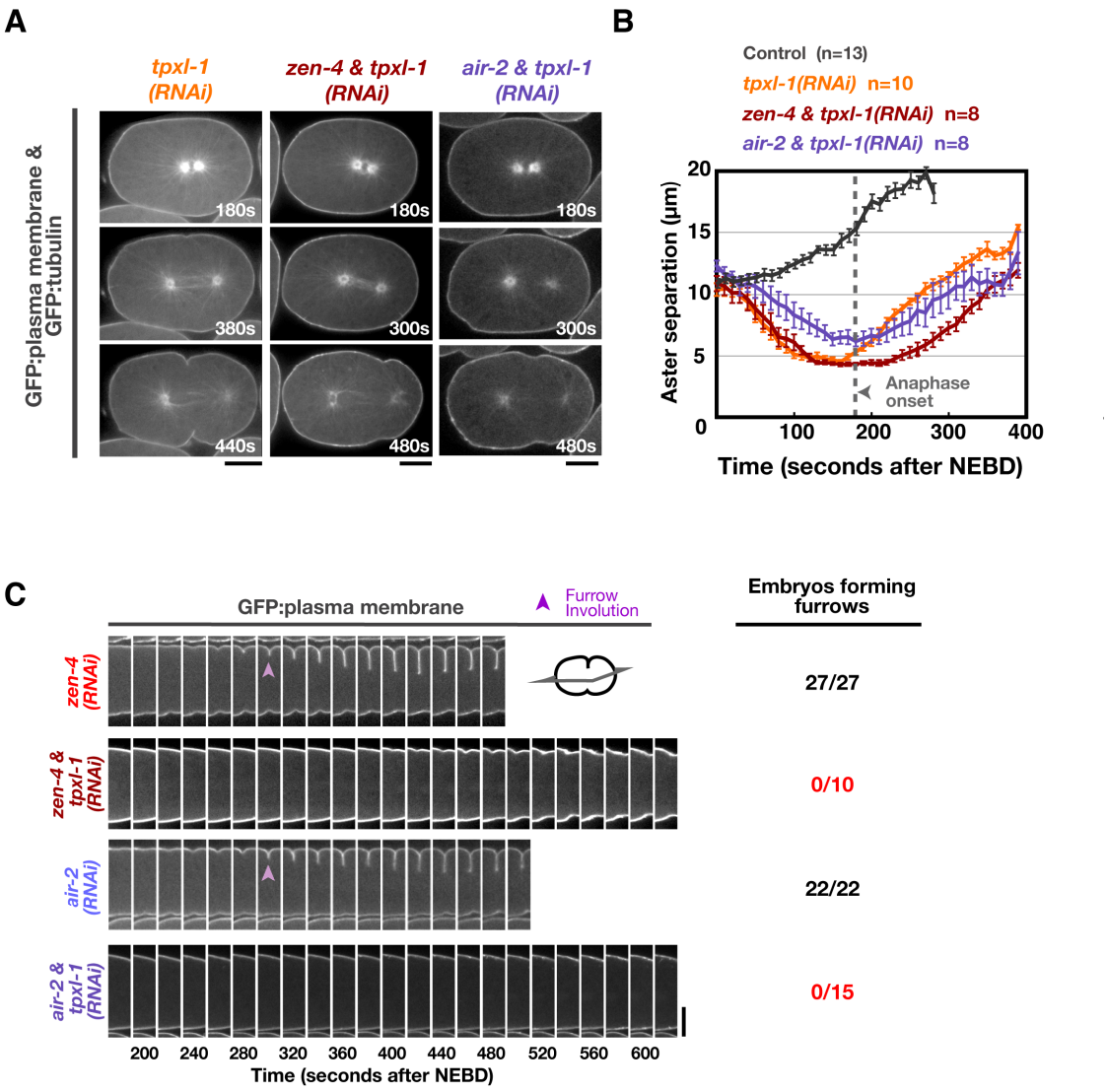

Figure 2.7 Midzone-localized signaling complexes become essential for furrow formation when aster separation is delayed.

(A) Confocal images of *tpxl-1(RNAi)*, *zen-4 & tpxl-1(RNAi),* and *air-2 & tpxl-1(RNAi)* embryos co-expressing GFP:β-tubulin and a GFP plasma membrane probe. (B) The mean aster-to-aster distance, measured from the sequences in A, is plotted versus time in seconds after NEBD for each condition. The control and *tpxl-1(RNAi)* curves from Fig. 2.1B are reproduced here for comparison. Error bars are SEM. (C) Central plane confocal images of embryos expressing a GFP plasma membrane probe. Montages of the equatorial region are shown: furrow involution is indicated (*purple arrowheads*). The number of embryos forming a double membrane furrow is indicated. Times are in seconds after NEBD. Scale bars are 10µm.

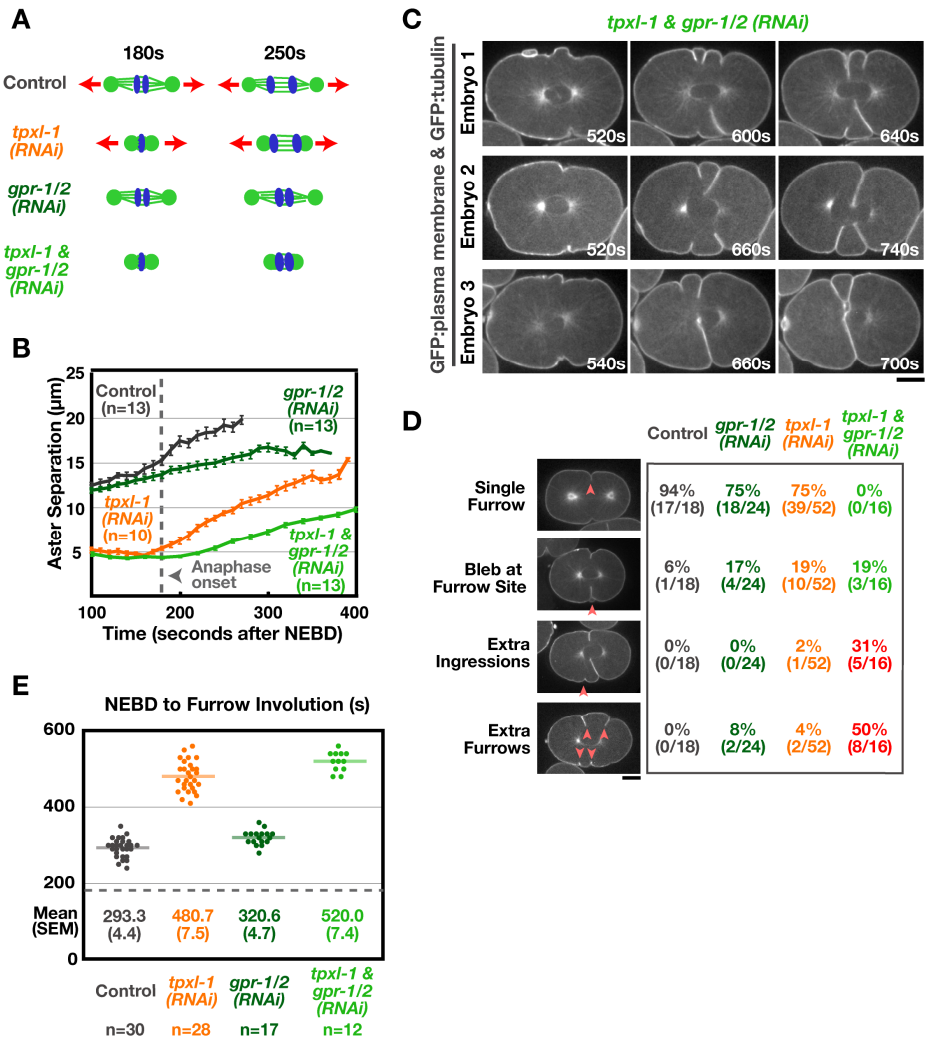

Figure 2.8 Multiple furrows form and simultaneously ingress towards the spindle center when aster separation is prevented.

(A) Schematics illustrating the effects of each perturbation. (B) Mean aster-to-aster distance, measured in confocal images of embryos co-expressing GFP:β-tubulin and a GFP plasma membrane probe, is plotted versus time in seconds after NEBD for *gpr-1/2(RNAi)* and *tpxl-1 & gpr1/2(RNAi)* embryos. The control and *tpxl-1(RNAi)* curves from Fig. 2.1B are reproduced here for comparison. Error bars are SEM. (C) Three examples of *tpxl-1 & gpr-1/2(RNAi)* embryos co-expressing the GFP plasma membrane probe and GFP:β-tubulin. Times are relative to NEBD. (D) Table showing the proportion of embryos exhibiting each phenotype. Red arrowheads indicate extra ingressions or furrows. (E) The interval between NEBD and furrow involution is plotted for individual embryos. The data for the control and *tpxl-1(RNAi)* embryos is reproduced from Fig. 2.2B for comparison. Solid line indicates the mean for each condition. Dashed line indicates mean time of anaphase onset in controls.

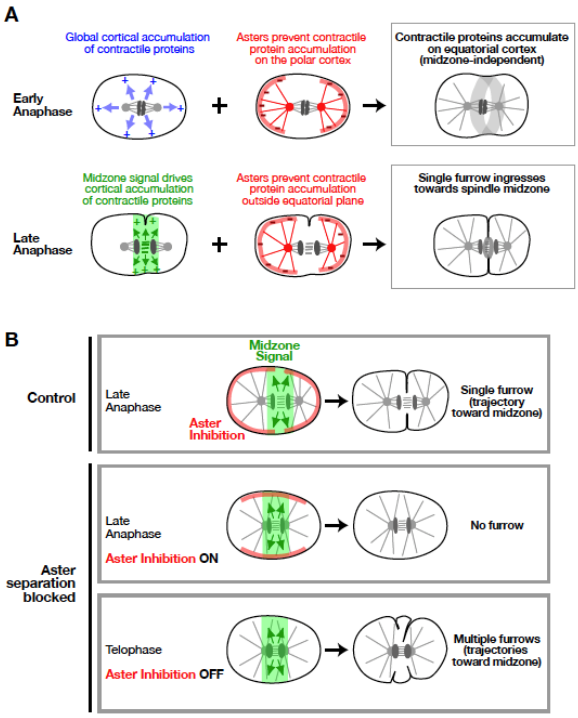

Figure 2.9 Aster-based inhibition makes two distinct contributions to cytokinesis.

(A) Model for the role of aster-based inhibition during cytokinesis. Anaphase onset triggers a rapid global increase in cortical contractility (*blue arrows*; Canman et al., 2000; Foe et al., 2000; Shuster and Burgess, 2002; Straight et al., 2003; Foe and von Dassow, 2008). Aster-based inhibition (*red lines*) prevents the contractile proteins from accumulating on the polar cortex in response to this cell-cycle trigger, leading to their relative enrichment on the equatorial cortex. This mechanism provides an initial midzone-independent signal for furrow formation. As the midzone assembles, it provides a second spatially restricted signal (mediated by Centralspindlin and the CPC; *green arrows*/*zone*) that promotes contractile protein accumulation. Aster-based inhibition prevents the accumulation of contractile proteins outside the equatorial plane in response to the midzone signal, confining furrow formation to a single site. (B) Model to explain the consequences of inhibiting aster separation. In control embryos at late anaphase, aster separation generates a central zone relatively devoid of aster-based inhibition. A signal generated by the spindle midzone (*green arrows*/*zone*), acts on this permissive zone to direct the formation of a single furrow that ingresses along a trajectory towards the spindle center (*control; top row*). When the asters fail to separate, there is no permissive zone, and aster-based inhibition blocks furrow formation by preventing the accumulation of contractile proteins on the equatorial cortex - no furrow forms during the time window when cytokinesis would normally occur (*Aster separation blocked- late anaphase; middle row*). Later, after furrowing has completed in controls, aster based inhibition decays (*Aster separation blocked- telophase; bottom row*), and the midzone acts on the cortex to promote furrow formation in the presence of the unseparated asters. In the absence of aster-based inhibition, the midzone-based signal lacks sufficient positional information to specify a single furrow, and it promotes the simultaneous formation of multiple furrows that ingress towards the spindle center.

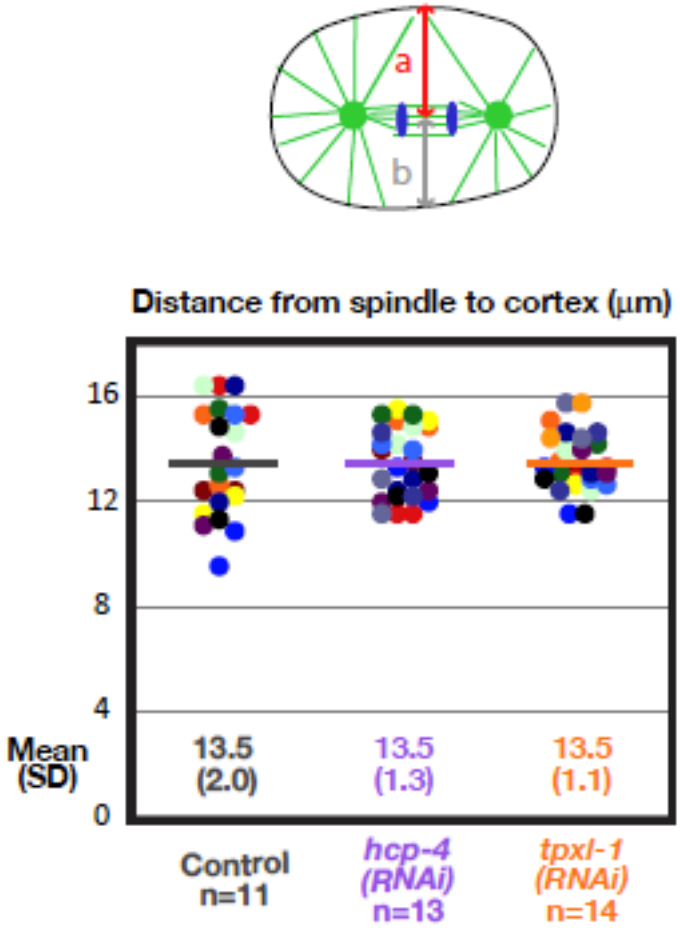

Figure S2.1 The distance from the spindle center to the cortex is not significantly changed by depletion of TPXL-1 or HCP-4.

The distance between the center of the spindle midzone and the cortex was measured 200s after NEBD in single, central plane images of embryos expressing GFP:PH domain and GFP:tubulin. As illustrated in the schematic, 2 measurements, one to the cortex on each side were made for each embryo (see schematic). The 2 measurements made for each embryo are shown in the same color in the distribution plot. The mean and standard deviation are also indicated for each condition.

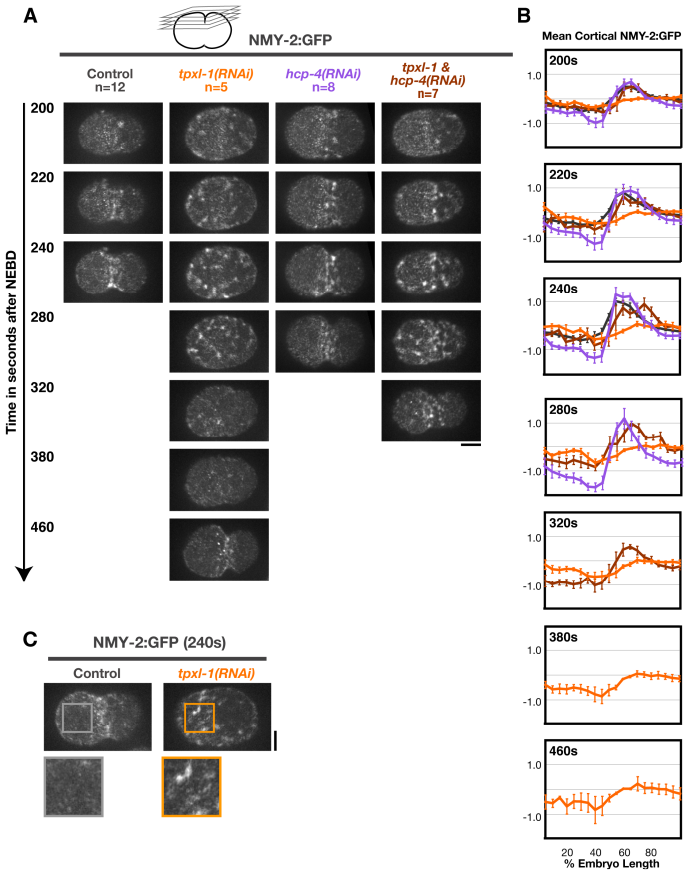

Figure S2.2 Delaying aster separation disrupts the early patterning of myosin II^{NMY-2} on the equatorial cortex.

(A) Confocal optics were used to image the cortex in embryos expressing NMY-2:GFP. Images are maximum intensity projections of 4 z-sections collected at 1µm intervals. During cytokinesis, NMY-2:GFP accumulates at the cell equator in a manner similar to GFP:Anillin. Delaying aster separation leads to the ectopic accumulation NMY-2:GFP on the polar corticies. A normal pattern of NMY-2:GFP accumulation is restored by co-depletion of HCP-4 along with TPXL-1. One difference between the localization patterns of NMY-2:GFP and GFP:Anillin is that prior to anaphase onset, cortical NMY-2 is present in an anterior cap that contributes to the polarity maintenance (Guo and Kemphues 1996; Shelton, Carter et al. 1999; Severson and Bowerman 2003; Munro 2004), whereas Anillin is not. In the early post-anaphase interval, this anterior cap localization is super-imposed with its accumulation at the cell equator. Times are in seconds after NEBD. (B) The mean post-anaphase accumulation of cortical NMY-2:GFP is plotted as a function of embryo length. The mean NMY-2:GFP in each segment, after subtraction of a background measurement made prior to anaphase onset, is plotted for each timepoint. Values were normalized by dividing by the average maximum value for controls. We note that although NMY-2:GFP accumulates with similar timing, the equatorial band of NMY-2:GFP remains detectable for slightly longer in embryos depleted of HCP-4 or co-depleted of TPXL-1 & HCP-4 than in controls due to the ~1 minute delay in furrow involution caused by HCP-4 depletion. Error bars are SEM. (C) Examples of cortical NMY-2:GFP accumulation in control and *tpxl-1(RNAi)* embryos 240 seconds after NEBD. Boxed regions are magnified 2x. Scale bars are 10 µm.

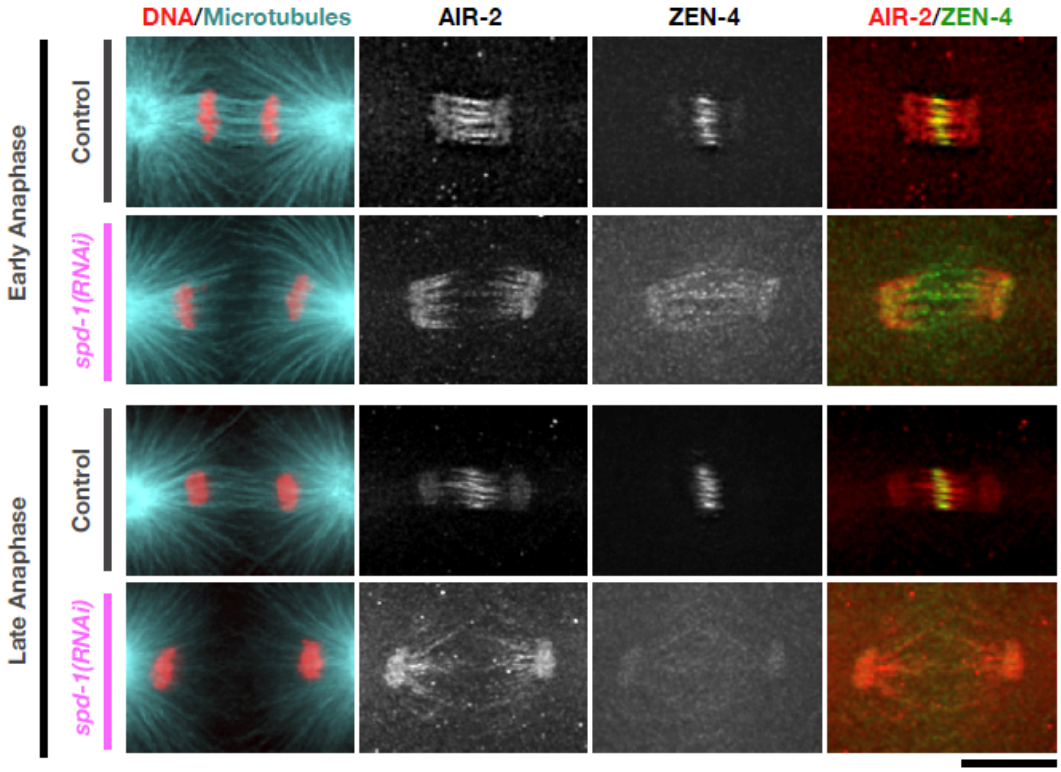

Figure S2.3 Localization of Centralspindlin and the CPC to microtubules in the midzone region in SPD-1 depleted embryos.

Fixed control (n>30) and *spd-1(RNAi)* (n=20) embryos were stained for DNA, α-tubulin, ZEN-4, and AuroraB^{AIR-2}. 3D widefield data stacks were collected and computationally deconvolved. Equivalently scaled maximum intensity projections of the central region of representative early (*top two rows*) and late (*bottom two rows*) anaphase embryos are shown. Embryos were staged based on spindle pole morphology, which changes in a reproducible way during this transition. Scale bar is 5 μm.

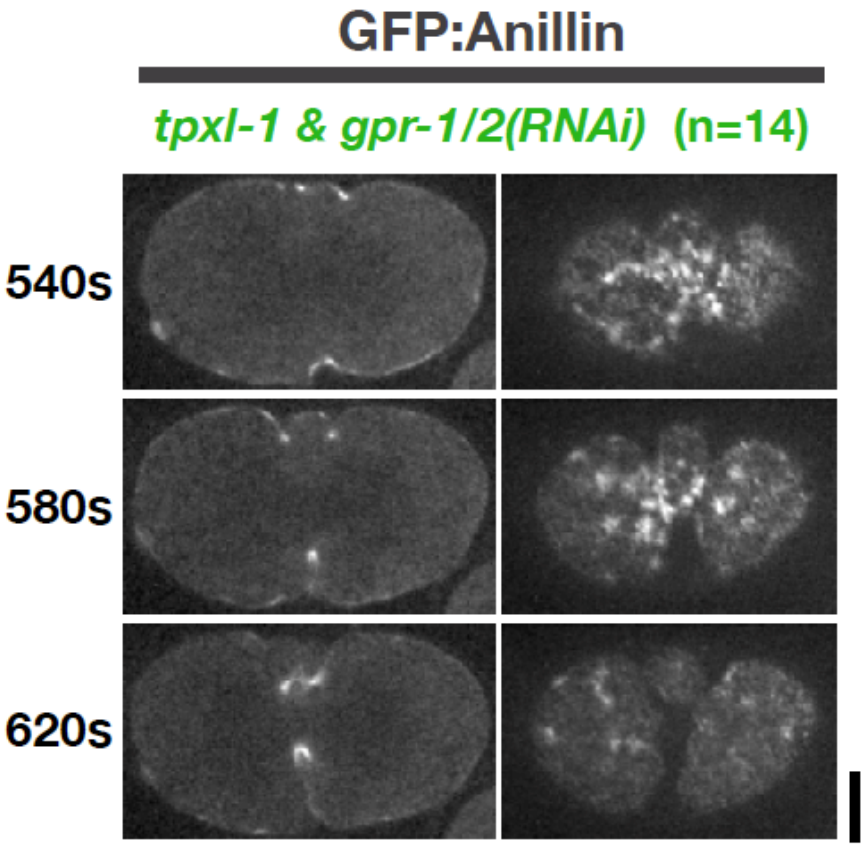

Figure S2.4 The equatorial accumulation of GFP:Anillin occurs over a substantially broader region when aster separation is prevented by co-depletion of TPXL-1 & GPR-1/2.

Central plane (left) and cortical (right) images of a *tpxl-1 & gpr-1/2(RNAi)* embryo expressing GFP:Anillin. After furrow formation, GFP:Anillin is enriched at the tips of the ingressing furrows. Times are in seconds after NEBD. Scale bar is 10 μm.

Table 2.1 Worm strains used in this study

Strain #	Genotype
N2	Ancestral N2 Bristol strain
OD38	unc-119(ed3) III; ltIs28 [pASM14; pie-1/GFP-TEV-STag::ani-1; unc-119 (+)]
OD58	unc-119(ed3) III; ltIs38 [pAA1; pie-1/GFP::PH(PLC1delta1); unc-119 (+)]
OD73	unc-119(ed3) III; ltIs38 [pAA1; pie-1/GFP::PH(PLC1delta1); unc-119 (+)]; ltIs24 [pAZ132; pie-1/GFP::tba-2; unc-119 (+)])
OD224	unc-119(ed3) III; ltIs37 [pAA64; pie-1/mCHERRY::his-58; unc-119 (+)]; ltIs14 [pASM05; pie-1/GFP-TEV-STag::air-2; unc-119 (+)] IV
JJ1473	unc-119(ed3) III; zuIs45[nmy-2::NMY-2::GFP; unc-119(+)] V

Table 2.2 dsRNAs used in this study

Gene	Oligo 1	Oligo 2	Template	Conc. mg/ml
Y39G10AR.12 (*tpxl-1*)	TAATACGACTCACTATAGGACGTCGGTGAGCAAATTGAC	AATTAACCCTCACTAAAGGTGTACACATATGATGGCACAGG	yk596b10	1.05
T03F1.9 (*hcp-4*)	AATTAACCCTCACTAAAGGGGAAATGTACGGAGCGAAAA	TAATACGACTCACTATAGGACATTGTTGGTGGGTCCAAT	N2 genomic	1.36
C38C10.4 (*gpr-2*, also targets *gpr-1*)	TAATACGACTCACTATAGGAGCATGTGATTCCACACGTC	AATTAACCCTCACTAAAGGTCTGGCAGCAGACAGTTCAG	N2 genomic	2.27
M03D4.1 (*zen-4*)	AATTAACCCTCACTAAAGGAATTGGTTATGGCTCCGAGA	TAATACGACTCACTATAGGATTGGAGCTGTTGGATGAGC	yk35d10	1.28
Y34D9A.4 (*spd-1*)	TAATACGACTCACTATAGGTCGTTGACGCGTACTCAACT	AATTAACCCTCACTAAAGGGAATTCGAAATCCGACTCCA	N2 genomic	3.11
B0207.4 (*air-2*)	AATTAACCCTCACTAAAGGTTTCGAGATCGGAAGACCAC	TAATACGACTCACTATAGGCAACGACAAGCAATCTTCCA	yk483g8	1.49
CTF13 (*S. cerevisiae gene*)	TAATACGACTCACTATAGGTGTGGAGCTTCCAGGAAAAC	AATTAACCCTCACTAAAGGCTCGATGTTCCACCACTTGA	*S. cerevisiae* genomic	1.84

Chapter 3: Inhibition of Rac by the GAP Activity of Centralspindlin is Essential for Cytokinesis

3.1 Summary

During cytokinesis, the GTPase RhoA orchestrates contractile ring assembly and constriction. RhoA signaling is controlled by the central spindle—a set of microtubule bundles that forms between the separating chromosomes. Centralspindlin, a protein complex consisting of the kinesin-6 ZEN-4, and the Rho family GAP CYK-4, is required for central spindle assembly and cytokinesis. However, the importance of the CYK-4 GAP activity and whether it regulates RhoA remain unclear. Here, we found that two separation-of-function mutations in the GAP domain of *C. elegans* CYK-4 lead to cytokinesis defects that mimic centralspindlin loss-of-function. These defects could be rescued by depletion of Rac or its effectors, but not RhoA. Thus, inactivation of Rac by centralspindlin functions in parallel with RhoA activation to drive contractile ring constriction during cytokinesis.

3.2 Introduction

Cytokinesis completes mitosis, partitioning a single cell into two. To coordinate cell division with chromosome segregation, the mitotic apparatus

directs the assembly and constriction of a contractile ring composed of filamentous actin and myosin II that physically divides the cell (Glotzer 2005). Understanding how the mitotic apparatus communicates with the cell cortex during cytokinesis is a major current challenge. One critical mediator of this signaling is the small GTPase RhoA (Glotzer 2004; Bement, Benink et al. 2005; Glotzer 2005). RhoA signaling is thought to be controlled by an array of anti-parallel microtubule bundles, called the central spindle, that forms between the separating chromosomes during anaphase (Glotzer 2005). Consistent with a central role in cytokinesis, RhoA and its activating GEF (Guanine nucleotide Exchange Factor) ECT-2 are essential for contractile ring assembly and constriction (Yuce 2005; Kamijo, Ohara et al. 2006; Nishimura 2006).

3.3 Results

Centralspindlin, a conserved heterotetrameric complex consisting of two molecules of kinesin-6 (ZEN-4 in *C. elegans*) and two molecules of a protein containing a GTPase activating (GAP) domain (CYK-4 in *C. elegans*), is critical for central spindle assembly and cytokinesis (Mishima, Kaitna et al. 2002; Glotzer 2005). The current dominant model proposes that centralspindlin targets the ECT-2 GEF to the central spindle, thereby contributing to the equatorial activation of RhoA (Somers and Saint 2003; Yuce 2005; Nishimura 2006). Formation of the heterotetrameric

centralspindlin complex requires an interaction between the N-terminal region of CYK-4 and the central region of ZEN-4 (Fig. 3.1A; Mishima, Kaitna et al. 2002; Pavicic-Kaltenbrunner, Mishima et al. 2007). Mutant forms of CYK-4 and ZEN-4 that disrupt centralspindlin assembly lead to a phenotype similar to that resulting from depletion of centralspindlin subunits by RNAi (Fig. 3.1C,D)—failure to form a central spindle accompanied by a defect in contractile ring constriction (Powers, Bossinger et al. 1998; Raich, Moran et al. 1998; Jantsch-Plunger, Gonczy et al. 2000; Severson, Hamill et al. 2000).

The conserved GAP domain in the CYK-4 C-terminus is predicted to inactivate Rho family GTPases (Fig. 3.1A; Jantsch-Plunger, Gonczy et al. 2000). However, the role of the CYK-4 GAP domain in cytokinesis and the identity of the Rho family GTPase that it targets are unknown (Jantsch-Plunger, Gonczy et al. 2000; Minoshima, Kawashima et al. 2003; D'Avino, Savoian et al. 2004; Yamada, Hikida et al. 2006). In vitro, the GAP domains of CYK-4 and its homologs are active towards all three subclasses of Rho family GTPases: RhoA, Rac, and CDC-42 (Toure, Dorseuil et al. 1998; Jantsch-Plunger, Gonczy et al. 2000; Kawashima, Hirose et al. 2000). It has been assumed that the CYK-4 GAP activity acts on RhoA because it is the only Rho family member essential for cytokinesis (Toure, Dorseuil et al. 1998; Jantsch-Plunger, Gonczy et al. 2000; Kawashima, Hirose et al. 2000). CYK-4 has been proposed to either promote RhoA cycling (Bement, Miller et al. 2006) or to inactivate RhoA after cytokinesis during contractile ring disassembly

(Glotzer 2005). It is also possible that RhoA is not the critical target of the CYK-4 GAP domain. Supporting this hypothesis, haplo-insufficiency of Rac can suppress the rough-eye phenotype induced by RNAi of the *Drosophila* CYK-4 homolog (D'Avino, Savoian et al. 2004). Although cytokinesis was not examined, this result indicates that in some contexts CYK-4 may oppose Rac activation.

To study the role of the CYK-4 GAP domain in cytokinesis (Methods can be found in supplementary online material), we characterized two conditional *C. elegans* alleles that lead to residue substitutions within the GAP domain (Encalada, Martin et al. 2000)—a Glu to Lys change at residue 448 (CYK-4$^{GAP(E448K)}$) and a Thr to Ile change at residue 546 (CYK-4$^{GAP(T546I)}$), respectively (Fig. 3.1A, B). Based on the X-ray structure of the human CYK-4 homolog (PDBID: 2OVJ), the charge reversal resulting from the Glu to Lys substitution would disrupt a network of salt-bridge and hydrogen-bond interactions that positions the arginine-finger (Arg 459), a conserved residue essential for GAP activity (Fig. 3.1B; Ahmed, Lee et al. 1994; Rittinger, Walker et al. 1997; Kawashima, Hirose et al. 2000). Although the effects of the Thr to Ile substitution are less clear, the larger isoleucine side chain may clash with surrounding residues and also interfere with arginine-finger positioning. Both alleles are strictly recessive (Fig. S3.1), temperature-sensitive, and fast-inactivating—showing a fully penetrant cytokinesis defect within one minute of

shifting to the restrictive temperature. Thus, these are loss-of-function alleles affecting the CYK-4 GAP domain.

We used quantitative live-imaging assays to characterize cytokinesis in the CYK-4 GAP mutant embryos. Although no obvious defects were evident during the initial stages of contractile ring assembly (Fig. S3.2B,C), the GAP mutants exhibited a severe defect in contractile ring constriction. The constriction rate was ~3 fold slower than that in control embryos, and cleavage furrows only ingressed to ~50% of the initial cell diameter before regressing. This ingression defect mimicked that in the centralspindlin-assembly mutants and in embryos depleted of CYK-4 by RNAi (Fig. 3.1C,D; S3.3; Movie S1; Severson, Hamill et al. 2000). Thus, the CYK-4 GAP domain is fundamental to the role of centralspindlin in promoting contractile ring constriction.

Because centralspindlin is also required for assembly of the central spindle (Powers, Bossinger et al. 1998; Raich, Moran et al. 1998; Jantsch-Plunger, Gonczy et al. 2000), we next examined central spindle structure in the GAP mutant embryos. In contrast to the absence of a central spindle following depletion of the kinesin-6 ZEN-4, there were no clear defects in central spindle organization or ZEN-4 targeting in the GAP mutants (Fig. 3.2A). The recruitment of a GFP fusion with AuroraB^{AIR-2} kinase (the enzymatic component of the Chromosomal Passenger Complex) to the central spindle was also not affected in the GAP mutants (Fig. 3.2B; Movie S2). Disrupting central spindle structure in *C. elegans* embryos leads to abrupt

centrosome separation following anaphase onset (Oegema, Desai et al. 2001). This phenotype was not observed in the CYK-4 GAP mutants confirming a mechanically intact central spindle (Fig. 3.2C). Thus, CYK-$4^{GAP(E448K)}$ and CYK-$4^{GAP(T546I)}$ are separation-of-function mutants that uncouple the role of CYK-4 in contractile ring constriction from its role in central spindle assembly.

CYK-4 GAP activity is expected to down-regulate a Rho family GTPase, therefore RNAi-mediated depletion of the target GTPase should rescue the cytokinesis defect in CYK-4 GAP mutant embryos. There are five Rho family members in *C. elegans*: $RhoA^{RHO-1}$, Rac^{CED-10}, Rac^{RAC-2}, $RhoG^{MIG-2}$, and CDC-42 (Lundquist 2006). Because $RhoA^{RHO-1}$ depletion results in a cytokinesis defect on its own (Toure, Dorseuil et al. 1998; Jantsch-Plunger, Gonczy et al. 2000; Kawashima, Hirose et al. 2000), we tested if partial depletion of $RhoA^{RHO-1}$ or its activating ECT-2 GEF could suppress the GAP mutant phenotype. Instead of suppressing, partial depletion of either $RhoA^{RHO-1}$ or ECT-2 enhanced the CYK-$4^{GAP(E448K)}$ cytokinesis defect, suggesting that $RhoA^{RHO-1}$ is not the main target of CYK-4 GAP activity (Fig. 3.3A,B; Fig. S3.4A).

Unlike depletion of $RhoA^{RHO-1}$, RNAi of the other Rho family members does not affect cytokinesis in control embryos (Fig. 3.3C). RNAi of CDC-42 or $RhoG^{MIG-2}$ also did not ameliorate the CYK-$4^{GAP(E448K)}$ cytokinesis phenotype (Fig. 3.3D). However, RNAi of Rac^{CED-10} or Rac^{RAC-2} led to substantial rescue,

allowing 70% and 24%, respectively, of CYK-4$^{GAP(E448K)}$ embryos to successfully complete the first cytokinesis (Fig. 3.3A,D). Simultaneous RNAi of Rac^{CED-10} and Rac^{RAC-2} did not increase the efficiency of rescue over RNAi of Rac^{CED-10} alone (Fig. S3.4D). These results indicate that CYK-4 GAP activity promotes furrow ingression by down-regulating Rac. Consistent with a role for CYK-4 in Rac inactivation, over-expressing a GAP-dead CYK-4 mutant in dividing mammalian cells was previously found to increase the level of active Rac at the cell equator (Yoshizaki, Ohba et al. 2003).

If CYK-4 GAP activity is critical for the role of centralspindlin in contractile ring constriction, Rac^{CED-10} depletion should also rescue the furrow ingression defect resulting from inhibiting centralspindlin assembly. Indeed, 85% of furrows in ZEN-4$^{CSA(D520N)}$ embryos ingressed fully when Rac^{CED-10} was depleted (Fig. S3.4B). However, Rac^{CED-10} depletion was less efficient in rescuing cytokinesis completion in the ZEN-4$^{CSA(D520N)}$ mutant compared to the CYK-4 GAP mutant (Fig. S3.4B). This result suggests an additional role for either centralspindlin or the central spindle in the completion of cytokinesis that is independent of the GAP activity. Importantly, Rac^{CED-10} depletion had no effect on furrow ingression in AuroraB$^{AIR-2(P265L)}$ embryos which have a similar spectrum of defects in central spindle assembly and furrow ingression to that resulting from centralspindlin disruption (Fig. S3.4C; Severson, Hamill et al. 2000), confirming the specificity of the rescue.

Why is inhibition of Rac signaling important for contractile ring constriction? Rac promotes activation of the Arp2/3 complex via its effectors WASp^{WSP-1} and WAVE^{WVE-1}, resulting in the formation of a branched meshwork of short cross-linked actin filaments (Pollard 2007). Possibly, these Rac effectors interfere with actin filaments nucleated by the cytokinesis formin, CYK-1, which function with myosin II to drive cytokinesis. To test this idea, we determined whether depletion of WASp^{WSP-1}/WAVE^{WVE-1} or the Arp2/3 complex could also rescue the CYK-4$^{GAP(E448K)}$ cytokinesis defect (Fig. 3.4A,B; Severson, Baillie et al. 2002; Withee, Galligan et al. 2004). Although their individual depletions did not dramatically suppress the CYK-4$^{GAP(E448K)}$ cytokinesis defect, co-depletion of WASp^{WSP-1} and WAVE^{WVE-1} led to significant rescue (Fig 3.4A)—69% of furrows ingressed fully and 38% of embryos successfully completed cytokinesis (Fig 3.4A). RNAi of Arp2^{ARX-2} also significantly suppressed the CYK-4$^{GAP(E448K)}$ cytokinesis defect, with 74% of furrows ingressing fully and 52% of embryos completing division (Fig. 3.4B). Thus, cytokinesis depends on CYK-4 GAP to inactivate Rac, thereby reducing activation of the Arp2/3 complex via WASp and WAVE. Active Arp2/3 complex in the furrow region may disrupt contractile ring constriction by branching formin-nucleated actin filaments. Alternatively, active Arp2/3 complex could nucleate the formation of an independent branched actin network that competes for essential contractile ring components or presents a structural barrier to furrow ingression.

3.4 Discussion

We have uncovered a negative regulation cascade that is essential for successful cytokinesis. Although negative regulation has been proposed to be important during cytokinesis, previous models have emphasized inhibition of cortical contractility by astral microtubules that contact the polar regions of the cell (Dechant and Glotzer 2003; Rappaport 1997). A requirement for negative regulation of an inhibitory pathway at the cell equator has not been widely considered. Our findings lead to a model in which inactivation of Rac by CYK-4 GAP functions in parallel with activation of RhoA to drive contractile ring constriction during cytokinesis (Fig. S3.7).

3.5 Materials and Methods

3.5.1 Mutant cloning and rescue experiments

The *cyk-4(or570ts)* and *cyk-4(or749ts)* (CYK-4$^{GAP(T546I)}$ and CYK-4$^{GAP(E448K),}$ respectively) mutants were isolated in EMS and ENU mutagenesis screens, respectively, for conditional (temperature-sensitive) embryonic-lethal mutants as described (Kemphues, Priess et al. 1988; Encalada, Martin et al. 2000). The mutations were mapped to LG::III using strains *MT3751* and *MT464*. Mutations were identified by sequencing, after refining their location by 3-factor visible marker mapping as described (Fay 2006) using strains

DR104 and *CB2053* for *cyk-4(or570ts*) and *cyk-4(or749ts)* respectively. To confirm that the *cyk-4* mutations were the cause of the cytokinesis defect, we rescued the embryonic lethality by expression of a GFP fusion with CYK-4. To test for rescue, the *cyk-4(or570ts)* and *cyk-4(or749ts)* mutants were crossed with *WH0279* non-Unc hermaphrodites. First, *cyk-4(or749ts)* and *cyk-4(or570ts)* were linked to *unc-119(ed3)* and homozygosed then, *ojIs12[cyk-4::GFP unc-119(+)]*/+ (which is lethal when homozygous) progeny were screened for the ability to rescue embryonic lethality at restrictive temperature. Both *cyk-4(or570ts)* and *cyk-4(or749ts)* were back-crossed six times prior to mating into fluorescent protein expressing strains for phenotypic analysis (*him-8(e1489)* first cross, N2 remaining out-crosses). All analysis was done in non-Him strains to avoid possible phenotypic complications.

3.5.2 Temperature control

Strains were maintained at the permissive temperature of 16ºC. For all live imaging experiments, the temperature was controlled by heating the room to 26ºC for at least one hour prior to filming or until the microscope temperature reached 26ºC. Embryos were maintained at 16ºC until immediately prior to filming. The temperature was continuously monitored during filming using a thermometer probe wedged into the microscope body near the stage. For some experiments, a heated stage was also used (20/20 Technology Inc, Wilmington, NC).

3.5.3 Imaging and quantitative analysis

Live imaging was performed on newly fertilized embryos mounted on agarose pads as previously described (Gonczy, Schnabel et al. 1999). Embryos were filmed using a spinning disk confocal as described (Audhya, Hyndman et al. 2005) using a 60x, 1.4 NA PlanApochromat lens with 2x2 binning. For all movies, Differential Interference Contrast (DIC) images and/or images of an $RFP^{mCherry}$ fusion with histone H2B were collected in parallel to monitor cell cycle progression. The rate of furrow ingression was measured in strains expressing a GFP labeled plasma membrane probe. A z-series consisting of 14 or 15 planes at 2.5μm intervals was collected every 20s and the data from the equatorial region of the embryo was isolated, rotated by 90^{o}, and projected to generate an "end on" view that was used to measure furrow diameter. To test for suppression of the mutant phenotype, central plane images of mutant embryos depleted of the indicated protein by RNAi were collected at 10s intervals. GFP::$AuroraB^{AIR-2}$ was imaged by collecting 5 z-planes at 1.5 μm intervals every 10s.

NMY-2::GFP (Myosin II heavy chain) was imaged by acquiring 4 z-planes at 1 μm intervals at the cell cortex, followed by a single central plane image every 10s. Analysis of the post-anaphase accumulation of cortical NMY-2::GFP as a function of embryo length was performed on maximum-intensity projections of the cortical z-series. A line bisecting the embryo was drawn from the anterior to the posterior tip of the embryo, and MetaMorph

software (Molecular Devices, Downingtown, PA) was used to generate an average intensity line scan (50 pixels wide ~1/2 of the width of the embryo) for each time point. Embryos were divided into 20 equal length segments from anterior (0% embryo length) to posterior (100% embryo length), and the mean NMY-2::GFP in each segment was calculated for each time point, after subtraction of a background measurement for that segment made just prior to anaphase onset. The values for each data set were normalized by dividing all intensity values by the average maximum value for controls (55-65% embryo width). The amount of NMY-2::GFP in the contractile ring at the leading edge of the ingressing furrow was quantified using the central plane images as outlined in Fig. S3.3A.

3.5.4 Immunofluoresence and imaging fixed embryos

Methanol fixation was performed as described (Oegema, Desai et al. 2001) on worms that were pre-shifted to restrictive temperature for 1-2 hours, and dissection was done in a 26ºC room. Images were acquired as described (Cheeseman, Niessen et al. 2004) using a Deltavision microscope equipped with a 100x Plan Apo 1.35 N.A. objective. All antibodies were used at a concentration of 1µg/ml.

3.5.5 RNAi

dsRNA was made as described (Oegema, Desai et al. 2001). After injection, worms were allowed to recover for 44-50 hrs at 16℃ prior to filming unless the dsRNA led to sterility in which case the worms were allowed to recover for 12-15 hrs (*ect-2*), 22-24 hrs (*cyk-4*), and 36-38 hrs (*rho-1*), respectively.

3.6 Acknowledgements

We thank all members of the Oegema, Desai, and Bowerman labs. We thank A. Maddox, J. Dumont, and R. Green for reading this manuscript; J. Dumont for making dsRNAs; Y. Kohara for cDNA clones; and the CGC for strains. J.C.C. was funded by the JCC-MF and by the LLS. L.L. was supported by the NIH/NIGMS (T32 GM008666) and by the NCI. K.O. and A.D. were funded by the LICR. B.B. was funded by the NIH (GM058017).

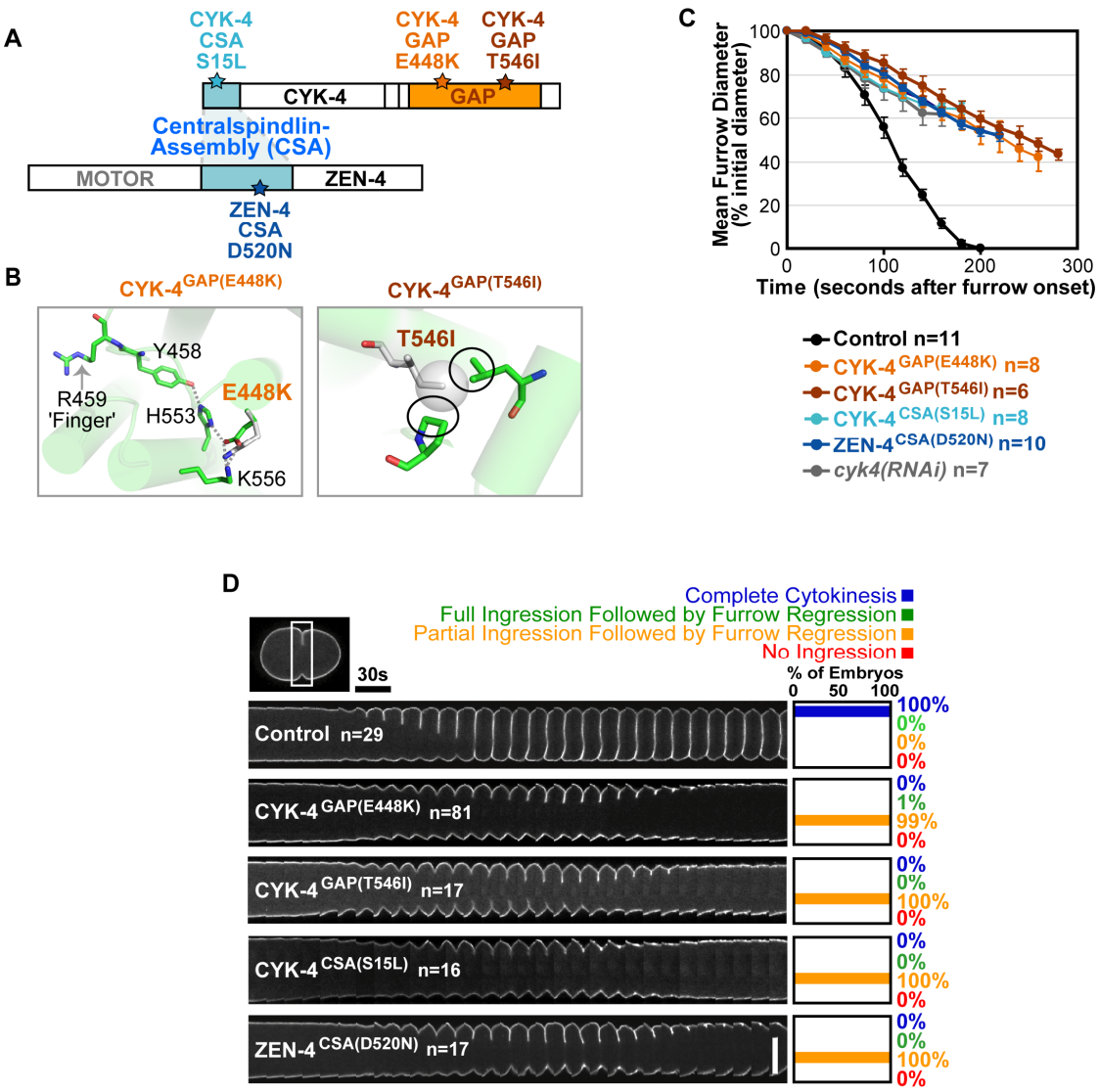

Figure 3.1 CYK-4 GAP domain mutants phenocopy centralspindlin loss-of function.

A) Residues changed in CYK-4 and ZEN-4 mutant proteins. B) The E448K and T546I substitutions destabilize CYK-4 GAP domain structure. C) Plot of mean furrow diameter versus time. Error bars=SEM. D) Time-lapse montage of the furrow region in embryos expressing a GFP::plasma membrane marker. Series begin at anaphase onset. Scale bar, 20μm.

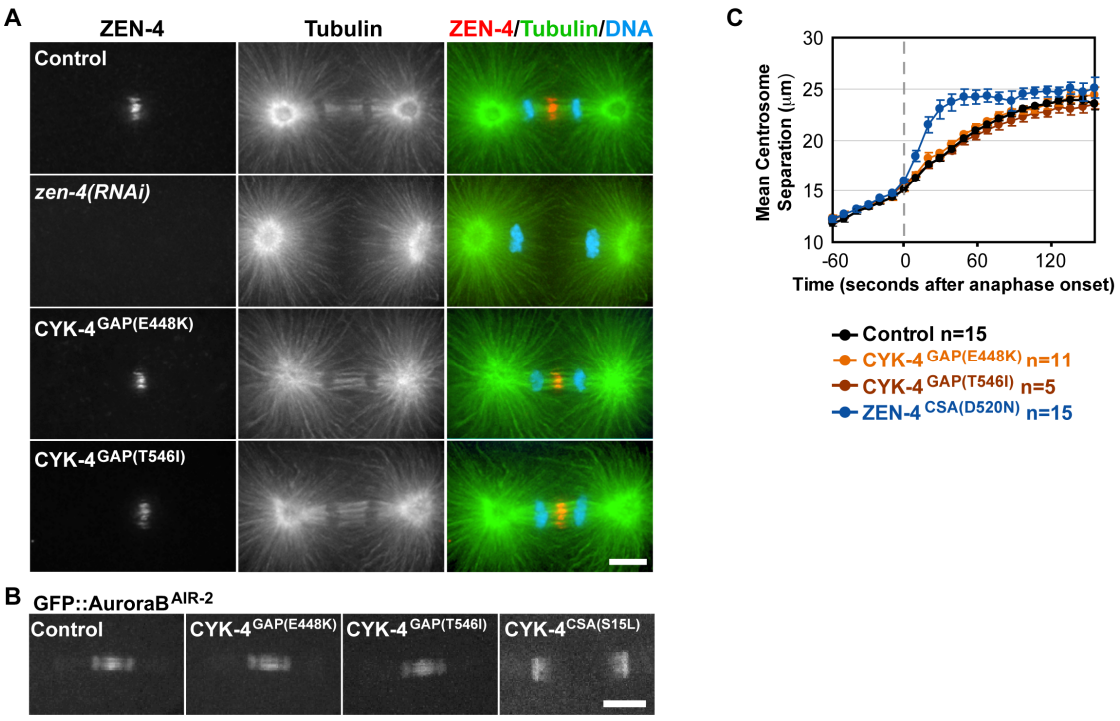

Figure 3.2 Central spindle assembly is not disrupted in the GAP mutants. A) Immunofluorescence staining for tubulin, ZEN-4, and DNA. B) Images of GFP::AuroraB^{AIR-2} 40s post-anaphase onset. C) Plot of mean centrosome separation verses time. Error bars=SEM. Scale bars, 10 μm.

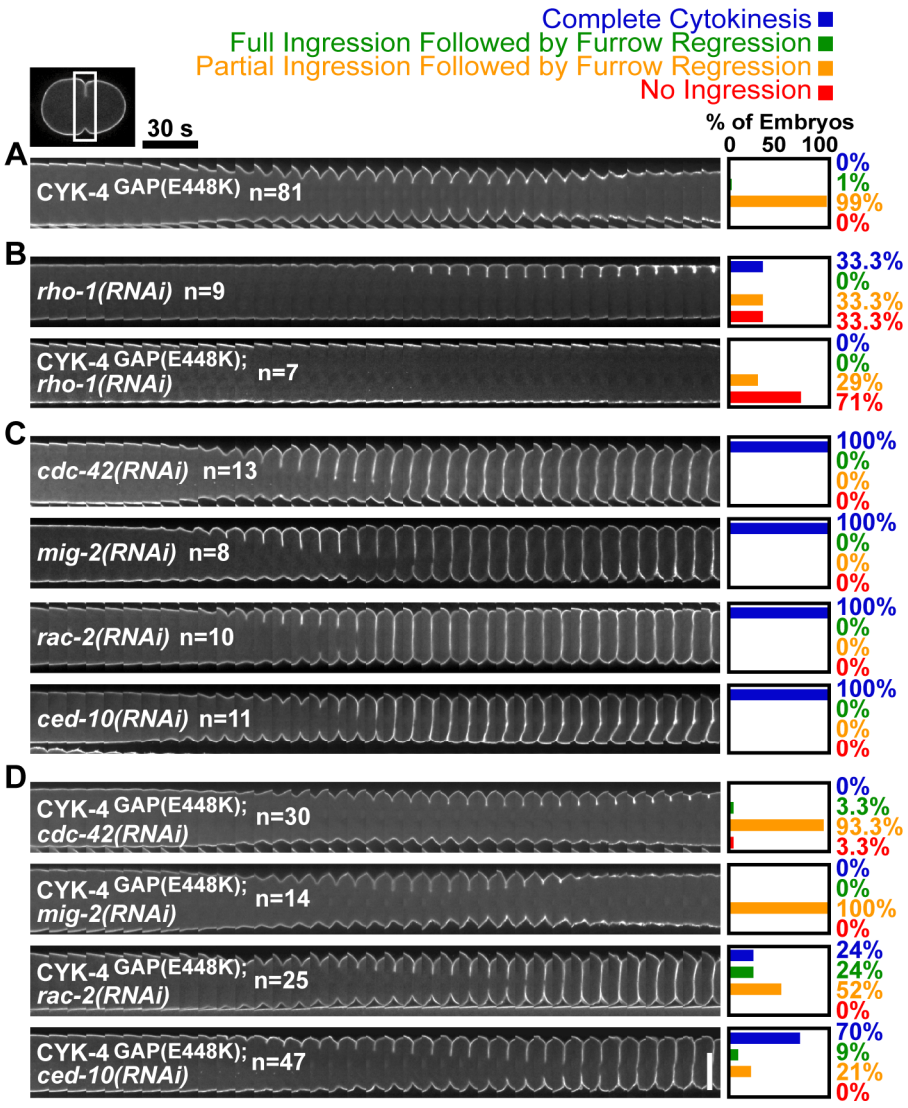

Figure 3.3 Rac depletion suppresses the cytokinesis defect in CYK-4$^{GAP(E448K)}$ embryos.

Time-lapse montage of the furrow region in embryos expressing a GFP::plasma membrane marker. Series begin at anaphase onset. A) CYK-4$^{GAP(E448K)}$ embryos exhibit partial furrow ingression followed by regression. B) Partial depletion of RhoA^{RHO-1} enhances the CYK-4$^{GAP(E448K)}$ cytokinesis defect. C) RNAi of other Rho family members does not disrupt cytokinesis. D) RNAi of Rac^{CED-10} or Rac^{RAC-2} rescues cytokinesis success in CYK-4$^{GAP(E448K)}$ embryos. Scale bar, 20 µm.

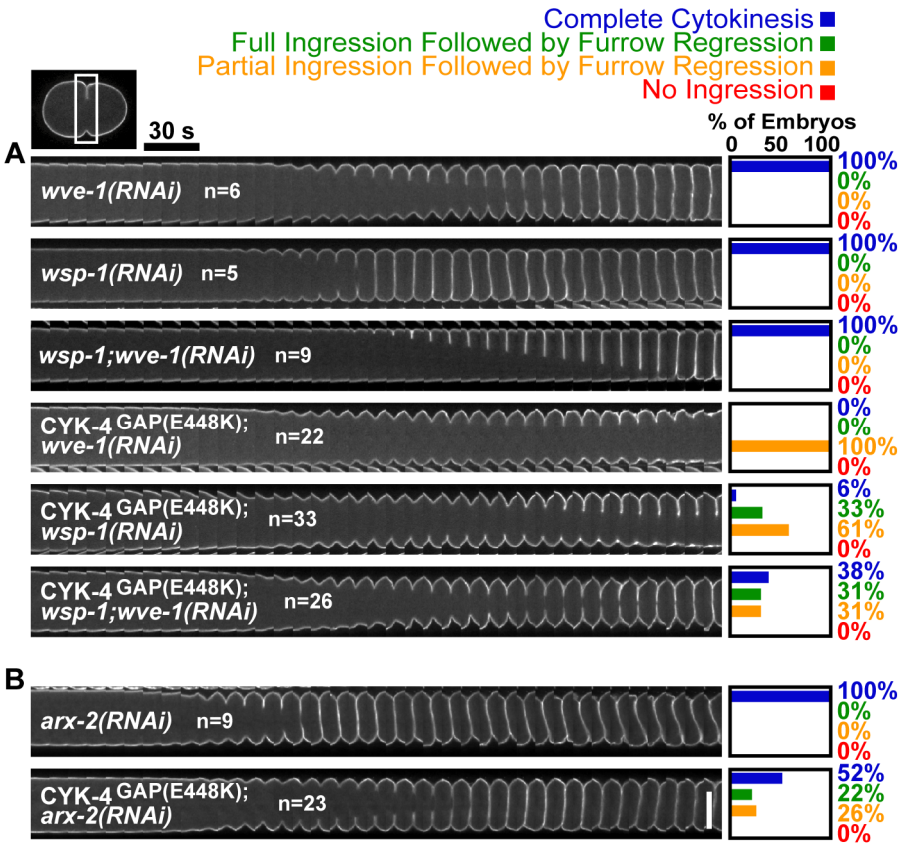

Figure 3.4 CYK-4 GAP inactivates Rac and its effectors, WASp/WAVE and the Arp2/3 complex, to promote cytokinesis.
Cytokinesis in CYK-4$^{GAP(E448K)}$ embryos is rescued by A) co-depletion of WASp^{WSP-1} and WAVE^{WVE-1} or B) depletion of Arp2^{ARX-2}. Scale bar, 20 μm.

Genetic Interactions and Rescue of *cyk-4* Alleles at 25ºC

Genotype	Average/Median % Embryonic Lethal	Viable/Total # Embryos
cyk-4(or749ts) / *cyk-4(or749ts)*	100/100%	0/495
cyk-4(or570ts) / *cyk-4(or570ts)*	100/100%	0/276
cyk-4(or570ts) / *cyk-4(or749s)*	99/100%	2/311
cyk-4(or749ts) / +	1/0%	530/533
cyk-4(or570ts) / +	1/0%	343/348
unc-32(e189) cyk-4(t1689ts) / *unc-32(e189) cyk-4(t1689ts)*	100/100%	0/503
unc-32(e189) cyk-4(t1689ts) / *cyk-4(or749ts)*	95/99%	30/698
unc-32(e189) cyk-4(t1689ts) / *cyk-4(or570ts)*	85/87%	140/888
unc-32(e189) cyk-4(t1689ts) / +	41/26%	362/540
unc-119(ed3) cyk-4(or749ts) / *unc-119(ed3) cyk-4(or749ts)* ; *unc-119+ gfp::cyk-4+* / +	39/36%	213/601
unc-119(ed3) cyk-4(or570ts) / *unc-119(ed3) cyk-4(or570ts)* ; *unc-119+ gfp::cyk-4+* / +	29/23%	222/911
unc-119(ed3) / *unc-119(ed3)* ; *unc-119+ gfp::cyk-4+* / +	1/0%	5/373

Figure S3.1 Genetic interactions and rescue of cyk-4 GAP alleles.
Genetic data demonstrating that *cyk-4(or749ts)* and *cyk-4(or570ts)* (CYK-4$^{GAP(E448K)}$ and CYK-4$^{GAP(T546I)}$, respectively) are strictly recessive (orange), fail to complement each other (brown), and also fail to fully complement *cyk-4(t1689ts)* (CYK-4$^{CSA(S15L)}$, an allele that affects centralspindlin assembly, CSA). Expression of a GFP fusion with CYK-4 from a transgene rescues the embryonic lethality of both *cyk-4(or749ts)* and *cyk-4(or570ts)* (green).

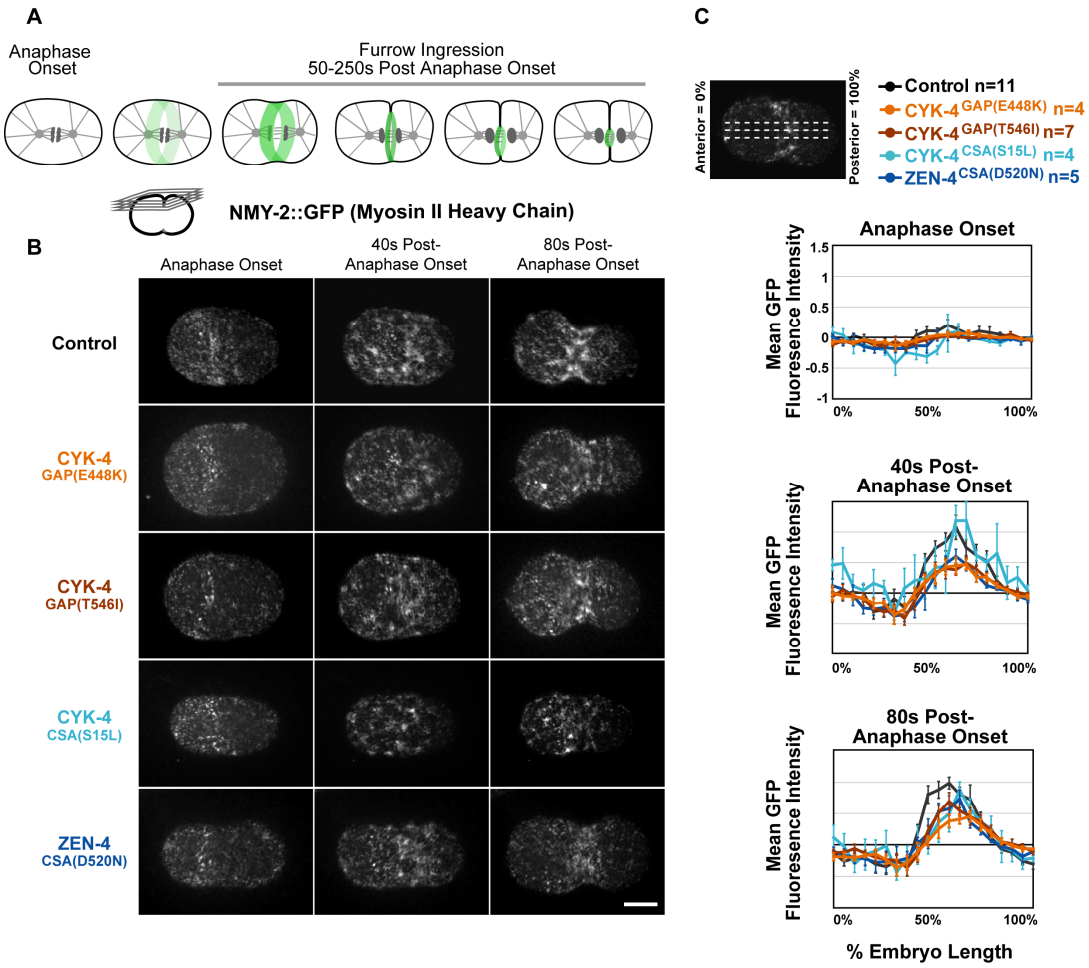

Figure S3.2 Centralspindlin mutations do not affect the accumulation of myosin II on the equatorial cortex prior to furrow ingression.

A) Schematic summarizing the temporal progression of cytokinesis at 25ºC. Immediately following anaphase onset, myosin II becomes enriched on the equatorial cortex, forming a band that encircles the cell equator. The cortex subsequently buckles inwards to form a furrow that ingresses inwards towards the spindle center, closing the hole between the daughter cells. B,C) During the 80s immediately following anaphase onset, the amount and distribution of cortical myosin II in the GAP domain and centralspindlin assembly mutants is similar to that in controls. B) Images of the cortex from time-lapse series of embryos expressing a GFP-fusion to the *C. elegans* myosin II heavy chain (NMY-2::GFP). Scale bar, 10 μm. C) The mean post-anaphase accumulation of cortical NMY-2::GFP fluorescence is plotted as a function of embryo length for control and centralspindlin mutant embryos at the indicated time points. Values were normalized by dividing by the average maximum value for controls (between 55-65% embryo length). Error bars=SEM. NOTE: Prior to anaphase onset, cortical NMY-2::GFP is present in an anterior cap that contributes to cellular polarity maintenance. In the early post-anaphase interval, this localization is super-imposed with its accumulation at the cell equator. In the quantification shown in C, the post-anaphase accumulation is measured by subtracting the distribution at anaphase onset from the distribution at subsequent time points to eliminate the contribution from the anterior cap.

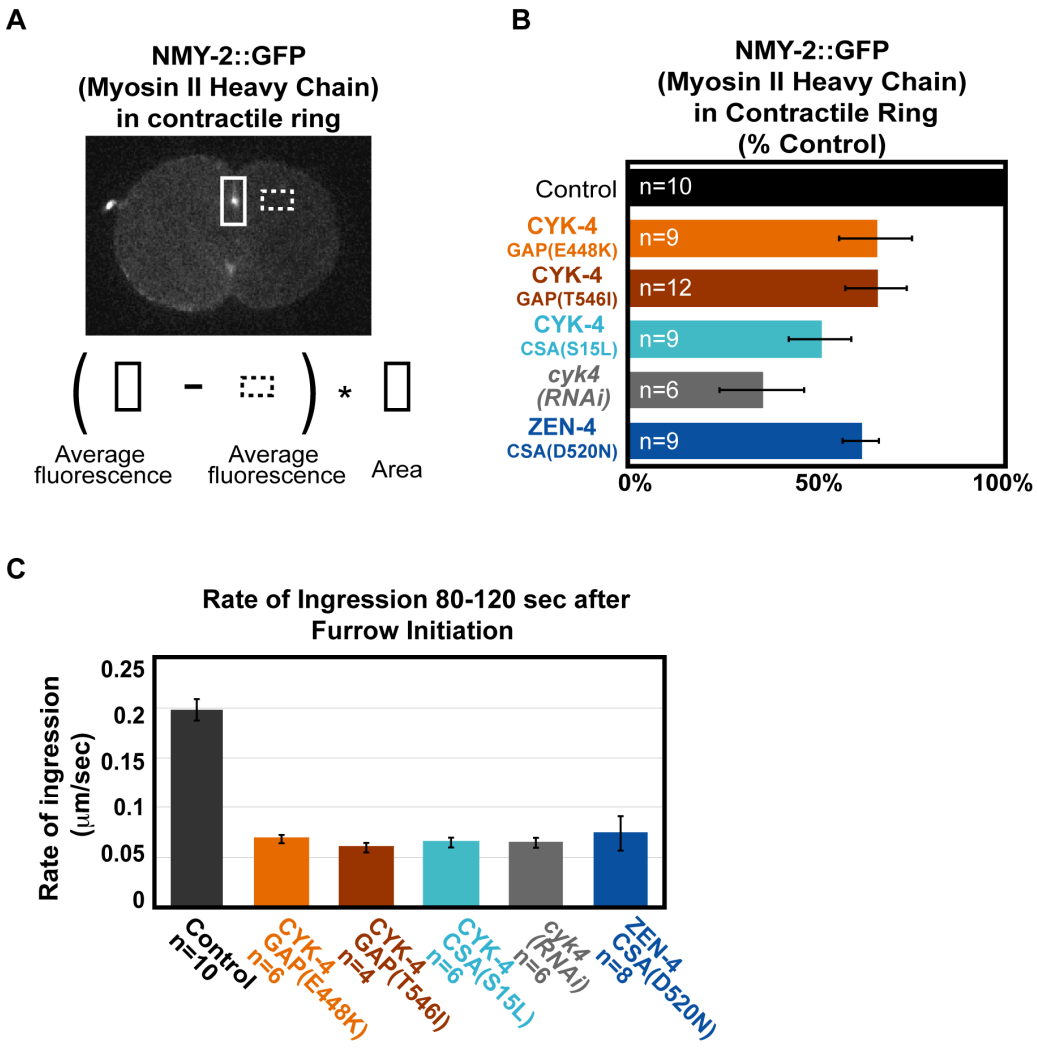

Figure S3.3 Myosin II levels at the furrow tip and the rate of furrow ingression are reduced in centralspindlin mutants.

A) Schematic illustrating the quantification method used to measure the amount of myosin II heavy chain (NMY-2::GFP) at the furrow tip. B) Mean NMY-2::GFP fluorescence at the furrow tip, measured ~180s after anaphase onset, is reduced in centralspindlin mutants relative to controls. Error bars=SEM. C) The mean rate of furrow ingression in the CYK-4 GAP mutants is nearly identical to that in mutants disrupting centralspindlin assembly and following RNAi-mediated depletion of CYK-4, and is reduced ~3-fold relative to controls. Error bars=SEM.

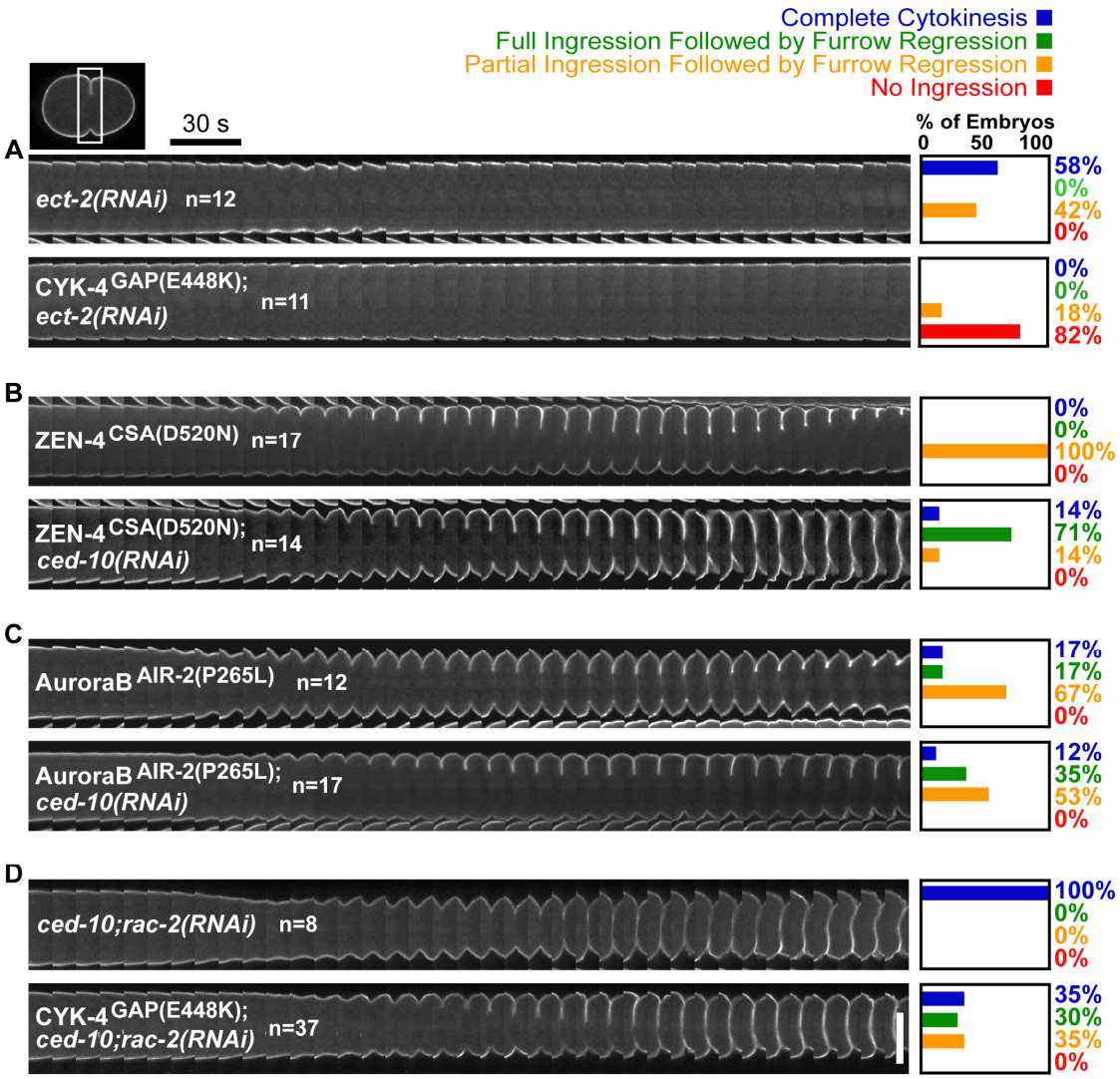

Figure S3.4 Partial depletion of the ECT-2 GEF enhances the CYK-4$^{GAP(E448K)}$ cytokinesis defect, and Rac^{CED-10} depletion rescues furrow ingression in ZEN-4$^{CSA(D520N)}$ but not in AuroraB$^{AIR-2(P265L)}$ embryos.

A) Partial depletion of the ECT-2 GEF by RNAi enhances the CYK-4$^{GAP(E448K)}$ cytokinesis defect. B) Rac^{CED-10} depletion rescues the furrow ingression defect in the centralspindlin assembly mutant ZEN-4$^{CSA(D520N)}$, allowing 85% of the furrows to ingress to completion. However, in 71% of these embryos cytokinesis fails to complete and the furrow ultimately regresses. C) Rac^{CED-10} depletion does not suppress the cytokinesis phenotype in AuroraB$^{AIR-2(P265L)}$ mutants which also fail to form a central spindle and have a partial furrow ingression defect. D) Co-depletion of Rac^{CED-10} and Rac^{RAC-2} by RNAi did not increase the efficiency of rescue over that observed following depletion of Rac^{CED-10} alone (Fig. 3.3D). However, due to two (30-40 bp) stretches of identity at the nucleotide level we cannot rule out that RNAi depletion of Rac^{CED-10} also targets Rac^{RAC-2} (albeit less-efficiently) and vice versa. Scale bar, 20 μm.

Worm strains used in the study

Strain #	Genotype
N2	*wild-type (ancesteral)*
CB1309	*lin-2(e1309)X.*
CB1489	*him-8(e1489)IV.*
MT3751	*dpy-5(e61)I; rol-6(e187)II; unc-32(e189)III.*
MT464	*unc-5(e53)IV; dpy-11(e224)V; lon-2(e678)X.*
DR104	*dpy-18(e364) unc-25(e156)III.*
CB2053	*dpy-18(e364) unc-64(e246)III.*
EU1303	*cyk-4(or570ts)III.*
EU1302	*cyk-4(or570ts)III; him-8(e1489)IV.*
OD227	*cyk-4(or749ts)III.*
OD228	*unc-32(e189) cyk-4(t1689ts)III.*
WH0279	*unc-119(ed3)III; ojIs12[cyk-4::GFP unc-119(+)]/+*
OD229	*cyk-4(or749ts) unc-119(ed3)III; ojIs12[cyk-4::GFP unc-119(+)]/+*
OD230	*cyk-4(or570ts) unc-119(ed3)III; ojIs12[cyk-4::GFP unc-119(+)]/+*
EU716	*zen-4(or153ts)IV.*
OD27	*unc-119(ed3)III; ltIs14 [pASM05; pie-1/GFP-TEV-STag::air-2; unc-119 (+)]IV.*
OD231	*cyk-4(or570ts)III; ltIs14 [pASM05; pie-1/GFP-TEV-STag::air-2; unc-119 (+)]IV.*
OD232	*cyk-4(or749ts)III; ltIs14 [pASM05; pie-1/GFP-TEV-STag::air-2; unc-119 (+)]IV.*
OD233	*unc-32(e189) cyk-4(t1689ts)III; ltIs14 [pASM05; pie-1/GFP-TEV-STag::air-2; unc-119 (+)]IV.*
JJ1473	*unc-119(ed3)III; zuIs45[nmy-2::NMY-2::GFP + unc-119(+)]V.*
OD234	*cyk-4(or570ts)III; zuIs45[nmy-2::NMY-2::GFP + unc-119(+)]V.*
OD235	*cyk-4(or749ts)III; zuIs45[nmy-2::NMY-2::GFP + unc-119(+)]V.*
OD236	*zen-4(or153ts)IV; zuIs45[nmy-2::NMY-2::GFP + unc-119(+)]V.*
OD237	*unc-32(e189) cyk-4(t1689ts)III; zuIs45[nmy-2::NMY-2::GFP + unc-119(+)]V.*
OD95	*unc-119(ed3) ltIs38 [pAA1; pie-1/GFP::PH(PLC1delta1)III; unc-119 (+)]; ltIs37 [pAA64; pie-1/mCHERRY::his-58; unc-119 (+)]IV*
OD238	*zen-4(or153ts)IV; ltIs38 [pAA1; pie-1/GFP::PH(PLC1delta1)III.*
OD105	*air-2(or207ts)I; ltIs38 [pAA1; pie-1/GFP::PH(PLC1delta1)III.*
OD239	*cyk-4(or749ts) ltIs38 [pAA1; pie-1/GFP::PH(PLC1delta1) unc-119 (+)]III; ltIs37 [pAA64; pie-1/mCHERRY::his-58; unc-119 (+)]IV*
OD240	*cyk-4(or570ts) ltIs38 [pAA1; pie-1/GFP::PH(PLC1delta1) unc-119 (+)]III; ltIs37 [pAA64; pie-1/mCHERRY::his-58; unc-119 (+)]IV*
OD241	*cyk-4(t1689ts) ltIs38 [pAA1; pie-1/GFP::PH(PLC1delta1) unc-119 (+)]III; tIs37 [pAA64; pie-1/mCHERRY::his-58; unc-119 (+)]IV*

Figure S3.5 Strains used in this study.
Genotype and strain names used in this study. Note: CYK-4$^{GAP(E448K)}$ is *cyk-4(or749ts)*, CYK-4$^{GAP(T546I)}$ is *cyk-4(or570ts),* CYK-4$^{CSA(S15L)}$ is *cyk-4(t1689ts)*, and ZEN-4$^{CSA(D520N)}$ is *zen-4(or153ts)* in this manuscript.

dsRNAs used in the study

Gene	Oligo 1	Oligo 2	Template	Conc. (mg/mL)
zen-4 (M03D4.1)	AATTAACCCTCACTAA AGGAATTGGTTATGG CTCCGAGA	TAATACGACTCACTAT AGGATTGGAGCTGTT GGATGAGC	Kohara cDNA yk35d10	1.3
cyk-4 (K08E3.6)	TAATACGACTCACTAT AGGCGCAAGCTGTGG AAAGATTC	AATTAACCCTCACTAA AGGTTGCGATGTCAC GAGTTGTT	N2 genomic	2.0
rho-1 (Y51H4A.3)	TAATACGACTCACTAT AGGTGGCTGCGATTA GAAAGAAG	AATTAACCCTCACTAA AGGCCTCACGAATTC CGTCCTTA	Kohara cDNA yk435f7	2.0
ect-2 (T19E10.1)	TAATACGACTCACTAT AGGTGGATCCGATTC TCGAACTT	AATTAACCCTCACTAA AGGACATTTGGCTTTG TGCTTCC	N2 genomic	1.7
ced-10 (C09G12.8)	TAATACGACTCACTAT AGGTCAAATGTGTCGT CGTTGGT	AATTAACCCTCACTAA AGGATCGCCTCATCGA AAACTTG	N2 cDNA	1.0
rac-2 (K03D3.10)	TAATACGACTCACTAT AGGAAATGTGTCGTCG TTGGTGA	AATTAACCCTCACTAA AGGCTCGTTTGTGGTG TTTGTGG	N2 cDNA	1.2
cdc-42 (R07G3.1)	TAATACGACTCACTAT AGGGATCAAGTGCGT CGTCGTT	AATTAACCCTCACTAA AGGGAGAATATTGCA CTTCTTCTTCTTCTC	N2 cDNA	0.7
mig-2 (C35C5.4)	TAATACGACTCACTAT AGGGGAGACGGAACAG TTGGAAA	AATTAACCCTCACTAA AGGGGTTTCGGATGAA GAATGGA	N2 cDNA	1.6
arx-2 (K07C5.1)	TAATACGACTCACTAT AGGTCAGCTTCGTCAA ATGCTTG	AATTAACCCTCACTAA AGGTGCAATACGCGA TCCAAATA	N2 genomic	1.7
wsp-1 (C07G1.4)	AATTAACCCTCACTAAA GGTCTTCAGGAATCGG ATCCAC	TAATACGACTCACTATA GGCGGCTCCAGAAGT CGTACTC	N2 cDNA	4.1
wve-1 (R06C1.3)	AATTAACCCTCACTAA AGGCTCTAACAAAACG GGCGGTA	TAATACGACTCACTAT AGGGGAGGTGGTGGAG GGATATT	N2 cDNA	4.8

Figure S3.6 dsRNAs used in this study.
Primers, template, and concentrations of the dsRNAs used in this study.

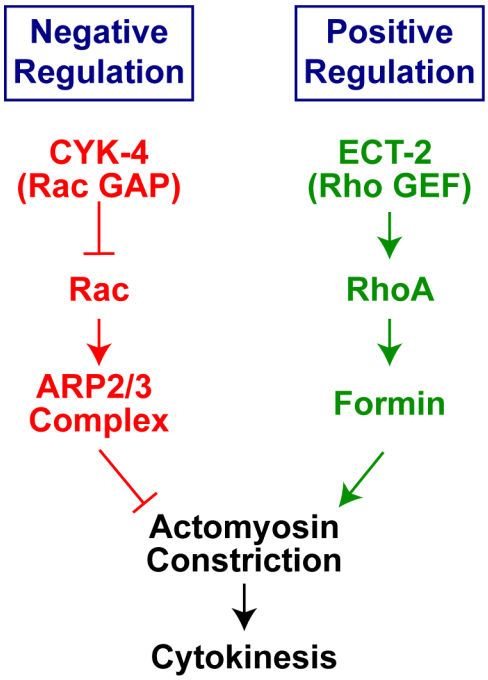

Figure S3.7 Negative regulation of Rac and its effectors, WASp/WAVE and the Arp2/3 complex, by CYK-4 GAP activity is essential for cytokinesis.
Model for signaling during cytokinesis.

Chapter 4: Centralspindlin and the Chromosomal Passenger Complex are part of independent pathways to promote furrow ingression

4.1 Summary

Cytokinesis, the final step of cell division, is accomplished by formation and constriction of an actin-myosin contractile ring. Two midzone-localized signaling complexes – Centralspindlin and the Chromosomal Passenger Complex (CPC) – are dispensable for furrow formation, but they are required to drive furrow ingression. Although previous work put the two complexes within a linear pathway, with the CPC being upstream of Centralspindlin, our work shows that these complexes are promoting furrow ingression via distinct molecular pathways. The key role of the Centralspindlin complex is via inactivation of the Rac pathway. Interestingly, depletion of either Anillin or the septins, two components of the contractile ring, is able to rescue CPC mutants, suggesting that one of these contractile ring components could be the key target of the CPC during furrow ingression. Therefore, this suggests that the key role of the CPC could be to destabilize the contrctile ring during furrow ingression.

4.2 Introduction

Cytokinesis is the final step of mitosis, which physically divides a single cell into two daughter cells. In animal cells, cytokinesis is achieved via a progressive remodeling of the cortex that changes the shape of the cell to partition its contents. To ensure that each daughter cell receives a single genomic complement, assembly of the cytokinetic furrow is spatially and temporally coordinated with chromosome segregation (Glotzer 2004; Eggert, Mitchison et al. 2006). Although it is known that continuous communication between the spindle and the cortex is required to assemble and maintain the furrow (Rappaport 1996; Wheatley and Wang 1996; Larkin and Danilchik 1999; Alsop and Zhang 2004; Bement, Benink et al. 2005), the mechanisms by which the anaphase spindle directs cortical remodeling are current topics of investigation.

The idea that the spindle midzone generates a signal that promotes furrowing was originally suggested by studies in grasshopper spermatocytes, echinoderm eggs, and newt kidney epithelial cells (Ris 1949; Rappaport and Rappaport 1974; Kawamura 1977). Subsequently, this idea re-emerged following a study in which vertebrate somatic cells were “perforated” between the midzone and the adjacent equatorial cortex (Cao and Wang 1996). In these cells, furrowing was limited to the side of the perforation adjacent to the midzone, suggesting that the midzone generates a non-diffusible signal that promotes furrow formation.

Consistent with this idea, a number of protein complexes that localize to the midzone have been implicated in cytokinesis (Glotzer 2005; Eggert, Mitchison et al. 2006). One of these is the Chromosomal Passenger Complex (CPC), a four-protein complex composed of the mitotic kinase Aurora B^{AIR-2}, INCENP^{ICP-1}, Survivin^{BIR-2}, and Borealin^{CSC-1}. The CPC localizes to chromosomes during prophase and then transitions to midzone microtubules at anaphase. In all metazoans examined to date, inhibition of the CPC by RNAi or expression of mutant subunits leads to a late cytokinesis defect in which the furrow forms and ingresses deeply but later regresses (Rev. Ruchaud, Carmena et al. 2007). The role of the CPC during furrow ingression has remained a mystery, although it is known that the kinase activity is required (Murata-Hori and Wang 2002; Honda, Korner et al. 2003). A number of AuroraB targets have been identified, but the one that seems most likely to be involved in promoting cytokinesis is the regulatory light chain of myosin (MRLC), which is known to be phosphorylated downstream of Rho activation during cytokinesis to promote the myosin's motor activity (Murata-Hori, Fumoto et al. 2000). However, whether this is an actual *in vivo* target of the CPC has not been fully assessed.

A second conserved complex that localizes to the midzone is Centralspindlin, a heterotetramer (Pavicic-Kaltenbrunner, Mishima et al. 2007) composed of two molecules of the plus end directed kinesin-6, MKLP-1^{ZEN-4}, and two molecules of MgcRacGAP^{CYK-4}, whose distinguishing feature is a

GAP domain for Rho family GTPases. Depletion of Centralspindlin proteins leads to cytokinesis defects that range in severity in different systems from no furrow ingression in *Drosophila* (Adams, Tavares et al. 1998; Somma, Fasulo et al. 2002; Somers and Saint 2003) to late cytokinesis defects in *C. elegans* (Powers, Bossinger et al. 1998; Raich, Moran et al. 1998; Jantsch-Plunger, Gonczy et al. 2000; Severson, Hamill et al. 2000). In vertebrates and *Drosophila*, Centralspindlin has been proposed to serve as an anchoring site for the polo-kinase dependent targeting of the RhoGEF, ECT2, which promotes equatorial Rho activation and contractile ring assembly (Somers and Saint 2003; Yuce 2005; Zhao and Fang 2005; Chalamalasetty, Hummer et al. 2006; Kamijo, Ohara et al. 2006; Nishimura 2006; Brennan, Peters et al. 2007; Burkard, Randall et al. 2007; D'Avino, Archambault et al. 2007; Petronczki, Glotzer et al. 2007). In addition, a role for the GAP domain of CYK-4 in down-regulating Rac activity during cytokinesis has been observed (Canman, Lewellyn et al. 2008).

Previously, the Centralspindlin complex and the CPC have been put within a common, linear pathway to promote cytokinesis, with the CPC being upstream of the Centralspindlin complex. This model is based on the fact that the CPC is able to phosphorylate both members of the Centralspindlin Complex (Minoshima, Kawashima et al. 2003; Guse, Mishima et al. 2005), and one of these sites was shown to be required for completion of cytokinesis, but not for localization to the spindle midzone (Guse, Mishima et al. 2005). Using

conditional alleles in the early *C. elegans* embryo, Severson (2000) showed that AuroraB^{AIR-2} is required during metaphase and early anaphase to promote chromosome segregation and the localization of ZEN-4 to the spindle midzone, but it is dispensable during furrow ingression. In contrast, they found that ZEN-4 was not required until late cytokinesis. Further, embryos homozygous for mutations in ZEN-4 and AuroraB^{AIR-2} did not show an enhanced phenotype, suggesting that the two complexes act within a common pathway.

Here, we show that disrupting both Centralspindlin and the CPC has a more severe effect on furrow ingression than either single perturbation, suggesting that the CPC is likely performing an additional function distinct from the Centralspindlin complex and its role in Rac inactivation. We show that this function is distinct from its role during meiosis, chromosome segregation, and midzone formation. We find that depletion of Rho kinase, which is known to phosphorylate and activate myosin regulatory light chain, enhances the *air-2(or207ts)* mutant, but depletion of the myosin phosphatase subunit, MEL-11, is unable to rescue it: this suggests that AuroraB^{AIR-2} is not functioning as a myosin kinase. Finally, we show that depletion of the septin, UNC-59, or the filament linker protein, Anillin^{ANI-1}, is able to rescue the AuroraB^{AIR-2} mutant, suggesting that one function of the CPC might be to promote disassembly of the contractile ring during furrow ingression.

4.3 Results

4.3.1 Centralspindlin and the CPC are required to promote furrow ingression

Centralspindlin and the Chromosomal Passenger Complex (CPC) are both required for successful cell division in all systems, and most reports have put the two complexes in a common pathway to promote cytokinesis (Rev. Glotzer 2005). Because the first division of the *C. elegans* embryo is highly stereotypical, we are able to develop quantitative assays to characterize the phenotype of embryos depleted of these complexes. Depletion of either the Centralspindlin complex (ZEN-4) or the CPC (AuroraB^{AIR-2}) disrupts formation of the midzone bundles of microtubules (Fig. 4.1A) and leads to failure of the first division (Fig. 4.1B). These embryos only ingress ~50% of their starting diameter, and the rate of furrow ingression is ~3-4 fold slower than in controls (Fig. 4.1D,E; Lewellyn, Dumont et al. 2009). Therefore, depletion of either Centralspindlin or the CPC causes a decrease in the rate of furrow ingression, not just a late failure of cytokinesis, as was previously reported.

Because these complexes are thought to act in the same pathway, we asked whether co-depleting both ZEN-4 and AuroraB^{AIR-2} would have a more dramatic effect on furrow ingression. In contrast to previous reports, embryos co-depleted of both ZEN-4 and AuroraB^{AIR-2} showed an enhanced phenotype compared to either single depletion. The co-depleted embryos only ingressed ~20% of their starting diameter, compared to ~50% for either single depletion

(Fig. 4.1B,D,E). Quantitative Western blotting confirmed that these embryos were thoroughly depleted of both ZEN-4 and AuroraB^{AIR-2} (Fig. 4.1C). Therefore, depletion of both Centralspindlin and the CPC enhances the ingression defect seen in either single depletion, and it suggests that these complexes might be functioning in separate pathways to promote furrow ingression.

4.3.2 An AIR-2 mutant can be used to bypass the meiotic defect in CPC depletions

Although much work has been done to characterize the molecular mechanism through which the Centralspindlin complex promotes furrow ingression, little is known about what the CPC is doing during cytokinesis. This gap in our understanding is partially explained by the wide range of phenotypes associated with disruption of the CPC. One significant complication with the *air-2(RNAi)* condition is that these embryos show a complete failure of meiotic chromosome segregation, due to the role of AuroraB^{AIR-2} in the phosphorylation and degradation of the meiotic cohesin, REC-8 (Kaitna, Pasierbek et al. 2002; Rogers, Bishop et al. 2002). This leads to the addition of a large polyploid female pronucleus to the mitotic spindle, which could be causing the enhanced phenotype we see in embryos depleted of ZEN-4 and AuroraB^{AIR-2} (Fig. S4.1A,B). Therefore, we chose to use a previously characterized allele of AuroraB^{AIR-2}, *air-2(or207ts)* (Severson,

Hamill et al. 2000), to continue our analysis. *air-2(or207ts)* contains a point mutation within the kinase domain of the protein, which has been shown to compromise the kinase activity *in vitro* (Bishop 2002). Dissected embryos could be shifted to the restrictive temperature after the completion of meiosis, bypassing the requirement for the CPC during meiosis (Fig. S4.1A,B). At the restrictive temperature, AuroraB^{AIR-2} remained localized to the segregated chromosomes, and to the chromosome bridges (Fig. S4.1C; *arrowheads*; Severson, Hamill et al. 2000). However, in contrast to previous results, we found that ZEN-4 was still present in the midzone region of the cell; however, the levels were dramatically reduced compared to embryos fixed at the permissive temperature (Fig. S4.1C). These shifted embryos could be used for further analysis, since they allowed us to simplify the AuroraB^{AIR-2} phenotype and focus solely on its role during mitosis.

4.3.3 Mutation of AuroraB^{AIR-2} enhances the Centralspindlin depletion phenotype

First, we characterized the *air-2(or207ts)* mutant embryos at restrictive temperature, to determine whether the cytokinesis defect was similar to depletion of AuroraB^{AIR-2}. Shifting to the restrictive temperature (~26.5^{o}C) after the completion of meiosis (usually during pronuclear migration) produced a phenotype that was comparable, although less severe, than embryos depleted of AuroraB^{AIR-2}. Embryos showed ~2 fold decrease in the rate of ingression relative to controls, and they ingressed ~60% of their starting

diameter before regressing (Fig. 4.2B,C). We then combined depletion of ZEN-4 with the *air-2(or207ts)* mutation, to test whether we still observed the enhanced phenotype. Similar to embryos co-depleted of both ZEN-4 and AuroraB^{AIR-2}, depletion of ZEN-4 in the *air-2(or207ts)* background enhanced the phenotype of the *zen-4(RNAi)* embryos. In fact, *zen-4(RNAi);air-2(or207ts)* embryos ingressed slower and to a significantly reduced extent compared to *zen-4(RNAi)* alone (Fig. 4.2B,C). Comparisons were made to the *zen-4(RNAi)* phenotype because this condition provides a more severe phenotype than the *air-2(or207ts)*; further, depletion of ZEN-4 in a previously characterized mutant background (*zen-4(or153ts)*; Severson, Hamill et al. 2000) does not enhance the *zen-4(RNAi)* phenotype (Fig. 4.2B,C), suggesting that the *zen-4(RNAi)* condition is close to the null phenotype. Therefore, similar to the double RNAi condition, mutation of the kinase, AuroraB^{AIR-2}, significantly enhances the ZEN-4 depletion phenotype.

4.3.4 Disrupting chromosome segregation and midzone formation does not enhance ZEN-4 depletion

In addition to its role in cytokinesis, the CPC is also required to promote chromosome segregation and formation of the spindle midzone (Fig. 4.2A). In the original characterization, Severson (2000) showed that shifting the *air-2(or207ts)* mutant to the restrictive temperature during early anaphase did not affect cytokinesis, which would be consistent with the kinase performing its

essential functions prior to significant furrow ingression. If the role of the CPC during cytokinesis were strictly via promoting chromosome segregation and formation of the midzone, then we would expect that depletion of an inner kinetochore protein, CenpC^{HCP-4}, which also disrupts chromosome segregation and midzone formation (Fig. 4.2A) would similarly enhance the *zen-4(RNAi)* phenotype. However, we found that co-depletion of CenpC^{HCP-4} & ZEN-4 was not significantly different from *zen-4(RNAi)* (Fig. 4.2B,C). We additionally tested whether co-depletion of ZEN-4 and SPD-1, a microtubule bundling protein that also localizes to the spindle midzone and is required for formation of the bundles during anaphase (Fig. S4.2A; Verbrugghe 2004) would enhance the *zen-4(RNAi)* phenotype. The rate and maximum extent of ingression of embryos depleted of SPD-1 & ZEN-4 were not significantly different from embryos depleted of ZEN-4 alone (Fig. S4.2B,C). Together, this data suggests that AuroraB^{AIR-2} is driving furrow ingression independently of its role in promoting chromosome segregation and spindle midzone formation. Consistent with this result, depletion of SPD-1, ZEN-4, or SPD-1 & ZEN-4 did not prevent the localization of AuroraB^{AIR-2} to the remnants of the spindle midzone (Fig. S4.2D).

4.3.5 AuroraB^{AIR-2} is part of a Rac-independent pathway that is downstream of Rho to promote furrow ingression

From this data, we are left with the idea that the CPC (AuroraB^{AIR-2}) is promoting furrow ingression via a mechanism that is distinct from its role of promoting chromosome segregation and midzone formation. Further, the additive phenotype that we see upon co-depletion of Centralspindlin and the CPC suggests that the two complexes are promoting furrow ingression through different pathways; however, we cannot yet rule out the possibility that the more severe phenotype is due to compromising two components of the same pathway. Recent work suggests that the key function of the Centralspindlin complex is to inactivate the small GTPase, Rac, via the GAP activity of CYK-4. Depletion of the Rac homologs, CED-10 or RAC-2, or the downstream effector, Arp2^{ARX-2}, was able to rescue mutations in the Centralspindlin complex. In that work, it was shown that depletion of Rac^{CED-10} was not able to rescue *air-2(or207ts)* mutants (Fig. 4.3A; Canman, Lewellyn et al. 2008), which suggests that AuroraB^{AIR-2} is not functioning as part of the Rac inactivation pathway to promote furrow ingression.

We wanted to further confirm that the CPC was not acting upstream of Centralspindlin to promote Rac inactivation by using our assays to monitor the rate and maximum extent of furrow ingression in embryos depleted of either Rac^{CED-10} or Arp2^{ARX-2}. Depletion of Rac^{CED-10} or Arp2^{ARX-2} led to a decrease in the rate of ingression, but these embryos always completed the first division

(Fig. 4.3B,C). Depletion of Rac^{CED-10} or Arp2^{ARX-2} in the *zen-4(or153ts)* mutant embryos did not affect the rate of ingression, but it did significantly increase the maximum extent that these embryos were able to ingress (Fig. 4.3B,C). However, unlike *cyk-4(or749ts)* GAP mutant embryos (Canman, Lewellyn et al. 2008), depletion of Rac^{CED-10} or Arp2^{ARX-2} did not allow the full completion of the first division. This could be due to the fact that *cyk-4(or749ts)* embryos did not disrupt midzone formation (Canman, Lewellyn et al. 2008), which might aid in the final steps of cytokinesis. In contrast, depletion of Rac^{CED-10} or Arp2^{ARX-2} in *air-2(or207ts)* embryos did not affect the maximum extent of ingression, but it did significantly decrease to the rate of ingression (Fig. 4.3B,C). Together, this data shows that depletion of proteins in the Rac pathway are able to rescue Centralspindlin mutants, but not CPC mutants, suggesting that the CPC is part of an independent pathway to promote furrow ingression.

One possibility is that AuroraB^{AIR-2} is promoting activation of another small GTPase, Rho, which is required for cytokinesis in all systems (Glotzer 2005). This possibility is unlikely, however, because depletion of AuroraB^{AIR-2} has a much less severe phenotype than depletion of a known Rho activator, the guanine nucleotide exchange factor (GEF), ECT-2. Depletion of ECT-2 prevents the equatorial accumulation of contractile ring proteins (Fig. S4.3B,C) and completely blocks furrow formation and ingression (Fig. S4.3A). In contrast, even combining depletion of AuroraB^{AIR-2} with the mutant background

(*air-2(RNAi);air-2(or207ts)*) did not block the localization of contractile ring proteins during early anaphase (Fig. S4.4) or furrow ingression. Therefore, if AuroraB^{AIR-2} is part of the Rho pathway, it is likely acting downsteam of Rho activation to promote furrow ingression.

4.3.6 Depletion of the septin, UNC-59, is able to rescue mutation in AuroraB^{AIR-2}

What could the CPC be doing to promote furrow ingression, downstream of Rho activation? Although there is a long list of AuroraB targets, including histone H3, myosin regulatory light chain (MRLC), CENP-A, INCENP, MgcRacGAP, vimentin, desmin, survivin, and MCAK (Rev. Vagnarelli and Earnshaw 2004), none have proven to be the key to promoting furrow ingression. One of the more intriguing targets of AuroraB^{AIR-2} came from an *in vitro* experiment showing that the AuroraB homolog, AIM-1, could phosphorylate MRLC (Murata-Hori, Fumoto et al. 2000). Therefore, we wanted to genetically test whether this could be the critical role that AuroraB^{AIR-2} is performing during cytokinesis.

Regulation of the motor activity of myosin, but not its localization (Miyauchi, Yamamoto et al. 2006; Beach and Egelhoff 2009), is primarily through phosphorylation of the regulatory light chain. Rho kinase (RhoK) is a known Rho effector, which phosphorylates MRLC during cytokinesis (Fig. 4.4A; Matsumura 2005). Disruption of RhoK$^{LET-502}$ in the *C. elegans* embryo

led to a decrease in the rate of ingression, but these embryos always completed the first division (Fig. 4.4B; Piekny and Mains 2002; Maddox, Lewellyn et al. 2007). Depletion of RhoK$^{LET-502}$ enhanced the ingression phenotype of the *air-2(or207ts)* mutant embryos: both the rate and maximum extent of ingression were significantly decreased relative to the mutant alone (Fig. 4.4B). This could indicate that AuroraB^{AIR-2} is also acting as a myosin kinase, and that depletion of both kinases severely cripples the contractile ring; however, the other possibility is that we are disturbing two separate pathways which drive furrow ingression.

To distinguish between these two possibilities, we wanted to further explore the potential similarities between RhoK$^{LET-502}$ and AuroraB^{AIR-2}. In addition to regulating MRLC during cytokinesis, RhoK phosphorylates and inactivates the myosin phosphatase, which removes the activating phosphorylation from MRLC, and thereby inhibits contractility. Disruption of the myosin binding subunit of the phosphatase (MEL-11) leads to an increase in the rate of furrow ingression (Fig. 4.4B,C; Piekny and Mains 2002; Gally, Wissler et al. 2009). Mutation of MEL-11 was able to rescue the embryonic lethality of the RhoK$^{LET-502}$ mutant (Piekny and Mains 2002). If AuroraB^{AIR-2} is similarly promoting myosin activation or inhibiting MEL-11, then we would expect to be able to at least partially rescue the *air-2(or207ts)* phenotype by depleting MEL-11. However, in contrast to RhoK$^{LET-502}$, depletion of MEL-11 was unable to rescue the AuroraB^{AIR-2} mutant embryos (Fig. 4.4B,C: *mel-*

11(RNAi);air-2(or207ts)). This suggests that AuroraB^{AIR-2} is not promoting inactivation of the myosin phosphatase.

Previously, a synthetic interaction was observed between RhoK$^{LET-502}$ and the septin, UNC-59. On its own, depletion of septin^{UNC-59} does not have a dramatic effect on cytokinesis. The rate of ingression is slower than in controls (Fig. 4.5B,C), and the normal asymmetric localization of contractile ring proteins and asymmetry of furrowing is disrupted (Fig. 4.5A; Maddox, Lewellyn et al. 2007), but cytokinesis is ultimately successful. It was shown previously, however, that co-depletion of RhoK$^{LET-502}$ and septin^{UNC-59} significantly enhanced either single depletion, causing cytokinesis failure in >60% of the embryos (compared to 0% in either single depletion; Maddox, Lewellyn et al. 2007). Therefore, the septins (and furrow asymmetry) are not normally necessary for successful division; however, if the robustness of the contractile ring is compromised, such as by decreasing the levels of active myosin, then cytokinesis will fail. If AuroraB^{AIR-2} were promoting the localization or activation of myosin motor proteins, or otherwise contributing to the robustness of the contractile ring, then depletion of septin^{UNC-59} should similarly enhance the *air-2(or207ts)* mutant phenotype. Surprisingly, depletion of septin^{UNC-59} actually suppressed the AuroraB^{AIR-2} phenotype. Although the rate of ingression was not significantly different from the mutant alone (Fig. 4.5C), depletion of septin^{UNC-59} increased the maximum extent of ingression, resulting in successful division in 5/18 embryos (Fig. 4.5B,C; compared to 0/14

for *air-2(or207ts)* uninjected). This rescue was specific to the AuroraB^{AIR-2} mutant, since depletion of septin^{UNC-59} in the *zen-4(or153ts)* background enhanced the ingression defect of the mutant alone (Fig. 4.5C). This points to a role for the CPC in negatively regulating the septins during furrow ingression.

After seeing this rescue of the *air-2(or207ts)* phenotype following depletion of septin^{UNC-59}, we wanted to test whether depletion of the filament linker protein, Anillin^{ANI-1}, is also able to rescue the mutant. Anillin^{ANI-1} localizes to the contractile ring independently of myosin II and the septins, but it is required to target the septins to the contractile ring. Similar to the septins, Anillin^{ANI-1} promotes asymmetric furrow ingression, but it is not required for cytokinesis (Fig. 4.5A,B; Maddox, Habermann et al. 2005; Maddox, Lewellyn et al. 2007). Therefore, we tested whether depletion of Anillin^{ANI-1} would similarly rescue the *air-2(or207ts)* mutant. Full depletion of Anillin^{ANI-1} (dsRNA injections done ~45-48hrs prior to imaging) in *air-2(or207ts)* mutant embryos caused a variable phenotype: 2/19 embryos completed the first division, 13/19 showed partial ingression and regression, and 4/19 showed no ingression. Because of this highly variable range in phenotypes, we tried a more subtle depletion condition (embryos from worms injected ~24 hours prior to imaging). In these *ani-1(RNAi);air-2(or207ts)* embryos, we saw 7/15 embryos complete the first division, 6/15 showed partial ingression and regression, and 2/15 showed no ingression (Fig. 4.5B). Partial depletion of Anillin^{ANI-1} in *zen-*

4(or153ts) was unable to rescue the mutant phenotype (Fig. 4.5B,C). This data further confirms that Centralspindlin and the CPC are participating in distinct pathways during furrow ingression; further, it suggests that the role of the CPC is likely to promote disassembly of the contractile ring.

4.4 Discussion

Here, we have shown that depletion of Centralspindin and the Chromosomal Passenger Complex leads to an enhanced defect in furrow ingression, suggesting that the CPC is performing a function distinct from the Centralspindlin complex. The role of the CPC during cytokinesis has been complicated by its involvement in meiosis, midzone formation, and chromosome segregation. By using the *air-2(or207ts)* temperature sensitive mutant, we were able to dissect the mechanism by which the CPC is promoting furrow ingression. We were able to confirm that the role of the CPC during furrow ingression is independent of chromosome segregation, midzone formation, and inactivation of the small GTPase, Rac. Because disruption of AuroraB^{AIR-2} does not affect the recruitment of contractile ring proteins, we believe that the CPC is functioning downstream of Rho activation. Depletion of the myosin kinase, RhoK$^{LET-502}$, enhances the AuroraB^{AIR-2} phenotype, and depletion of the myosin phosphatase subunit, MEL-11, is unable to rescue it. This suggests that the role of the CPC during furrow ingression is not through regulation of myosin activation. Finally, depletion of septin^{UNC-59} or the

filament liker protein, Anillin^{ANI-1}, is able to rescue the *air-2(or207ts)* mutant. Therefore, our data points to a role for AuroraB^{AIR-2} in regulating the septins or Anillin during furrow ingression, potentially by promoting their dynamics or disassembly.

4.4.1 Centralspindlin complex and the CPC are coordinately required to promote furrow ingression

All previous work on Centralspindlin and the CPC has suggested that the two complexes function in a single linear pathway, with the CPC acting upstream of Centralspindlin. AuroraB^{AIR-2} can phosphorylate both members of the Centralspindlin Complex - MgcRacGAP and Mklp1/ZEN-4, and this regulation is required for the completion of cytokinesis (Minoshima, Kawashima et al. 2003; Guse, Mishima et al. 2005). Further, embryos homozygous for mutations in both ZEN-4 (*zen-4(or153ts)*) and AuroraB^{AIR-2} (*air-2(or207ts)*) did not show an enhancement of the phenotype seen in the single mutants alone (Severson, Hamill et al. 2000). In contrast, our work has shown that disruption of both Centralspindlin and the CPC significantly enhances the furrow ingression defect seen in either single perturbation (Fig. 4.1, 4.2). One potential explanation for the difference we see compared to the initial characterization of the mutants (Severson, Hamill et al. 2000) is that the temperature sensitive alleles are hypomorphic, and so in order to see this enhancement, RNAi depletion must be combined with the mutants.

We could not initially rule out the possibility that the enhanced phenotype that we see is simply due to disrupting two components of the same pathway. However, combining out data with recent work has provided more evidence to suggest the two complexes have at least some independent functions. Canman et al. (2008) has shown that one of the critical functions of the Centralspindlin complex is to promote inactivation of the small GTPase, Rac, during furrow ingression via the GAP domain of CYK-4. In fact, depletion of Rac^{CED-10} is able to rescue completion of cytokinesis in ~70% of the CYK-4 GAP mutant embryos, and depletion of the downstream effect, $Arp2^{ARX-2}$ is able to rescue 52% of the embryos. In contrast, depletion of Rac^{CED-10} was unable to rescue the *air-2(or207ts)* mutant embryos, suggesting that the CPC is not promoting Rac inactivation through regulation of the Centralspindlin complex. To strengthen this argument, we further analyzed the rate and extent of ingression of mutant embryos depleted of Rac^{CED-10} or $Arp2^{ARX-2}$. We found that depletion of either protein significantly increased the maximum extent of ingression of *zen-4(or153ts)* embryos, but it caused a significant decrease in the rate of ingression of *air-2(or207ts)* embryos, without affecting the maximum extent (Fig. 4.3). This further supports the idea that the Centralspindlin complex is promoting Rac inactivation during cytokinesis, whereas the CPC is not (although there is likely a role for the CPC in localizing the Centralspindlin complex to the spindle midzone, even if just by promoting normal midzone bundle formation; Fig. S4.1C). It is interesting that although

depletion of Rac^{CED-10} or Arp2^{ARX-2} provides a significant rescue of the extent of ingression Centralspindlin mutants, it does not fully rescue the rate of ingression. This suggests that there might be another role for the Centralspindlin Complex during cytokinesis that is independent of the Rac pathway.

4.4.2 The role of the CPC/AuroraB^{AIR-2} during furrow ingression is independent of its role in promoting chromosome segregation and midzone formation

In contrast to the extensive work that has been done on the role of the Centralspindlin complex during cytokinesis, very little is known about the specific function of the CPC. Work on the CPC was limited by the range of processes that AuroraB^{AIR-2} participates in during meiosis and mitosis. Therefore, we tried to simplify our approach by using the temperature sensitive strain *air-2(or207ts)*, which contains a point mutation within the kinase domain that severely compromises the kinase activity *in vitro* (Bishop 2002). We were able to bypass the meiotic requirement for the CPC and show that there was still and additive defect in furrow ingression when ZEN-4 was depleted in the *air-2(or207ts)* background (Fig. 4.2). We then analyzed embryos depleted of ZEN-4 and the inner kinetochore protein, CenpC^{HCP-4}. Like disruption of the CPC, depletion of CenpC^{HCP-4} disrupts chromosome segregation and midzone formation; however, its co-depletion did not enhance the *zen-4(RNAi)*

phenotype (Fig. 4.2). Therefore, we concluded that the CPC is promoting furrow ingression independently of its role in promoting chromosome segregation and midzone formation. This is different from the model proposed by Severson (2000), which suggested that AuroraB^{AIR-2} was required to during prometaphase, metaphase, and early anaphase, but it was dispensable during furrow ingression.

4.4.3 AuroraB^{AIR-2} is likely not promoting furrow ingression through myosin phosphorylation

What could the CPC be doing to promote furrow ingression, independent from the Centralspindlin complex and its role in promoting chromosome segregation and midzone formation? The kinase activity of AuroraB is required for its role during cytokinesis (Terada, Tatsuka et al. 1998; Murata-Hori and Wang 2002), and a number of different substrates for AuroraB have been identified, including histone H3, myosin regulatory light chain (MRLC), CENP-A, INCENP, MgcRacGAP, vimentin, desmin, survivin, and MCAK (Rev. Vagnarelli and Earnshaw 2004). The clearest link to furrow ingression was the regulation of the regulatory light chain of myosin, which was able to be phosphorylated by the homolog, AIM-1, *in vitro* (Murata-Hori, Fumoto et al. 2000). Myosin motor activity and interaction with f-actin is regulated by phosphorylation of its regulatory light chain on Ser19/Thr18 (Rev. Matsumura 2005). In addition, recent cryo-electron microscopy work has

shown that active myosin motors can promote actin disassembly via the progressive unbundling and depolymerization of filaments (Haviv, Gillo et al. 2008).

In order to test whether AuroraB^{AIR-2} is performing its critical function during cytokinesis by regulating MRLC, we wanted to compare AuroraB^{AIR-2} to another well-characterized kinase, Rho kinase$^{LET-502}$, which is known to phosphorylate both MRLC and MEL-11, the myosin binding subunit of the myosin phosphatase. In *C. elegans*, depletion of RhoK$^{LET-502}$ slowed the rate of furrow ingression, but the first division was always successful (Fig. 4.4B,C; Piekny and Mains 2002; Maddox, Lewellyn et al. 2007). Mutation of RhoK$^{LET-502}$ caused embryonic lethality, but this was rescued by mutation of the myosin binding subunit of the phosphatase, MEL-11 (Piekny and Mains 2002). Depletion of RhoK$^{LET-502}$ did enhance the *air-2(or207ts)* mutant phenotype, but depletion of MEL-11 did not have a significant effect on the rate or maximum extent of ingression of the mutant (Fig. 4.4). The fact that depletion of RhoK$^{LET-502}$ enhances the AuroraB^{AIR-2} mutant phenotype is not particularly informative, since it doesn't tell us whether the two kinases are both activating myosin, or whether AuroraB^{AIR-2} is involved in a distinct mechanism to drive furrow ingression. However, the fact that depletion of MEL-11 does not affect the *air-2(or207ts)* embryos suggests that the defect in the mutant embryos is not due to a decreased myosin activation or hyperactivity of the myosin phosphatase. Although further biochemistry or other *in vivo* monitoring of

myosin activation is needed to be more conclusive, our data suggests that the CPC is likely not regulating myosin activity during cytokinesis (either directly or indirectly via inhibition of the myosin phosphatase).

4.4.4 Depletion of Septin or Anillin is able to rescue the AuroraB^{AIR-2} mutant embryos

Another characteristic of the RhoK$^{LET-502}$ phenotype is that it is significantly enhanced by co-depletion of the septin^{UNC-59}. Septins are a nonpolar filament system that localizes to the contractile ring (John, Hite et al. 2007). In *C. elegans*, the septins are not required for cytokinesis to occur; however, like the filament linker protein, Anillin^{ANI-1}, they are required to promote asymmetric ingression of the furrow. Furrow asymmetry is not required for cytokinesis, but it does make ingression more robust, especially in conditions where contractility is compromised (such as depletion of RhoK$^{LET-502}$; Maddox, Lewellyn et al. 2007). Here, we see that instead of enhancing the mutant phenotype, depletion of septin^{UNC-59} actually suppresses the *air-2(or207ts)* ingression defect (Fig. 4.5). Although the rate of ingression is not significantly different, the maximum extent of ingression is much greater than the mutant alone, and ~30% of the embryos complete the first division (compared to 0% for the uninjected mutant embryos). This rescue was specific to AuroraB^{AIR-2}, since depletion of septin^{UNC-59} was unable to rescue the ZEN-4 mutant (Fig. 4.5B,C). This would suggest that the contractile ring in

the *zen-4(or153ts)* embryos is compromised to begin with, and disrupting the septins^{UNC-59} makes enhances this defect. In contrast, it suggests that *air-2(or207ts)* embryos are building a normal contractile ring, but something about the constriction of the ring is defective in these embryos. Taken together with the additive phenotype seen upon disruption of both complexes (Fig. 4.1, 4.2), this data further supports the finding that Centralspindlin and the CPC are functioning in separate pathways to promote furrow ingression (Fig. 4.5D).

Depletion of AuroraB^{AIR-2} does not affect the initial localization of septin^{UNC-59} to the equatorial cortex or to the leading edge of the furrow (*data not shown)*, but it is possible that AuroraB^{AIR-2} could be regulating septin dynamics within the ring during constriction. In *C. elegans,* the concentration of septins^{UNC-59} (like Anillin^{ANI-1} and myosin^{NMY-2}) in the contractile ring does not vary during cytokinesis (Carvalho, Desai et al. 2009), suggesting that the septins are being disassembled during ingression. Because depletion of septin^{UNC-59} is able to rescue the *air-2(or207ts)* embryos, it suggests that one possible role for the CPC is to promote disassembly of the contractile ring during ingression. Consistent with this idea, partial depletion of Anillin^{ANI-1}, a linker protein that interacts with myosin, septins, and f-actin (Field and Alberts 1995; Oegema, Savoian et al. 2000; Kinoshita, Field et al. 2002; Maddox, Habermann et al. 2005; Straight, Field et al. 2005), provides an even greater rescue of the *air-2(or207ts)* mutant embryos, with almost half of the embryos completing the first division. Because Anillin^{ANI-1} is linking the different

filament systems of the contractile ring together, partial depletion could make the ring slightly unstable, allowing for easy disassembly. A full depletion of Anillin^{ANI-1}, however, might make the ring too unstable, and thereby prevent proper constriction, which could explain why 4/19 fully depleted *ani-1(RNAi);air-2(or207ts)* did not ingress at all. There is some evidence from other systems linking the CPC to septins. In human cells, AuroraB is able to phosphorylate Septin1 (Qi, Yu et al. 2005), the homolog of UNC-59. In addition, disruption of the interaction between Sli15 and Bir1, members of the CPC in budding yeast, leads to defects in disassembly of the septin ring in the mother cell (Thomas and Kaplan 2007), although disruption of the kinase, Ipl1, did not affect septin dynamics (Gillis, Thomas et al. 2005). Therefore, our work has shown that Centralspindlin and the CPC are participating in distinct molecular pathways to promote furrow ingression. Although the precise role of the CPC during cytokinesis is not known, our work suggests that one critical role could be to promote disassembly of the contractile ring through regulation of Anillin or the septins.

4.5 Materials and Methods

4.5.1 Strains and live imaging

The genotypes of all strains used are listed in Supplemental Table I. The strains OD58 (Audhya, Hyndman et al. 2005), OD38, and OD73 (Maddox,

Lewellyn et al. 2007) were described previously. The strain JJ1473 expressing NMY-2:GFP (Nance, Munro et al. 2003) was a gift of Edwin Munro. Strains were maintained at 20° C, except for the temperature sensitive strains, which were maintained at 16° C. Live imaging was performed on newly fertilized embryos mounted as previously described (Oegema, Desai et al. 2001). Embryos were filmed using a spinning disk confocal mounted on a Nikon TE2000-E inverted microscope controlled by the Andor iQ software (Andor Technology, Belfast, Ireland) equipped with an electron multiplication back-thinned charge-coupled device camera (iXon) and solid state 100 mW lasers. In all cases a 60x, 1.4 NA PlanApochromat lens with 2x2 binning was used. For cortical imaging, 4 z-sections were collected at 1µm intervals. For end-on projections, 11 z-sections were collected at 2.5µm intervals, and the region of the furrow was isolated, projected, and rotated 90° using MetaMorph software. For temperature sensitive strains, imaging was done at restrictive temperature, which was monitored using a Digi-Sense Type T Thermocouple thermometer (Cole Palmer, Vernon Hill, IL).

4.5.2 RNA-mediated interference

dsRNAs were prepared as described (Oegema, Desai et al. 2001) using the primers listed in Supplemental Table II to amplify regions from N2 genomic or specific cDNAs. L4 hermaphrodites were injected with dsRNA and incubated at 20˚C (or 16° for the mutant strains) for 45-48 hours. Depletions

of ECT-2 were done at 20˚C for 20-24 hours because these depletions cause sterility. For double depletions, RNAs were mixed to obtain equal concentrations for each RNA.

4.5.3 Western Blotting

Western blotting of control, *air-2(RNAi), zen-4(RNAi),* and *air-2 & zen-4(RNAi)* worms was performed as described (Hannak, Kirkham et al. 2001). Western blots were initially probed using 2 µg/ml rabbit anti–ZEN-4 or anti-AIR-2, which was detected using a HRP-conjugated secondary antibody (1:10,000; Bio-Rad Laboratories). The same blot was subsequently probed for α-tubulin using the monoclonal DM1α (1:100; Sigma-Aldrich) followed by an alkaline-phosphatase–conjugated anti-mouse secondary antibody (1:3,750; Jackson ImmunoResearch Laboratories).

4.6 Acknowledgements

We thank members of the Oegema and Desai labs, especially Julie Canman and Ana Carvalho, for their support. K.O. and A.D. receive salary and additional support from the Ludwig Institute for Cancer Research. K.O. is a Pew Scholar in the Biomedical Sciences. L.L. was supported by the NIH/NIGMS funded UCSD Genetics Training Program (T32 GM008666) and a training from the National Cancer Institute.

4.7 Abbreviations

NEBD- Nuclear Envelope Breakdown;

CPC- Chromosomal Passenger Complex

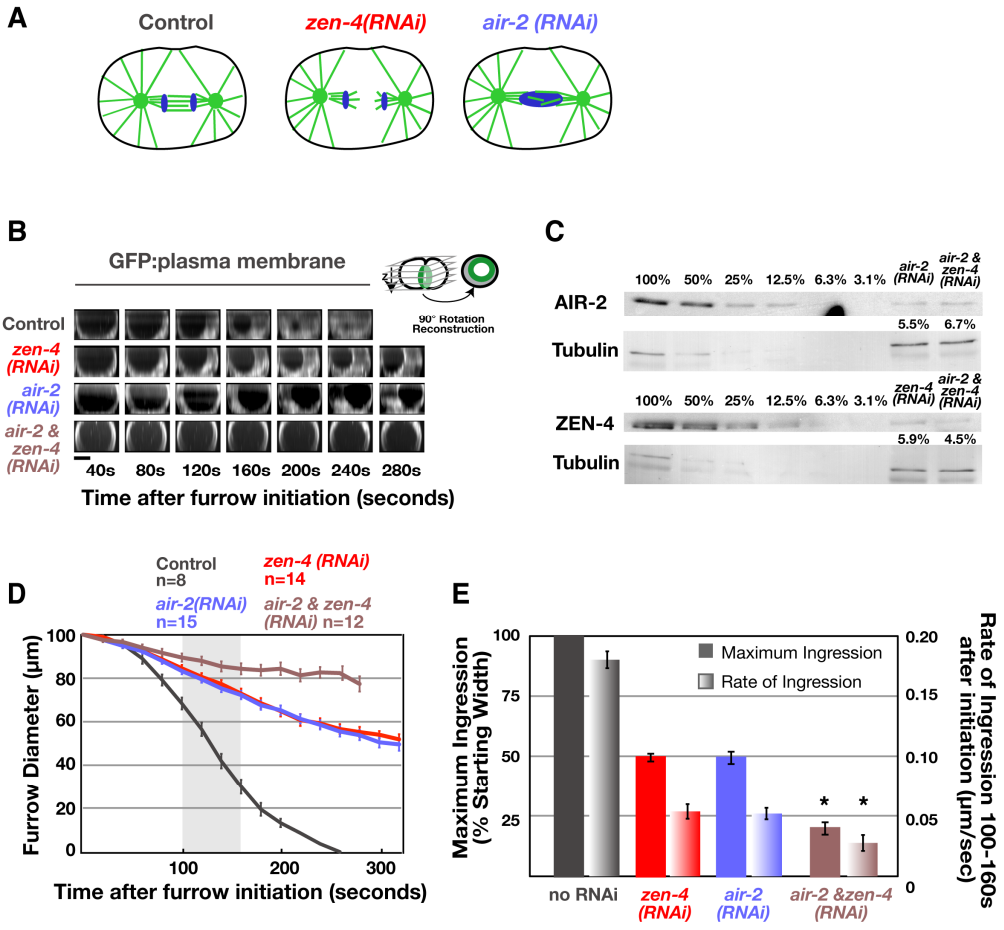

Figure 4.1 Centralspindlin and the Chromosomal Passenger Complex are coordinately required to promote furrow ingression.

(A) Schematic of the effect of each depletion on the morphology of the anaphase spindle and chromosome segregation. (B) End on reconstructions of control (n=8), *zen-4(RNAi)* (n=14), *air-2(RNAi)* (n=15), and *air-2 & zen-4(RNAi)* (n=12) embryos expressing the GFP plasma membrane marker. Time is in seconds after furrow initiation. Scale bar is 10 µm. (C) Western blot of control, *air-2(RNAi)*, *zen-4(RNAi),* and *air-2 & zen-4(RNAi)* worms. Serial dilutions of the control lysate were used to quantify the amount of AuroraB^{AIR-2} or ZEN-4 in the RNAi samples (percentage of amount in 100% control indicated above each lane), which is indicated at right. (D) The average furrow diameter, measured from end-on reconstructions, is plotted versus time (in seconds after furrow initiation). Error bars are SEM. (E) The mean maximum extent of furrow ingression (solid bars), measured as a percentage of initial diameter, and the rate of ingression (shaded bars; in µm/sec) over the time interval 100-160 seconds after furrow initiation is shown for the indicated conditions. Error bars are SEM. Asterisk indicates average values for the *air-2 & zen-4(RNAi)* are significantly different from either single depletion.

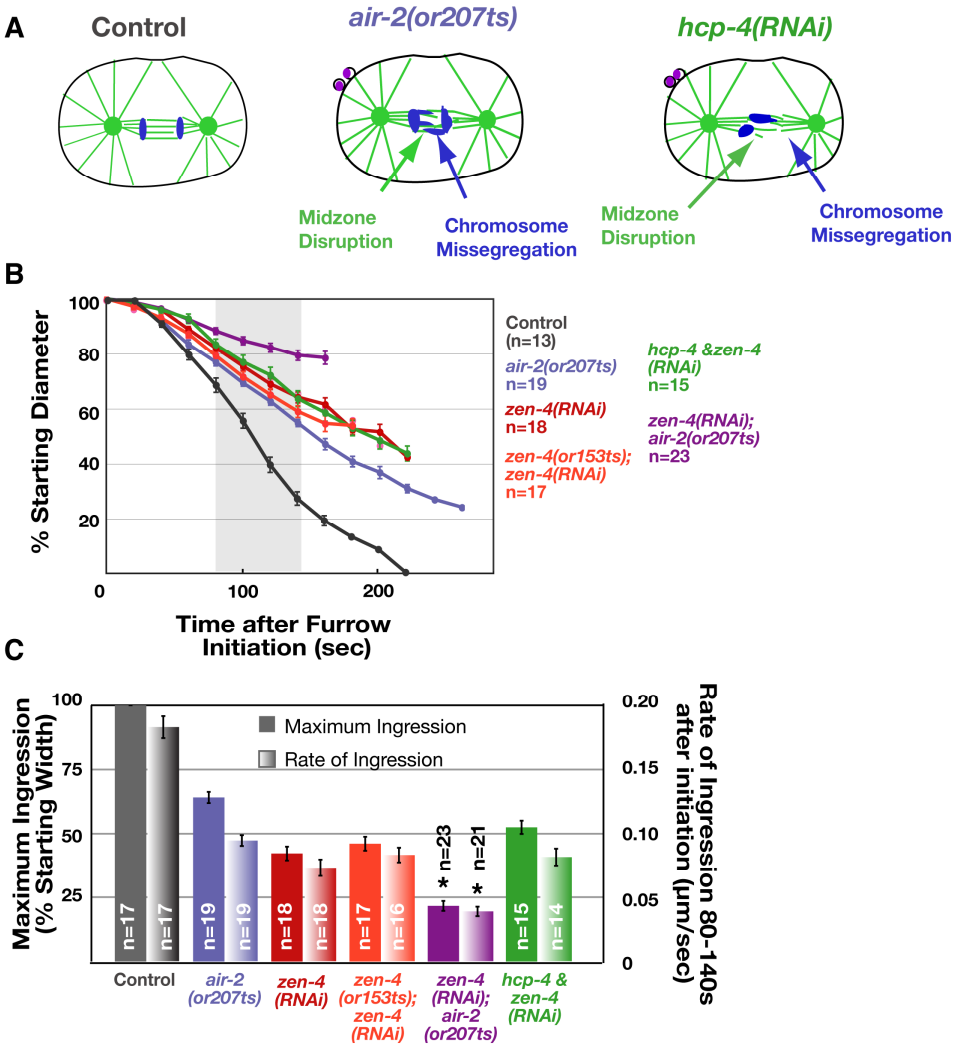

Figure 4.2 Mutation of AIR-2 enhances depletion of ZEN-4, whereas depletion of the inner kinetochore protein, HCP-4, does not.

(A) Schematic of the effect of HCP-4 depletion on chromosome segregation and midzone formation. (B) The average furrow diameter (measured from end-on reconstructions as in 4.1B) is plotted versus time (in seconds after furrow initiation). Error bars are SEM. (C) The mean maximum extent of furrow ingression (solid bars), measured as a percentage of initial diameter, and the rate of ingression (shaded bars; in µm/sec) over the time interval 80-140 seconds after furrow initiation is shown for the indicated conditions. Error bars are SEM. All imaging was done at the restrictive temperature for the mutant. Asterisk indicates that average values for *zen-4(RNAi);air-2(or207ts)* are significantly different (2-tailed t-test, $p<0.05$) from *zen-4(RNAi)* and *air-2(or207ts)*.

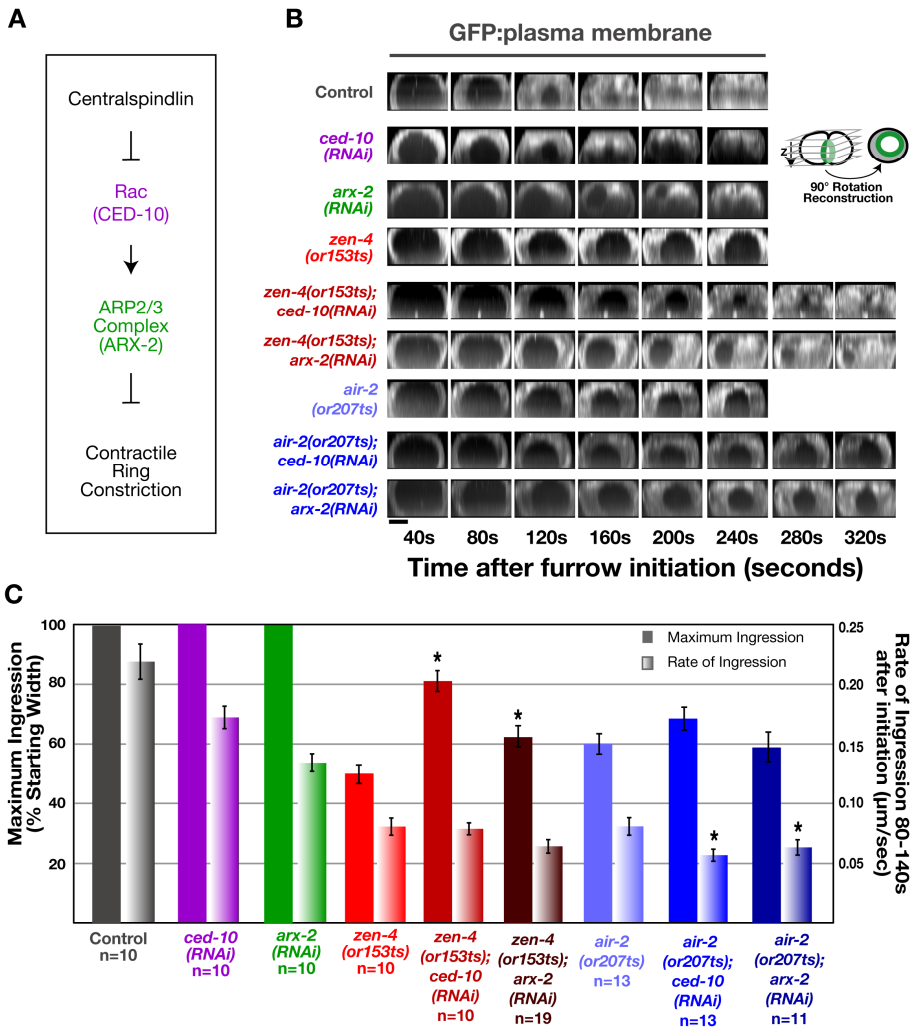

Figure 4.3 Depletion of Rac^{CED-10} or Arp2^{ARX-2} partially rescues a ZEN-4 mutant, but not an AuroraB^{AIR-2} mutant.

(A) Schematic of the role of Centralspindlin in Rac inactivation during cytokinesis. (B) Representative end-on reconstructions of embryos depleted of Rac^{CED-10} or Arp2^{ARX-2}. (C) The mean maximum extent of furrow ingression (solid bars), measured as a percentage of initial diameter, and the rate of ingression (shaded bars; in µm/sec) over the time interval 80-140 seconds after furrow initiation is shown for the indicated conditions. Error bars are SEM. All imaging was done at the restrictive temperature for the mutant. Asterisk indicates that average values that are significantly different (2-tailed t-test, $p<0.05$) from the uninjected mutant (at restrictive temperature).

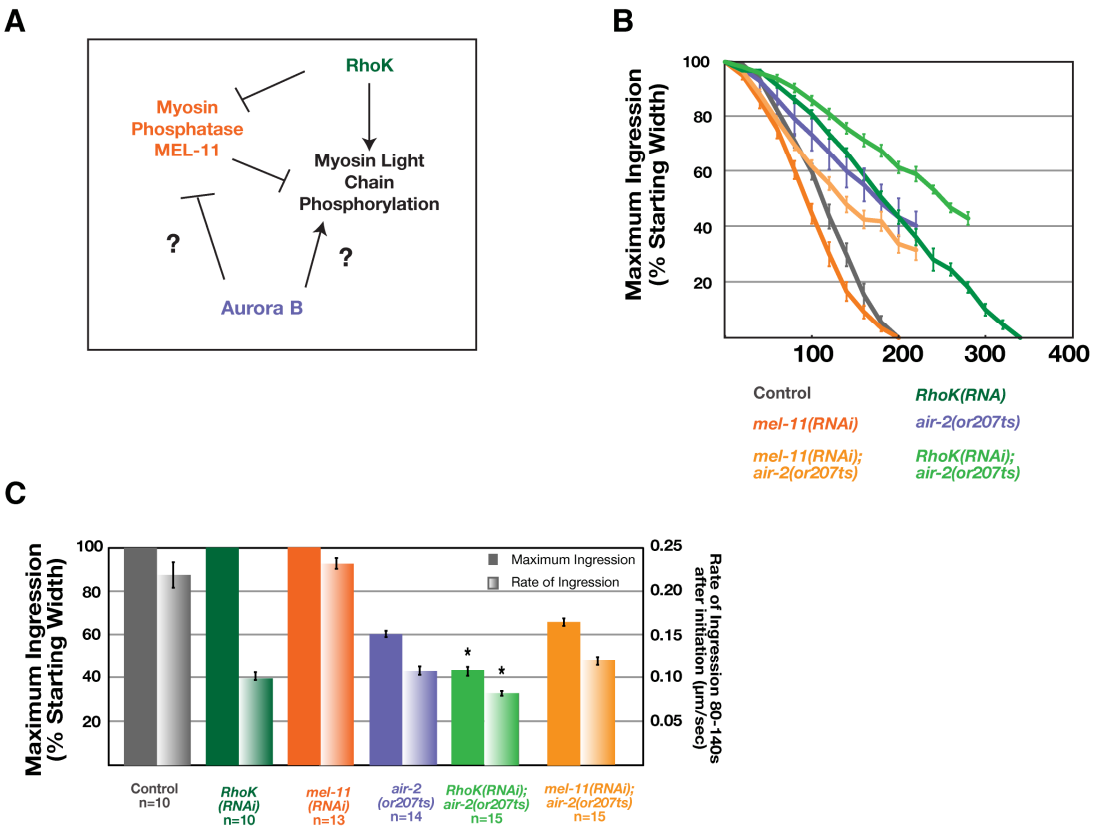

Figure 4.4 Depletion of RhoK$^{LET-502}$ enhances *air-2(or207ts)* mutant embryos, but depletion of the myosin phosphatase, MEL-11, does not rescue it.

(A) Schematic of the role of Rho kinase in promoting myosin activation through direct phosphorylation of myosin regulatory light chain and through inhibition of the myosin phosphatase. The putative role for AuroraB is indicated. (B) The average furrow diameter (measured from end-on reconstructions as in 4.1B) is plotted versus time (in seconds after furrow initiation). Error bars are SEM. (C) The mean maximum extent of furrow ingression (solid bars), measured as a percentage of initial diameter, and the rate of ingression (shaded bars; in µm/sec) over the time interval 80-140 seconds after furrow initiation is shown for the indicated conditions. Error bars are SEM. All imaging was done at the restrictive temperature for the mutants. Asterisks indicate significant differences (2-tailed t-test, $p<0.05$) as compared to uninjected mutants at the restrictive temperature.

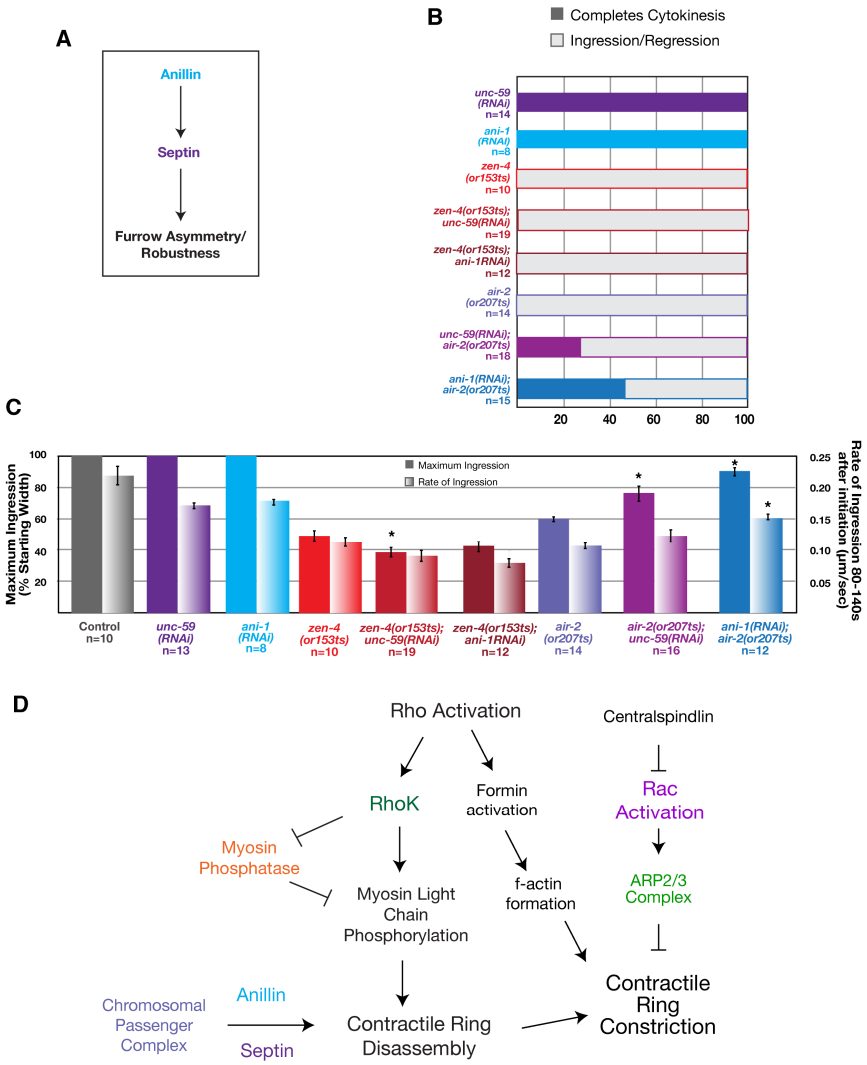

Figure 4.5 Depletion of Anillin^{ANI-1} or septin^{UNC-59} is able to rescue AuroraB^{AIR-2} mutant embryos.

(A) Schematic showing that targeting of septins to the contractile ring is dependent on the presence of Anillin. Both Anillin and the septins are required to promote asymmetric localization of other contractile ring proteins and asymmetric furrow ingression. (B) Percentage of embryos that complete the first division (measured from end-on reconstructions as in Fig. 4.1B). (C) The mean maximum extent of furrow ingression (solid bars), measured as a percentage of initial diameter, and the rate of ingression (shaded bars; in µm/sec) over the time interval 80-140 seconds after furrow initiation is shown for the indicated conditions. Error bars are SEM. All imaging was done at the restrictive temperature for the mutants. Asterisks indicate that *unc-59(RNAi);zen-4(or153ts)* is significantly different (2-tailed t-test, $p<0.05$) as compared to *zen-4(or153ts)* at the restrictive temperature. (D) Model showing the potential role for the CPC in promoting contractile ring disassembly during furrow ingression.

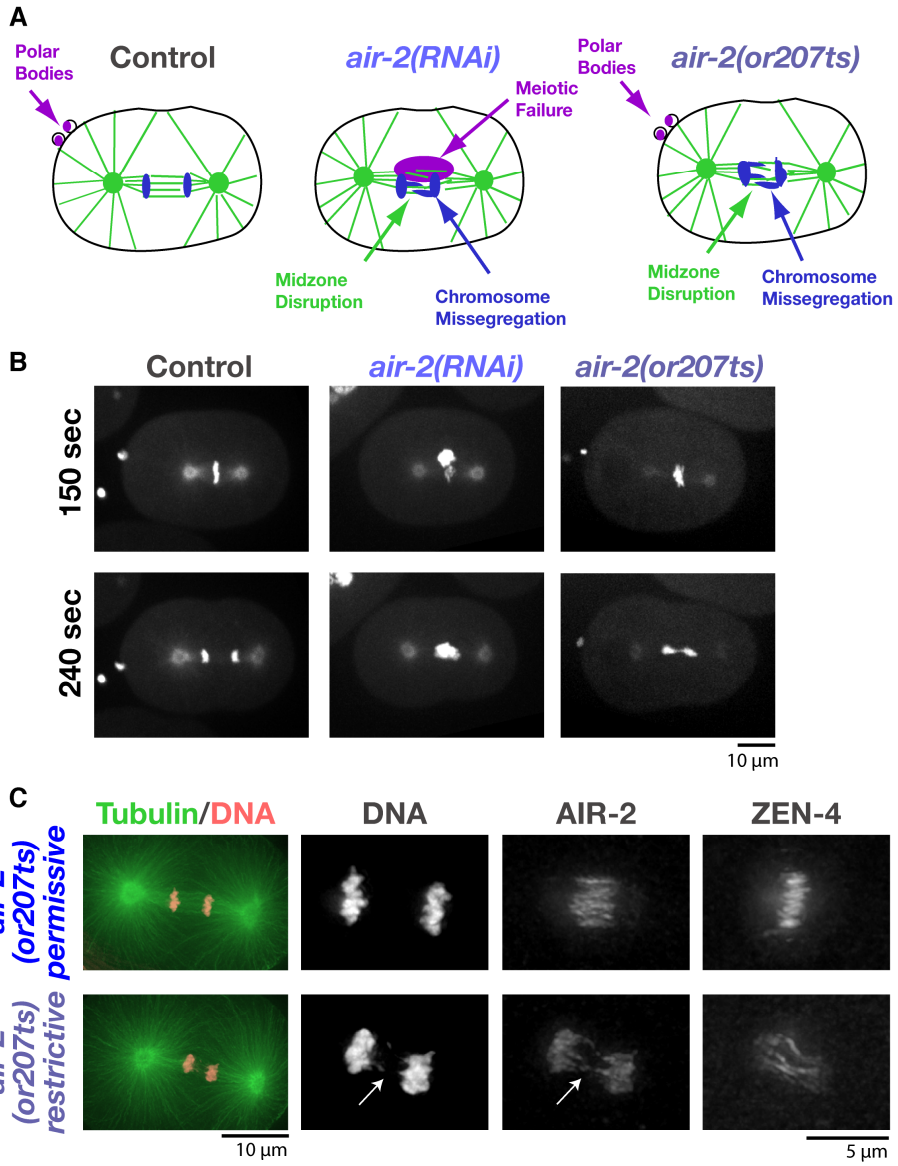

Figure S4.1 A temperature sensitive mutation in the kinase, AIR-2, is able to bypass the requirement for the CPC during meiosis.

(A) Schematic comparing the phenotype of control, *air-2(RNAi)*, and *air-2(or207ts)* mutant embryos shifted to the restrictive temperature after meiosis. (B) Maximum intensity projections of 5-2µm sections taken of embryos expressing GFP:tubulin and GFP:Histone H2B. All embryos were imaged at the restrictive temperature. (C) Immunofluorescence of *air-2(or207ts)* embryos fixed at the permissive or restrictive temperature. Images are maximum intensity projections of the midzone region of the cell. Arrows indicate chromosome bridges. Scale bars are 10µm.

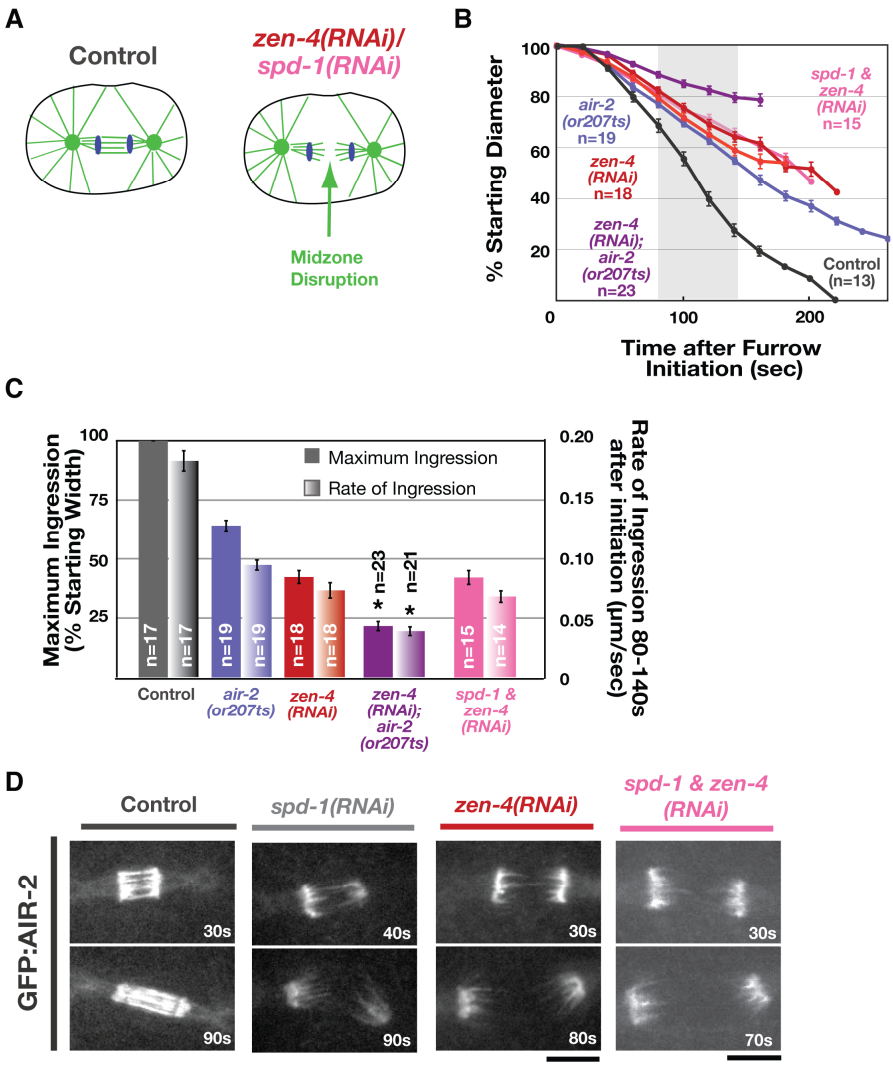

Figure S4.2 Depletion of the microtubule bundling protein, SPD-1, does not enhance depletion of ZEN-4.

(A) Schematic of the effect of ZEN-4 or SPD-1 depletion on midzone structure during anaphase. (B) The average furrow diameter (measured from end-on reconstructions as in 1B) is plotted versus time (in seconds after furrow initiation). Error bars are SEM. (C) The mean maximum extent of furrow ingression (solid bars), measured as a percentage of initial diameter, and the rate of ingression (shaded bars; in µm/sec) over the time interval 80-140 seconds after furrow initiation is shown for the indicated conditions. Error bars are SEM. All imaging was done at the restrictive temperature for the mutant. Average values for control, *air-2(or207ts),* *zen-4(RNAi),* and *zen-4(RNAi);or207ts)* are repeated from Fig. 4.3 for comparison. Asterisk indicates that average values for *zen-4(RNAi);air-2(or207ts)* are significantly different from *zen-4(RNAi)* and *air-2(or207ts)*. (D) Single plane confocal images from timelapse sequences of control (n=9), *spd-1(RNAi)* (n=12), *air-2(RNAi)* (n=11), and *air-2 & spd-1(RNAi)* (n=10) embryos expressing GFP:CYK-4. Time zero corresponds to the frame immediately preceding anaphase onset. Bars are 5 µm.

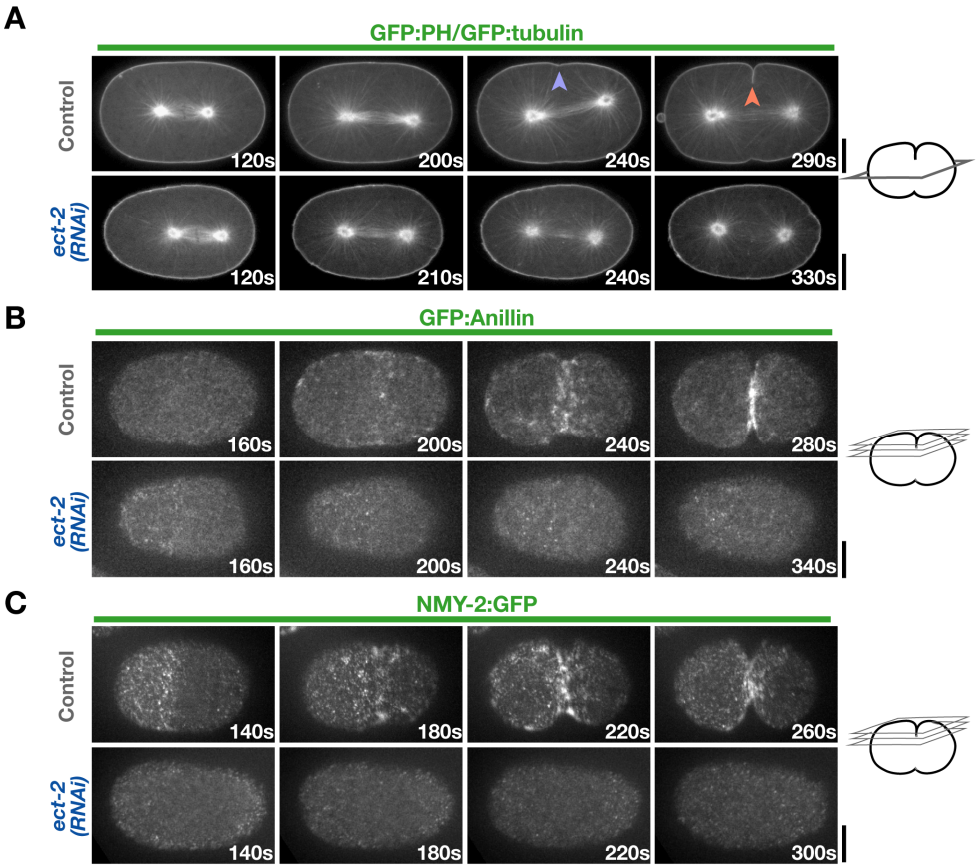

Figure S4.3 Depletion of the RhoGEF, ECT-2, inhibits recruitment of contractile ring proteins and furrow ingression.

Spinning disk confocal optics were used to image control and *ect-2(RNAi)* embryos (A) co-expressing GFP:β-tubulin and a GFP plasma membrane marker (control n=39, *ect-2(RNAi)* n=9), expressing (B) GFP:Anillin (control n>50, *ect-2(RNAi)* n=14), or (C) NMY-2:GFP (control n>100, *ect-2(RNAi)* n=16). Representative images, either a single central section or a maximum intensity projection of 4 sections collected at 1 μm intervals in z (*as indicated by schematics to the right*), are shown. Times are in seconds after nuclear envelope break down (NEBD). Arrowheads in (A) indicate the initial deformation of the cortex (*blue*) and furrow involution (*red*) in the embryo shown. Bar is 10 μm.

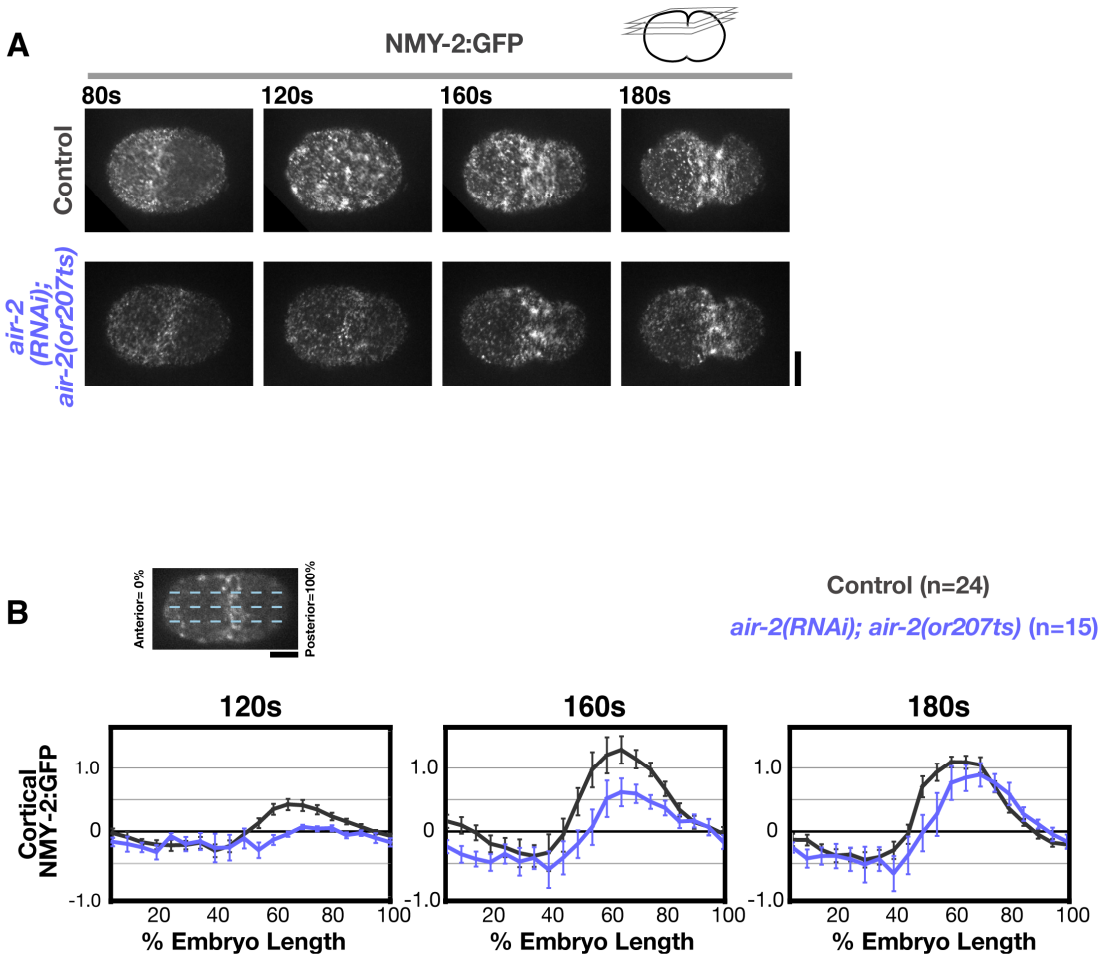

Figure S4.4 Depletion of AuroraB^{AIR-2} in the *air-2(or207ts)* mutant does not dramatically affect the recruitment of myosin to the cortex.

(A) Cortical imaging of control and *air-2(RNAi);air-2(or207ts)* embryos expressing NMY-2:GFP. (B) Quantification of the average post-anaphase cortical NMY-2:GFP, calculated as in Fig. 2.3. Average linescans (40 pixels wide) were drawn (anterior to the posterior) on maximum intensity projections, and divided into 20 equal segments. Value within that segment at a time point prior to anaphase onset was subtracted, and values were divided by the average maximum value of controls (55-65% embryo length at 180s). Bar is 10 µm.

Table 4.1 Worm strains used in this study

Strain #	Genotype
OD27	unc-119(ed3) III; ltIs14 [pASM05; pie-1/GFP::AIR-2;unc-119 (+)]
OD38	unc-119(ed3) III; ltIs28 [pASM14; pie-1/GFP::ANI-1; unc-119 (+)]
JJ1473	unc-119(ed3) III; zuIs45[nmy-2::NMY-2::GFP + unc-119(+)] V.
EU554	zen-4(or153ts) IV
EU630	air-2(or207ts) I
OD73	unc-119(ed3) III; ltIs38 [pAA1; pie-1/GFP::PH(PLC1delta1); unc-119 (+)]; ltIs24 [pAZ132; pie-1/GFP::tba-2; unc-119 (+)]
OD95	unc-119(ed3) III; ltIs37 [pAA64; pie-1/mCHERRY::his-58; unc-119 (+)] IV; ltIs38 [pAA1; pie-1/GFP::PH(PLC1delta1); unc-119 (+)]
OD106	zen-4(or153ts) IV; ltIs38 [pAA1; pie-1/GFP::PH(PLC1delta1); unc-119 (+)]
OD52	unc-119(ed3) ruIs32[pAZ132; pie-1/GFP::histone H2B] III; ltIs24 [pAZ132; pie-1/GFP::tba-2; unc-119 (+)]
OD253	air-2(or207ts) I; unc-119(ed3) ruIs32[pAZ132; pie-1/GFP::histone H2B] III; ltIs24 [pAZ132; pie-1/GFP::tba-2; unc-119 (+)]
OD283	air2(or207ts)I; zuIs45[nmy-2::NMY-2::GFP + unc-119(+)]V
OD105	air-2(or207ts) I; unc-119(ed3) III; ltIs38 [pAA1; pie-1/GFP::PH(PLC1delta1); unc-119 (+)]

Table 4.2 dsRNAs used in this study

Gene	Oligo 1	Oligo 2	Template	RNA Concentration (mg/ml)
Y34D9A.4 (*spd-1*)	TAATACGAC TCACTATAG GTCGTTGAC GCGTACTCA ACT	AATTAACCCT CACTAAAGGG AATTCGAAAT CCGACTCCA	N2 genomic	3.11
B0207.4 (*air-2*)	AATTAACCC TCACTAAAG GTTTCGAGA TCGGAAGAC CAC	TAATACGACT CACTATAGGC AACGACAAGC AATCTTCCA	yk483g8	1.49
M03D4.1 (*zen-4*)	AATTAACCC TCACTAAAG GAATTGGTT ATGGCTCCG AGA	TAATACGACT CACTATAGGA TTGGAGCTGT TGGATGAGC	yk35d10	1.28
W09C5.2 *(unc-59)*	TAATACGAC TCACTATAG GCGTGAAAC TCGTGGAGA ACA	AATTAACCCT CACTAAAGGT TGTGGTGGA GTTCAACGTG	Sep1-A	1.95
T03F1.9 *(hcp-4)*	AATTAACCC TCACTAAAG GGGAAATGT ACGGAGCG AAAA	TAATACGACT CACTATAGGA CATTGTTGGT GGGTCCAAT	N2 genomic	1.36
C10H11.9 *(let-502)*	TAATACGAC TCACTATAG GCCAGGAT CCTCGTCAT TTGT	AATTAACCCT CACTAAAGGT CGGTTTTTCG AGTCCAACT	N2 genomic	1.65
C06C3.1 *(mel-11)*	AATTAACCC TCACTAAAG GAAAAGGA GCCGATGT GAATG	TAATACGACT CACTATAGGT CGTTTCCGTT CACTTGTCA	N2 genomic	2.7
Y49E10.19 *(ani-1)*	TAATACGAC TCACTATAG GTCAAACTC AATGGAGAG GACAA	AATTAACCCT CACTAAAGGC ATTGTGCTTC AAATTCCTCA C	Anil3-A	2.18

Table 4.2 dsRNAs used in this study (continued)

Gene	Oligo 1	Oligo 2	Template	RNA Concentration (mg/ml)
T19E10.1A *(ect-2)*	TAATACGAC TCACTATAG GTGGATCC GATTCTCGA ACTT	AATTAACCCT CACTAAAGGA CATTTGGCTT TGTGCTTCC	N2 genomic	1.75

Chapter 5: Conclusions and Future Directions

My thesis work has focused on the process of cytokinesis, which physically separates a single cell into two daughter cells following chromosome segregation. In order to prevent aneuploidy, the process of cytokinesis must be precisely coupled to chromosome segregation. This coordination insures that division will not occur prematurely, before the chromosomes have separated, and that the plane of division will be positioned between the two chromosome masses. One of the most important questions within the cytokinesis field is how does a cell determine when and where to initiate furrow ingression, and further, once it begins, how is furrow ingression driven to completion.

5.1 Aster-based signaling

Because the process of cytokinesis must be coordinated with the events of nuclear division, it is logical that the position of the furrow would be correlated to the position of the spindle, the structure that is responsible for chromosome separation. As early as 1896, Boveri observed that cytokinesis occurrs between the asters, and two asters alone are sufficient to induce furrow formation (Rev. Rappaport 1996). The furrow is responsive to changes in the position of the spindle: movement of the spindle during anaphase or telophase results in repositioning of the furrow to correspond to the new

midpoint between the asters (Rappaport and Rappaport 1993). Therefore, the anaphase spindle is important to continuously signal to the cortex to position the furrow and promote ingression.

Most of the early work in the field concentrated on the role of the astral microtubules in promoting cytokinesis. Astral microtubules grow out from the centrosomes, producing a dense array of filaments that contact the cortex. One model put forth by Lewis Wolpert (1960) was that of “astral relaxation.” This model was expanded on by work from Schroeder (1981), and later modeled by White and Borisy (1983). The model proposed that there was a global increase in cortical tension, which was then inhibited in the polar regions due to the proximity of astral microtubules. In this way, there would be a local relaxation at the poles, and the equatorial tension would thereby promote furrowing. Since then, a role for the astral microtubules in inhibiting contraction has been supported by the observation that shortening or depolymerization of microtubules induces contractility (Canman, Hoffman et al. 2000; Kurz, Pintard et al. 2002), and that movement of the spindle to an ectopic location redistributes contractile proteins, such as myosin, away from the position of the spindle (Hird and White 1993; Werner, Munro et al. 2007). If this model were correct, then a cell would require a minimum of microtubule to contact the equatorial region of the cell to induce furrow formation, which is what has been observed (Dechant and Glotzer 2003).

In contrast, Ray Rappaport proposed that the distal tips of the astral microtubules deliver a positive signal to the cortex, and although the signal would be present throughout, the equatorial region would experience a higher concentration of the signal, thereby inducing furrow formation (Rev. Rappaport 1996). Based on later work, it was suggested that a subpopulation of stable astral microtubules that contact the cortex might provide the positive signal to induce furrowing (Canman, Cameron et al. 2003; Shannon, Canman et al. 2005; Foe and von Dassow 2008; Odell and Foe 2008). Although there has been much debate on whether the astral microtubules positively or negatively affect the cortex, they are not actually required for furrow ingression in many systems. *Drosophila asterless* mutants, which lack functional centrosomes, are still able to divide (Bonaccorsi, Giansanti et al. 1998), presumably due to signaling from the spindle midzone.

Later work began to look at the role of the spindle midzone, an array of anti-parallel bundles of microtubules that forms between the separating chromosomes during anaphase. Perforation of a cell between the midzone and the equatorial cortex blocked furrowing, even though astral microtubules were still able to contact the cortex (Cao and Wang 1996), suggesting that there was a critical positive signal that was generated by the spindle midzone to promote furrow ingression. Further, cells are still able to contract even following removal of centrosomes and chromosomes (Hiramoto 1971; Alsop

2003): this contractility was associated with bundles of microtubules at the cortex (Alsop 2003).

Although work on both astral microtubules and the spindle midzone were informative, they largely overlooked the possibility of the integration of these two signals, making work by Bringmann and Hyman (2005) influential in changing the thinking within the field. Using their laser severing assay, which spatially separated the position of the midzone from the point midway between the asters, they showed that two distinct furrows were formed: an initial furrow midway between the asters, and a second furrow corresponding to the position of the midzone. This suggests that the asters and midzone provide two sequential, redundant signals to promote furrow ingression. Although later work elaborated on this model (Dechant and Glotzer 2003; Bringmann and Hyman 2005; Bringmann and Hyman 2005; Foe and von Dassow 2008), our work was the first to demonstrate that signals from the asters are not in fact redundant with signals from the spindle midzone. Instead, we show that the asters are likely helping to pattern the cortex during early anaphase and generating a region in the equator that is primed for constriction, likely through inhibiting contractility in the polar regions. Proper aster separation insures that the astral microtubules contact the polar cortex during early anaphase. In sea urchin eggs, it was shown that the density of astral microtubules was higher at the poles during early anaphase: at the time of furrow initiation, the relative density at the poles was equal to that at the equator (Strickland, Wen et al.

2005). If it were critical for the astral microtubules to contact the polar cortex during early anaphase to inhibit contractility in these regions, then delaying aster separation (such as by depletion of TPXL-1) would disrupt normal patterning of contractility, which is exactly what we observed (Fig 2.3). Therefore, this suggests that the astral microtubules are inhibiting contractility in the poles, and this influence depends on proper aster separation.

In contrast to disruption of aster-based signaling, depletion of two key complexes that localize to the spindle midzone, Centralspindlin and the Chromosomal Passenger Complex (CPC), reduces the rate of furrow ingression and causes cytokinesis failure. Disrupting both aster separation and Centralspindlin or the CPC completely blocks early patterning of contractility and furrow ingression (Fig 2.7), which might be expected if you were disrupting two redundant signals. However, in contrast to the model proposed by Bringmann and Hyman (2005), our work suggests that these two signals are not functionally redundant. Preventing aster separation via simultaneous depletion of TPXL-1 and GPR-1/2 leads to formation of multiple furrows that ingress toward the spindle midzone (Fig 2.8); additionally, the patterning of contractile ring proteins on the cortex is completely disrupted (Fig S2.4). This implies that the aster-based signal is not necessary for furrow ingression, but it does help to limit the zone of contractility, which is primarily driven by signaling from the midzone (Fig 2.9). In sea urchin embryos, treatment with a low dose of nocodazole leads to depolymerization of dynamic

microtubules, leaving more stable astral microtubules and midzone microtubules intact: this treatment did not inhibit furrowing, but it did generate a broader region of active myosin in the equator (Foe and von Dassow 2008). Therefore, dynamic astral microtubules are not required to promote furrow formation, but they may help to refine the plane of division in embryonic cells, where the midzone is a point source within the large volume of the cell.

One of the major open questions that still remains is how do the dynamic astral microtubules inhibit the accumulation of contractile ring proteins on the polar cortex? One possibility is that this could be via Rho family GAPs and GEFs. It is known that the RhoGEF, GEF-H1, localizes to the ends of microtubules that contact the cortex. Depolymerization of microtubules leads to the release of GEF-H1, which then activates Rho, leading to contractility (Krendel, Zenke et al. 2002; Birkenfeld, Nalbant et al. 2007). If the microtubule bound form of GEF-H1 is inactive, then maybe in the polar regions of the cell, where the density of microtubules is greater during early anaphase (Strickland, Wen et al. 2005), there is less non-microtubule bound GEF-H1 available to promote Rho activation, effectively inhibiting contractility in those regions. Another possibility is that astral microtubules are somehow affecting the localization or activity of RhoGAPs, such as the recently identified RGA-3/4 in *C. elegans*. Depletion or mutation of RGA-3/4 leads to extreme ectopic contractility, due to the hyper-activity of Rho (Schmutz, Stevens et al. 2007; Schonegg, Constantinescu et al. 2007), which

is reminiscent of the phenotype following depletion of tubulin. An interesting experiment would be to look at the localization of RGA-3/4 following depolymerization of microtubules. If, for example, dynamic astral microtubules maintain RGA-3/4 on the polar cortices, then disruption of those microtubules could inhibit the localization of RGA-3/4 and increase the levels of Rho activity in those regions.

Another possibility is that astral microtubules in the polar regions are not directly influencing Rho activity, but they are instead promoting activation of other small GTPases, like Rac or Cdc42. In Chapter 3, we present a model in which the Centralspindlin complex is required to down-regulate Rac activity in the equator to promote furrow ingression (Canman, Lewellyn et al. 2008). It is known that Centralspindlin is not required for the early patterning of contractility (Fig 2.6, S3.2), which means that the CYK-4 GAP is likely not important for generating the equatorial band of contractile ring proteins. Maybe there is a microtubule-bound Rac (or Cdc42) GEF that is delivered to the cortex via dynamic astral microtubules. An interesting set of experiments would be to do a small RNAi screen with all of the known GEFs in the *C. elegans* genome to look at the early patterning of Anillin and myosin II. If that GEF were important for this microtubule-based inhibitory signal, then we would expect to see Anillin and myosin II across the entire cortex, and not limited to the equatorial region.

Along the same lines, it would also be very useful to develop probes to monitor the localization of active Rho, Rac, and Cdc42 during anaphase and cytokinesis. These types of probes have been developed in other systems, and they are based on the binding domains of effector molecules, which specifically interact with the active, GTP-bound form of the protein (Pertz and Hahn 2004; Benink and Bement 2005; Nakamura, Aoki et al. 2005). Developing such probes to use in the *C. elegans* embryo has proven to be quite challenging, but it would allow us to monitor the dynamic spatial localization and activation of these important small GTPases in wild type embryos and following experimental manipulation, such as disruption of aster separation.

5.2 The spindle midzone and cytokinesis

The other focus of my thesis has been on the role of the spindle midzone in promoting furrow ingression. From the results in Chapter 2, we believe that the spindle midzone is providing a positive signal to promote furrow formation and ingression. Disruption of midzone bundle formation, via depletion of the bundling protein, SPD-1, did not affect the early patterning of contractility or the rate or success of furrow ingression. In fact, depletion of SPD-1 actually increased the levels of anillin and myosin on the equatorial cortex and led to premature furrow formation (Fig 2.5, 2.6). This suggests that bundling of the midzone microtubules is not required for cytokinesis, but it is

important to sequester the positive midzone-based signal (mediated by Centralspindlin and the CPC) from acting on the cortex until after furrow initiation. My work has shown that depletion of Centralspindlin or the CPC did not affect the initial patterning of contractility, but it did cause a decrease in the rate of ingression and ultimately led to failure of the first division (Fig 2.5, 2.6). Although it has been known for many years that these two complexes are required for cytokinesis, the mechanism by which they are acting to promote furrow ingression has remained a mystery.

5.2.1 Centralspindlin and small GTPases

Work with a collaborator in the lab, Dr. Julie Canman, provided significant insight into the mode of action of the Centralspindlin Complex. Through a genetic screen for temperature sensitive sterile mutants, two novel mutations within the GAP domain of the Centralspindlin component, CYK-4, were identified. In contrast to previous Centralspindlin mutants, these GAP mutants did not affect formation of the spindle midzone or interaction with the other member of the complex, ZEN-4 (Fig. 3.2). However, mutation of the GAP domain led to a decreased rate of ingression and eventual failure of the first division (Fig. 3.1). Through a targeted RNAi screen, we showed that depletion of the Rac homologs, RAC-2 or CED-10, was able to rescue the CYK-4 GAP mutants (Fig. 3.3): about 70% of *ced-10(RNAi);cyk-4(or749ts)* embryos were able to complete the first division at restrictive temperature.

Further, depletion of the downstream effectors – Arp2^{ARX-2} or Wave^{WVE-1}/Wasp^{WSP-1} was also able to rescue the *cyk-4(or749ts)* phenotype (Fig 3.4), suggesting that the key role of the Centralspindlin complex is to promote inactivation of Rac in the equatorial region during furrow ingression.

The role of Centralspindlin in Rac inactivation is consistent with previous work showing that there is a local decrease in Rac activity in the equatorial region during cytokinesis (Yoshizaki, Ohba et al. 2003). In addition, overexpression of a dominant active form of Rac causes cytokinesis failure (Muris, Verschoor et al. 2002). One of the important open questions regarding the Centralspindlin complex is whether localization to the midzone bundles is important for its activity. Depletion of SPD-1 severely disrupts localization of the Centralspindlin complex to the midzone (Fig S2.3), and Verbrugghe (2004) showed that this perturbation promotes its association with the membrane and ingressing furrow. A recent modeling paper proposes that the Centralspindlin complex is transported along astral microtubules toward the cortex. When it is traveling along a dynamic microtubule, catastrophe will likely occur before the (+) end contacts the cortex; however, when the complex is associated with a stable microtubule, it will be able to walk along that track and eventually reach the cortex. Because there is a stable population of astral microtubules associated with the equatorial cortex (Canman, Cameron et al. 2003; Foe and von Dassow 2008), this model would predict an enrichment of Centralspindlin at the equator (Odell and Foe 2008), where it might promote cytokinesis. In

Drosophila cells, tethering the CYK-4 homolog, RacGAP50c, to the membrane was sufficient to induce cortical contractility (D'Avino, Savoian et al. 2006), suggesting that localization of Centralspindlin to the midzone is not required for its activity during cytokinesis.

Although we have shown that one of the key roles of the Centralspindlin complex in *C. elegans* is to inactivate Rac, in other systems, the Centralspindlin complex interacts with the RhoGEF, ECT-2, and is required for its localization to the spindle midzone (Somers and Saint 2003; Yuce 2005; Nishimura 2006). If the Centralspindlin complex was important to localize ECT-2 in addition to inactivating Rac, it would explain why depletion of Rac (or Arp2/3) was unable to completely rescue the rate of ingression of *zen-4(or153ts)* or *cyk-4(or749ts)* mutant embryos (Fig. 4.3; *data not shown*). Therefore, it would be interesting to test whether Centralspindlin interacts with ECT-2 in *C. elegans*. Yeast-two-hybrids, immunoprecipitations, and pull-down assays could be used to determine whether there is an interaction, and if so, which domains of ECT-2 and CYK-4/ZEN-4 are required for this interaction. If domains are mapped, those regions could be mutated to determine whether cytokinesis is affected. One could also repeat the tethering experiment to determine whether attaching the Centralspindlin complex to the cortex could induce furrowing, and if so, whether interaction with ECT-2 was required. One could also test whether tethering the Centralspindlin complex to the midzone (by fusing either ZEN-4 or CYK-4 to SPD-1) would disrupt furrow ingression.

From these experiments, we would hopefully learn a little more about the mechanism of the signal from the Centralspindlin complex.

5.2.2 Chromosomal Passenger Complex and Cytokinesis

The other midzone-localized complex that is known to be required for cytokinesis is the Chromosomal Passenger Complex (CPC). Because the CPC is also required for meiotic and mitotic chromosome segregation and midzone formation, it has been more complicated to determine the mechanism through which the CPC is promoting furrow ingression. However, using a temperature sensitive AuroraB^{AIR-2} mutant line, I have shown that the contribution of the CPC during cytokinesis is distinct from its role in meiosis, chromosome segregation, or midzone formation (Fig. 4.2, S4.2).

Previous work has focused on the role of the CPC in promoting the localization and activity of the Centralspindlin Complex (Severson, Hamill et al. 2000; Minoshima, Kawashima et al. 2003; Guse, Mishima et al. 2005), putting the two complexes in a linear pathway to promote furrow ingression. My work has shown that disruption of both Centralspindlin and the CPC enhances either single perturbation (Fig 4.1,4.2), which suggests that two complexes might be performing distinct functions. Further, if the CPC were strictly upstream of Centralspindlin in promoting Rac inactivation, then depletion of Rac or its downstream effectors should similarly be able to rescue mutations in the CPC. However, depletion of neither Rac^{CED-10} (Fig. 4.3; Canman, Lewellyn

et al. 2008) nor Arp2^{ARX-2} (Fig. 4.3) was able to rescue AuroraB^{AIR-2} mutant embryos.

It is known that the kinase activity of AuroraB is required for its role in cytokinesis (Murata-Hori and Wang 2002; Honda, Korner et al. 2003). Although a number of targets have been identified (Rev. Ruchaud, Carmena et al. 2007), none have been confirmed to be the critical target in cytokinesis. One of the more attractive targets is the myosin regulatory light chain (MRLC), whose phosphorylation leads to activation of the motor activity of myosin (Murata-Hori, Fumoto et al. 2000). I chose to compare mutation of AuroraB^{AIR-2} with depletion of a known myosin kinase, Rho kinase (RhoK$^{LET-502}$). MEL-11 is the myosin binding subunit of the myosin phosphatase that removes the activating phosphorylation from MRLC, thereby preventing the motor activity. RhoK not only phosphorylates MRLC to activate it, but it also phosphorylates MEL-11 to inhibit its activity. Because of this opposition, mutation of MEL-11 is able to rescue a RhoK$^{LET-502}$ mutant (Piekny and Mains 2002). We wanted to test whether depletion of MEL-11 would similarly be able to rescue a CPC mutant, which would suggest that AuroraB^{AIR-2} was functioning similarly to RhoK$^{LET-502}$ during cytokinesis. However, depletion of MEL-11 was not able to rescue *air-2(or207ts)* mutant embryos, suggesting that the CPC is likely not functioning redundantly with RhoK$^{LET-502}$.

In addition to the co-suppression of RhoK and the myosin phosphatase, there is a strong synthetic interaction between RhoK$^{LET-502}$ and septins:

embryos depleted of septin^{UNC-59} or RhoK$^{LET-502}$ alone always complete the first division, but co-depletion of both proteins causes >60% of embryos to fail the first division (Maddox, Lewellyn et al. 2007). Surprisingly, depletion of septin^{UNC-59} was actually able to rescue *air-2(or207ts)* mutant embryos. Further, partial depletion of Anillin^{ANI-1}, which is upstream of septin localization to the contractile ring, also rescued the AuroraB^{AIR-2} mutants (Fig. 4.5). Although Anillin^{ANI-1} and septin^{UNC-59} are required to promote the asymmetric localization of other contractile ring proteins around the circumference of the ring and asymmetric furrow ingression, depletion of either protein does not cause cytokinesis failure (Maddox, Habermann et al. 2005; Maddox, Lewellyn et al. 2007). Because depletion of these contractile ring proteins rescues the AuroraB^{AIR-2} mutant, it suggests that the role of the CPC during furrow ingression is to promote disassembly of the contractile ring through regulation of septins or Anillin.

The possibility that the CPC is regulating contractile ring disassembly leads to a number of potential experiments. For example, the first set of experiments would be to test whether AuroraB^{AIR-2} can directly phosphorylate Anillin or the septins and promote their disassembly. I have identified an AuroraB consensus site within the Anillin Homology domain (AHD) of the *C. elegans* protein. *In vitro* kinase assays could be performed, but more complicated biochemistry would probably be useful to determine whether

phosphorylation of the AHD would affect binding of Anillin to the other filament systems.

The septins are a non-polar filament system, and in *C. elegans*, there are two phosphorylation sites (one in either of the two septins – UNC-59 and UNC-61) that were identified via mass spectrometry of whole worms (www.phosphopep.org). Bacterially expressed septins are able to assemble into filaments *in vitro* (John, Hite et al. 2007), so an interesting experiment would be to perform an *in vitro* kinase assay with the septins and AuroraB^{AIR-2}, and determine whether phosphorylation of the septins changes their filament forming ability or dynamics. If phosphorylation sites are mapped within the septins, phospho-mimetic mutations can be made and re-introduced into the *C. elegans* embryo (in the septin mutant background). If this is the key role of the CPC during cytokinesis, then the phospho-mimetic mutation(s) should rescue the *air-2(or207ts)* mutant phenotype.

Overall, my thesis work has shed light on the mechanism by which the anaphase spindle signals to the cortex to promote furrow formation and ingression. I have shown that integration between aster and midzone based signaling is critical to promote formation of a signal furrow. Further, the midzone-based signal is dependent on input from both the Centralspindlin Complex and the Chromosomal Passenger Complex, which are promoting furrow ingression through distinct molecular pathways.

References

Adams, R. R., A. A. Tavares, et al. (1998). "pavarotti encodes a kinesin-like protein required to organize the central spindle and contractile ring for cytokinesis." Genes Dev **12**(10): 1483-1494.

Ahmed, S., J. Lee, et al. (1994). "Breakpoint cluster region gene product-related domain of n-chimaerin. Discrimination between Rac-binding and GTPase-activating residues by mutational analysis." J Biol Chem **269**(26): 17642-17648.

Ainsztein, A. M., S. E. Kandels-Lewis, et al. (1998). "INCENP centromere and spindle targeting: identification of essential conserved motifs and involvement of heterochromatin protein HP1." J Cell Biol **143**(7): 1763-1774.

Alsop, G. B. (2003). "Microtubules are the only structural constituent of the spindle apparatus required for induction of cell cleavage." The Journal of Cell Biology **162**(3): 383-390.

Alsop, G. B. and D. Zhang (2004). "Microtubules continuously dictate distribution of actin filaments and positioning of cell cleavage in grasshopper spermatocytes." J Cell Sci **117**(Pt 8): 1591-1602.

Audhya, A., F. Hyndman, et al. (2005). "A complex containing the Sm protein CAR-1 and the RNA helicase CGH-1 is required for embryonic cytokinesis in Caenorhabditis elegans." J Cell Biol **171**(2): 267-279.

Beach, J. R. and T. T. Egelhoff (2009). "Myosin II recruitment during cytokinesis independent of centralspindlin-mediated phosphorylation." J Biol Chem **284**(40): 27377-27383.

Bement, W. M., H. A. Benink, et al. (2005). "A microtubule-dependent zone of active RhoA during cleavage plane specification." J Cell Biol **170**(1): 91-101.

Bement, W. M., A. L. Miller, et al. (2006). "Rho GTPase activity zones and transient contractile arrays." Bioessays **28**(10): 983-993.

Benink, H. A. and W. M. Bement (2005). "Concentric zones of active RhoA and Cdc42 around single cell wounds." J Cell Biol **168**(3): 429-439.

Birkenfeld, J., P. Nalbant, et al. (2007). "GEF-H1 Modulates Localized RhoA Activation during Cytokinesis under the Control of Mitotic Kinases." Developmental Cell **12**(5): 699-712.

Bishop, J. D. (2002). "Phosphorylation of the Carboxyl Terminus of Inner Centromere Protein (INCENP) by the Aurora B Kinase Stimulates Aurora B Kinase Activity." Journal of Biological Chemistry **277**(31): 27577-27580.

Bonaccorsi, S., M. G. Giansanti, et al. (1998). "Spindle self-organization and cytokinesis during male meiosis in asterless mutants of Drosophila melanogaster." J Cell Biol **142**(3): 751-761.

Brennan, I. M., U. Peters, et al. (2007). "Polo-like kinase controls vertebrate spindle elongation and cytokinesis." PLoS ONE **2**(5): e409.

Bringmann, H., C. Cowan, et al. (2007). "LET-99, GOA-1/GPA-16, and GPR-1/2 Are Required for Aster-Positioned Cytokinesis." Current Biology **17**(2): 185-191.

Bringmann, H. and A. A. Hyman (2005). "A cytokinesis furrow is positioned by two consecutive signals." Nature **436**(7051): 731-734.

Bringmann, H. and A. A. Hyman (2005). "A cytokinesis furrow is positioned by two consecutive signals." Nature **436**(7051): 731-734.

Burkard, M. E., C. L. Randall, et al. (2007). "Chemical genetics reveals the requirement for Polo-like kinase 1 activity in positioning RhoA and triggering cytokinesis in human cells." Proc Natl Acad Sci USA **104**(11): 4383-4388.

Canman, J. C., L. A. Cameron, et al. (2003). "Determining the position of the cell division plane." Nature **424**(6952): 1074-1078.

Canman, J. C., D. B. Hoffman, et al. (2000). "The role of pre- and post-anaphase microtubules in the cytokinesis phase of the cell cycle." Current Biology **10**(10): 611-614.

Canman, J. C., L. Lewellyn, et al. (2008). "Inhibition of Rac by the GAP activity of centralspindlin is essential for cytokinesis." Science **322**(5907): 1543-1546.

Cao, L. G. and Y. L. Wang (1996). "Signals from the spindle midzone are required for the stimulation of cytokinesis in cultured epithelial cells." Mol Biol Cell **7**(2): 225-232.

Carvalho, A., A. Desai, et al. (2009). "Structural memory in the contractile ring makes the duration of cytokinesis independent of cell size." Cell **137**(5): 926-937.

Chalamalasetty, R. B., S. Hummer, et al. (2006). "Influence of human Ect2 depletion and overexpression on cleavage furrow formation and abscission." J Cell Sci **119**(Pt 14): 3008-3019.

Cheeseman, I. M., S. Niessen, et al. (2004). "A conserved protein network controls assembly of the outer kinetochore and its ability to sustain tension." Genes Dev **18**(18): 2255-2268.

D'Avino, P. P., V. Archambault, et al. (2007). "Recruitment of Polo kinase to the spindle midzone during cytokinesis requires the Feo/Klp3A complex." PLoS ONE **2**(6): e572.

D'Avino, P. P., M. S. Savoian, et al. (2006). "RacGAP50C is sufficient to signal cleavage furrow formation during cytokinesis." J Cell Sci **119**(Pt 21): 4402-4408.

D'Avino, P. P., M. S. Savoian, et al. (2004). "Mutations in sticky lead to defective organization of the contractile ring during cytokinesis and are enhanced by Rho and suppressed by Rac." J Cell Biol **166**(1): 61-71.

Dechant, R. and M. Glotzer (2003). "Centrosome separation and central spindle assembly act in redundant pathways that regulate microtubule density and trigger cleavage furrow formation." Dev Cell **4**(3): 333-344.

Desai, A., S. Rybina, et al. (2003). "KNL-1 directs assembly of the microtubule-binding interface of the kinetochore in C. elegans." Genes Dev **17**(19): 2421-2435.

Devore, J. J., G. W. Conrad, et al. (1989). "A model for astral stimulation of cytokinesis in animal cells." J Cell Biol **109**(5): 2225-2232.

Eckley, D. M., A. M. Ainsztein, et al. (1997). "Chromosomal proteins and cytokinesis: patterns of cleavage furrow formation and inner centromere protein positioning in mitotic heterokaryons and mid-anaphase cells." J Cell Biol **136**(6): 1169-1183.

Eggert, U. S., T. J. Mitchison, et al. (2006). "Animal cytokinesis: from parts list to mechanisms." Annu Rev Biochem **75**: 543-566.

Encalada, S. E., P. R. Martin, et al. (2000). "DNA replication defects delay cell division and disrupt cell polarity in early Caenorhabditis elegans embryos." Dev Biol **228**(2): 225-238.

Fay, D. (2006). "Genetic mapping and manipulation: chapter 1--Introduction and basics." Wormbook: 1-12.

Field, C. M. and B. M. Alberts (1995). "Anillin, a contractile ring protein that cycles from the nucleus to the cell cortex." J Cell Biol **131**(1): 165-178.

Foe, V. E. and G. von Dassow (2008). "Stable and dynamic microtubules coordinately shape the myosin activation zone during cytokinetic furrow formation." The Journal of Cell Biology **183**(3): 457-470.

Francis-Lang, H., J. Minden, et al. (1999). "Live confocal analysis with fluorescently labeled proteins." Methods Mol Biol **122**: 223-239.

Gally, C., F. Wissler, et al. (2009). "Myosin II regulation during C. elegans embryonic elongation: LET-502/ROCK, MRCK-1 and PAK-1, three kinases with different roles." Development **136**(18): 3109-3119.

Giet, R. and D. M. Glover (2001). "Drosophila aurora B kinase is required for histone H3 phosphorylation and condensin recruitment during chromosome condensation and to organize the central spindle during cytokinesis." J Cell Biol **152**(4): 669-682.

Gillis, A. N., S. Thomas, et al. (2005). "A novel role for the CBF3 kinetochore-scaffold complex in regulating septin dynamics and cytokinesis." J Cell Biol **171**(5): 773-784.

Glotzer, M. (2004). "Cleavage furrow positioning." J Cell Biol **164**(3): 347-351.

Glotzer, M. (2005). "The molecular requirements for cytokinesis." Science **307**(5716): 1735-1739.

Gonczy, P., H. Schnabel, et al. (1999). "Dissection of cell division processes in the one cell stage Caenorhabditis elegans embryo by mutational analysis." J Cell Biol **144**(5): 927-946.

Gonczy, P. a. R., L.S. (2005) "Asymmetric cell division and axis formation in the embryo." Wormbook.

Guo, S. and K. J. Kemphues (1996). "A non-muscle myosin required for embryonic polarity in Caenorhabditis elegans." Nature **382**(6590): 455-458.

Guse, A., M. Mishima, et al. (2005). "Phosphorylation of ZEN-4/MKLP1 by aurora B regulates completion of cytokinesis." Curr Biol **15**(8): 778-786.

Hannak, E., M. Kirkham, et al. (2001). "Aurora-A kinase is required for centrosome maturation in Caenorhabditis elegans." J Cell Biol **155**(7): 1109-1116.

Harris, A. K. and S. L. Gewalt (1989). "Simulation testing of mechanisms for inducing the formation of the contractile ring in cytokinesis." J Cell Biol **109**(5): 2215-2223.

Haviv, L., D. Gillo, et al. (2008). "A cytoskeletal demolition worker: myosin II acts as an actin depolymerization agent." J Mol Biol **375**(2): 325-330.

Hiramoto, Y. (1971). "Analysis of cleavage stimulus by means of micromanipulation of sea urchin eggs." Exp Cell Res **68**(2): 291-298.

Hird, S. N. and J. G. White (1993). "Cortical and Cytoplasmic Flow Polarity in Early Embryonic-Cells of Caenorhabditis-Elegans." Journal of Cell Biology **121**(6): 1343-1355.

Hirose, K. (2001). "MgcRacGAP Is Involved in Cytokinesis through Associating with Mitotic Spindle and Midbody." Journal of Biological Chemistry **276**(8): 5821-5828.

Honda, R., R. Korner, et al. (2003). "Exploring the functional interactions between Aurora B, INCENP, and survivin in mitosis." Mol Biol Cell **14**(8): 3325-3341.

Jantsch-Plunger, V., P. Gonczy, et al. (2000). "CYK-4: A Rho family gtpase activating protein (GAP) required for central spindle formation and cytokinesis." J Cell Biol **149**(7): 1391-1404.

John, C. M., R. K. Hite, et al. (2007). "The Caenorhabditis elegans septin complex is nonpolar." EMBO J **26**(14): 3296-3307.

Kaitna, S., M. Mendoza, et al. (2000). "Incenp and an aurora-like kinase form a complex essential for chromosome segregation and efficient completion of cytokinesis." Curr Biol **10**(19): 1172-1181.

Kaitna, S., P. Pasierbek, et al. (2002). "The aurora B kinase AIR-2 regulates kinetochores during mitosis and is required for separation of homologous Chromosomes during meiosis." Curr Biol **12**(10): 798-812.

Kamijo, K., N. Ohara, et al. (2006). "Dissecting the role of Rho-mediated signaling in contractile ring formation." Mol Biol Cell **17**(1): 43-55.

Kawamura, K. (1977). "Microdissection studies on the dividing neuroblast of the grasshopper, with special reference to the mechanism of unequal cytokinesis." Exp Cell Res **106**(1): 127-137.

Kawashima, T., K. Hirose, et al. (2000). "MgcRacGAP is involved in the control of growth and differentiation of hematopoietic cells." Blood **96**(6): 2116-2124.

Kemphues, K. J., J. R. Priess, et al. (1988). "Identification of genes required for cytoplasmic localization in early C. elegans embryos." Cell **52**(3): 311-320.

Kinoshita, M., C. M. Field, et al. (2002). "Self- and actin-templated assembly of Mammalian septins." Dev Cell **3**(6): 791-802.

Kozlowski, C., M. Srayko, et al. (2007). "Cortical microtubule contacts position the spindle in C. elegans embryos." Cell **129**(3): 499-510.

Krendel, M., F. T. Zenke, et al. (2002). "Nucleotide exchange factor GEF-H1 mediates cross-talk between microtubules and the actin cytoskeleton." Nat. Cell Biol. **4**(4): 294-301.

Kurz, T., L. Pintard, et al. (2002). "Cytoskeletal regulation by the Nedd8 ubiquitin-like protein modification pathway." Science **295**(5558): 1294-1298.

Larkin, K. and M. V. Danilchik (1999). "Microtubules are required for completion of cytokinesis in sea urchin eggs." Dev Biol **214**(1): 215-226.

Lens, S. M., J. A. Rodriguez, et al. (2006). "Uncoupling the central spindle-associated function of the chromosomal passenger complex from its role at centromeres." Mol Biol Cell **17**(4): 1897-1909.

Lewellyn, L., J. Dumont, et al. (2009). "Analyzing the Effects of Delaying Aster Separation on Furrow Formation during Cytokinesis in the C. elegans Embryo." Mol Biol Cell.

Lundquist, E. A. (2006). "Small GTPases." Wormbook: 1-18.

Mackay, A. M., A. M. Ainsztein, et al. (1998). "A dominant mutant of inner centromere protein (INCENP), a chromosomal protein, disrupts prometaphase congression and cytokinesis." J Cell Biol **140**(5): 991-1002.

Maddox, A. S., B. Habermann, et al. (2005). "Distinct roles for two C. elegans anillins in the gonad and early embryo." Development **132**(12): 2837-2848.

Maddox, A. S., L. Lewellyn, et al. (2007). "Anillin and the septins promote asymmetric ingression of the cytokinetic furrow." Dev Cell **12**(5): 827-835.

Maddox, A. S. and K. Oegema (2003). "Deconstructing cytokinesis." Nat Cell Biol **5**(9): 773-776.

Mastronarde, D. N., K. L. Mcdonald, et al. (1993). "Interpolar Spindle Microtubules in Ptk Cells." Journal of Cell Biology **123**(6): 1475-1489.

Matsumura, F. (2005). "Regulation of myosin II during cytokinesis in higher eukaryotes." Trends Cell Biol **15**(7): 371-377.

Matuliene, J. and R. Kuriyama (2002). "Kinesin-like protein CHO1 is required for the formation of midbody matrix and the completion of cytokinesis in mammalian cells." Mol Biol Cell **13**(6): 1832-1845.

Mcdonald, K., J. D. Pickettheaps, et al. (1977). "Mechanism of Anaphase Spindle Elongation in Diatoma-Vulgare." Journal of Cell Biology **74**(2): 377-388.

Minestrini, G., A. S. Harley, et al. (2003). "Localization of Pavarotti-KLP in living Drosophila embryos suggests roles in reorganizing the cortical cytoskeleton during the mitotic cycle." Mol Biol Cell **14**(10): 4028-4038.

Minoshima, Y., T. Kawashima, et al. (2003). "Phosphorylation by aurora B converts MgcRacGAP to a RhoGAP during cytokinesis." Developmental Cell **4**(4): 549-560.

Mishima, M., S. Kaitna, et al. (2002). "Central spindle assembly and cytokinesis require a kinesin-like protein/RhoGAP complex with microtubule bundling activity." Dev Cell **2**(1): 41-54.

Mishima, M., V. Pavicic, et al. (2004). "Cell cycle regulation of central spindle assembly." Nature **430**(7002): 908-913.

Miyauchi, K., Y. Yamamoto, et al. (2006). "Myosin II activity is not essential for recruitment of myosin II to the furrow in dividing HeLa cells." Biochem Biophys Res Commun **350**(3): 543-548.

Mollinari, C. (2002). "PRC1 is a microtubule binding and bundling protein essential to maintain the mitotic spindle midzone." The Journal of Cell Biology **157**(7): 1175-1186.

Mollinari, C., J.-P. Kleman, et al. (2002). "PRC1 is a microtubule binding and bundling protein essential to maintain the mitotic spindle midzone." J Cell Biol **157**(7): 1175-1186.

Mollinari, C., J. P. Kleman, et al. (2005). "Ablation of PRC1 by small interfering RNA demonstrates that cytokinetic abscission requires a central spindle bundle in mammalian cells, whereas completion of furrowing does not." Mol Biol Cell **16**(3): 1043-1055.

Munro, E. (2004). "Cortical Flows Powered by Asymmetrical Contraction Transport PAR Proteins to Establish and Maintain Anterior-Posterior Polarity in the Early C. elegans Embryo." Developmental Cell **7**(3): 413-424.

Murata-Hori, M., K. Fumoto, et al. (2000). "Myosin II regulatory light chain as a novel substrate for AIM-1, an aurora/Ipl1p-related kinase from rat." J Biochem **128**(6): 903-907.

Murata-Hori, M. and Y. L. Wang (2002). "Both midzone and astral microtubules are involved in the delivery of cytokinesis signals: insights from the mobility of aurora B." J Cell Biol **159**(1): 45-53.

Murata-Hori, M. and Y. L. Wang (2002). "The kinase activity of aurora B is required for kinetochore-microtubule interactions during mitosis." Curr Biol **12**(11): 894-899.

Muris, D. F., T. Verschoor, et al. (2002). "Constitutive active GTPases Rac and Cdc42 are associated with endoreplication in PAE cells." Eur J Cancer **38**(13): 1775-1782.

Nakamura, T., K. Aoki, et al. (2005). "Monitoring spatio-temporal regulation of Ras and Rho GTPase with GFP-based FRET probes." Methods **37**(2): 146-153.

Nance, J., E. M. Munro, et al. (2003). "C. elegans PAR-3 and PAR-6 are required for apicobasal asymmetries associated with cell adhesion and gastrulation." Development **130**(22): 5339-5350.

Neef, R., U. R. Klein, et al. (2006). "Cooperation between mitotic kinesins controls the late stages of cytokinesis." Curr Biol **16**(3): 301-307.

Nishimura, Y. (2006). "Centralspindlin regulates ECT2 and RhoA accumulation at the equatorial cortex during cytokinesis." Journal of Cell Science **119**(1): 104-114.

Odell, G. M. and V. E. Foe (2008). "An agent-based model contrasts opposite effects of dynamic and stable microtubules on cleavage furrow positioning." The Journal of Cell Biology **183**(3): 471-483.

Oegema, K., A. Desai, et al. (2001). "Functional analysis of kinetochore assembly in Caenorhabditis elegans." J Cell Biol **153**(6): 1209-1226.

Oegema, K. and T. J. Mitchison (1997). "Rappaport rules: cleavage furrow induction in animal cells." Proc Natl Acad Sci U S A **94**(10): 4817-4820.

Oegema, K., M. S. Savoian, et al. (2000). "Functional analysis of a human homologue of the Drosophila actin binding protein anillin suggests a role in cytokinesis." J Cell Biol **150**(3): 539-552.

Ozlü, N., M. Srayko, et al. (2005). "An essential function of the C. elegans ortholog of TPX2 is to localize activated aurora A kinase to mitotic spindles." Developmental Cell **9**(2): 237-248.

Pavicic-Kaltenbrunner, V., M. Mishima, et al. (2007). "Cooperative assembly of CYK-4/MgcRacGAP and ZEN-4/MKLP1 to form the centralspindlin complex." Mol Biol Cell **18**(12): 4992-5003.

Paweletz, N. (2001). "Walther Flemming: pioneer of mitosis research." Nat Rev Mol Cell Biol **2**(1): 72-75.

Pertz, O. and K. M. Hahn (2004). "Designing biosensors for Rho family proteins--deciphering the dynamics of Rho family GTPase activation in living cells." J Cell Sci **117**(Pt 8): 1313-1318.

Petronczki, M., M. Glotzer, et al. (2007). "Polo-like kinase 1 triggers the initiation of cytokinesis in human cells by promoting recruitment of the RhoGEF Ect2 to the central spindle." Developmental Cell **12**(5): 713-725.

Piekny, A. J. and P. E. Mains (2002). "Rho-binding kinase (LET-502) and myosin phosphatase (MEL-11) regulate cytokinesis in the early Caenorhabditis elegans embryo." Journal of Cell Science **115**(Pt 11): 2271-2282.

Pollard, T. D. (2007). "Regulation of actin filament assembly by Arp2/3 complex and formins." Annu Rev Biophys Biomol Struct **36**: 451-477.

Powers, J., O. Bossinger, et al. (1998). "A nematode kinesin required for cleavage furrow advancement." Curr Biol **8**(20): 1133-1136.

Qi, M., W. Yu, et al. (2005). "Septin1, a new interaction partner for human serine/threonine kinase aurora-B." Biochem Biophys Res Commun **336**(3): 994-1000.

Raich, W. B., A. N. Moran, et al. (1998). "Cytokinesis and midzone microtubule organization in Caenorhabditis elegans require the kinesin-like protein ZEN-4." Mol Biol Cell **9**(8): 2037-2049.

Rappaport, R. (1961). "Experiments concerning the cleavage stimulus in sand dollar eggs." J Exp Zool **148**: 81-89.

Rappaport, R. (1969). "Aster-Equatorial Surface Relations and Furrow Establishment." Journal of Experimental Zoology **171**(1).

Rappaport, R. (1982). "Cytokinesis: the effect of initial distance between mitotic apparatus and surface on the rate of subsequent cleavage furrow progress." J Exp Zool **221**(3): 399-403.

Rappaport, R. (1986). "Establishment of the mechanism of cytokinesis in animal cells." Int Rev Cytol **105**: 245-281.

Rappaport, R. (1996). Cytokinesis in Animal Cells. Cambridge, Press Syndicate of the University of Cambridge.

Rappaport, R. and G. W. Conrad (1963). "An Experimental Analysis of Unilateral Cleavage in Invertebrate Eggs." Journal of Experimental Zoology **153**(2).

Rappaport, R. and B. Rappaport (1983). "Cytokinesis - Effects of Blocks between the Mitotic Apparatus and the Surface on Furrow Establishment in Flattened Echinoderm Eggs." Journal of Experimental Zoology **227**(2): 213-227.

Rappaport, R. and B. N. Rappaport (1974). "Establishment of cleavage furrows by the mitotic spindle." J Exp Zool **189**(2): 189-196.

Rappaport, R. and B. N. Rappaport (1993). "Duration of division-related events in cleaving sand dollar eggs." Dev Biol **158**(1): 265-273.

Ris, H. (1949). "The anaphase movement of chromosomes in the spermatocytes of the grasshopper." Biol Bull **96**(1): 90-106.

Rittinger, K., P. A. Walker, et al. (1997). "Structure at 1.65 A of RhoA and its GTPase-activating protein in complex with a transition-state analogue." Nature **389**(6652): 758-762.

Rogers, E., J. D. Bishop, et al. (2002). "The aurora kinase AIR-2 functions in the release of chromosome cohesion in Caenorhabditis elegans meiosis." J Cell Biol **157**(2): 219-229.

Ruchaud, S., M. Carmena, et al. (2007). "Chromosomal passengers: conducting cell division." Nat Rev Mol Cell Biol **8**(10): 798-812.

Saxton, W. M. and J. R. McIntosh (1987). "Interzone microtubule behavior in late anaphase and telophase spindles." J Cell Biol **105**(2): 875-886.

Schmutz, C., J. Stevens, et al. (2007). "Functions of the novel RhoGAP proteins RGA-3 and RGA-4 in the germ line and in the early embryo of C. elegans." Development **134**(19): 3495-3505.

Schonegg, S., A. T. Constantinescu, et al. (2007). "The Rho GTPase-activating proteins RGA-3 and RGA-4 are required to set the initial size of PAR domains in Caenorhabditis elegans one-cell embryos." Proc Natl Acad Sci USA **104**(38): 14976-14981.

Schroeder, T. E. (1981). "The Origin of Cleavage Forces in Dividing Eggs - a Mechanism in 2 Steps." Experimental Cell Research **134**(1): 231-240.

Schumacher, J. M., A. Golden, et al. (1998). "AIR-2: An Aurora/Ipl1-related protein kinase associated with chromosomes and midbody

microtubules is required for polar body extrusion and cytokinesis in Caenorhabditis elegans embryos." J Cell Biol **143**(6): 1635-1646.

Severson, A. F., D. L. Baillie, et al. (2002). "A Formin Homology protein and a profilin are required for cytokinesis and Arp2/3-independent assembly of cortical microfilaments in C. elegans." Curr Biol **12**(24): 2066-2075.

Severson, A. F. and B. Bowerman (2003). "Myosin and the PAR proteins polarize microfilament-dependent forces that shape and position mitotic spindles in Caenorhabditis elegans." J Cell Biol **161**(1): 21-26.

Severson, A. F., D. R. Hamill, et al. (2000). "The aurora-related kinase AIR-2 recruits ZEN-4/CeMKLP1 to the mitotic spindle at metaphase and is required for cytokinesis." Curr Biol **10**(19): 1162-1171.

Shannon, K. B., J. C. Canman, et al. (2005). "Taxol-stabilized microtubules can position the cytokinetic furrow in mammalian cells." Mol Biol Cell **16**(9): 4423-4436.

Shelton, C. A., J. C. Carter, et al. (1999). "The nonmuscle myosin regulatory light chain gene mlc-4 is required for cytokinesis, anterior-posterior polarity, and body morphology during Caenorhabditis elegans embryogenesis." J Cell Biol **146**(2): 439-451.

Somers, W. G. and R. Saint (2003). "A RhoGEF and Rho family GTPase-activating protein complex links the contractile ring to cortical microtubules at the onset of cytokinesis." Dev Cell **4**(1): 29-39.

Somma, M. P., B. Fasulo, et al. (2002). "Molecular dissection of cytokinesis by RNA interference in Drosophila cultured cells." Mol Biol Cell **13**(7): 2448-2460.

Srayko, M., A. Kaya, et al. (2005). "Identification and characterization of factors required for microtubule growth and nucleation in the early C. elegans embryo." Developmental Cell **9**(2): 223-236.

Straight, A. F., C. M. Field, et al. (2005). "Anillin binds nonmuscle myosin II and regulates the contractile ring." Mol Biol Cell **16**(1): 193-201.

Strickland, L., Y. Wen, et al. (2005). "Interaction between EB1 and p150glued Is Required for Anaphase Astral Microtubule Elongation and Stimulation of Cytokinesis." Current Biology **15**(24): 2249-2255.

Teichmann, E. (1903). "Uber die Beziehung zwischen Astrospharen und Furchen: Experimentelle Untersuchungen am Seeigelei." Archiv fur Entwicklungsmechanik der Organismen **16**: 243-327.

Terada, Y., M. Tatsuka, et al. (1998). "AIM-1: a mammalian midbody-associated protein required for cytokinesis." EMBO J **17**(3): 667-676.

Thomas, S. and K. B. Kaplan (2007). "A Bir1p Sli15p kinetochore passenger complex regulates septin organization during anaphase." Mol Biol Cell **18**(10): 3820-3834.

Toure, A., O. Dorseuil, et al. (1998). "MgcRacGAP, a new human GTPase-activating protein for Rac and Cdc42 similar to Drosophila rotundRacGAP gene product, is expressed in male germ cells." J Biol Chem **273**(11): 6019-6023.

Vader, G., J. J. Kauw, et al. (2006). "Survivin mediates targeting of the chromosomal passenger complex to the centromere and midbody." EMBO Rep **7**(1): 85-92.

Vagnarelli, P. and W. C. Earnshaw (2004). "Chromosomal passengers: the four-dimensional regulation of mitotic events." Chromosoma **113**(5): 211-222.

Verbrugghe, K. (2004). "SPD-1 Is Required for the Formation of the Spindle Midzone but Is Not Essential for the Completion of Cytokinesis in C. elegans Embryos." Current Biology **14**(19): 1755-1760.

Verbrugghe, K. J. and J. G. White (2007). "Cortical centralspindlin and G alpha have parallel roles in furrow initiation in early C. elegans embryos." J Cell Sci **120**(Pt 10): 1772-1778.

Verni, F. (2004). "Feo, the Drosophila Homolog of PRC1, Is Required for Central-Spindle Formation and Cytokinesis." Current Biology **14**(17): 1569-1575.

Werner, M., E. Munro, et al. (2007). "Astral signals spatially bias cortical myosin recruitment to break symmetry and promote cytokinesis." Curr Biol **17**(15): 1286-1297.

Wheatley, S. P., A. Carvalho, et al. (2001). "INCENP is required for proper targeting of Survivin to the centromeres and the anaphase spindle during mitosis." Curr Biol **11**(11): 886-890.

Wheatley, S. P., C. B. O'Connell, et al. (1998). "Inhibition of chromosomal separation provides insights into cleavage furrow stimulation in cultured epithelial cells." Mol Biol Cell **9**(8): 2173-2184.

Wheatley, S. P. and Y. Wang (1996). "Midzone microtubule bundles are continuously required for cytokinesis in cultured epithelial cells." J Cell Biol **135**(4): 981-989.

White, J. G. and G. G. Borisy (1983). "On the Mechanisms of Cytokinesis in Animal-Cells." Journal of Theoretical Biology **101**(2): 289-316.

Withee, J., B. Galligan, et al. (2004). "Caenorhabditis elegans WASP and Ena/VASP proteins play compensatory roles in morphogenesis and neuronal cell migration." Genetics **167**(3): 1165-1176.

Wolpert, L. (1960). "The Mechanics and Mechanism of Cleavage." International Review of Cytology-a Survey of Cell Biology **10**: 163-216.

Yamada, T., M. Hikida, et al. (2006). "Regulation of cytokinesis by mgcRacGAP in B lymphocytes is independent of GAP activity." Exp Cell Res **312**(18): 3517-3525.

Yoshizaki, H., Y. Ohba, et al. (2003). "Activity of Rho-family GTPases during cell division as visualized with FRET-based probes." J Cell Biol **162**(2): 223-232.

Yuce, O. (2005). "An ECT2-centralspindlin complex regulates the localization and function of RhoA." The Journal of Cell Biology **170**(4): 571-582.

Zhao, W. M. and G. Fang (2005). "MgcRacGAP controls the assembly of the contractile ring and the initiation of cytokinesis." Proc Natl Acad Sci U S A **102**(37): 13158-13163.

Zhou, M. and Y. L. Wang (2008). "Distinct pathways for the early recruitment of myosin II and actin to the cytokinetic furrow." Mol Biol Cell **19**(1): 318-326.

Zhu, C., E. Bossy-Wetzel, et al. (2005). "Recruitment of MKLP1 to the spindle midzone/midbody by INCENP is essential for midbody formation and completion of cytokinesis in human cells." Biochem. J. **389**(2): 373.